The University Of Sheffield.

Access to Electronic Thesis

Author:	Tirthadipa Pradhan
Thesis title:	Function and regulation of the Drosophila planar polarity effector Multiple Wing Hairs (Mwh).
Qualification:	MPhil

This electronic thesis is protected by the Copyright, Designs and Patents Act 1988. No reproduction is permitted without consent of the author. It is also protected by the Creative Commons Licence allowing Attributions-Non-commercial-No derivatives.

This thesis was embargoed until 02nd March 2016.

If this electronic thesis has been edited by the author it will be indicated as such on the title page and in the text.

Function and regulation of the *Drosophila* planar polarity effector Multiple Wing Hairs (Mwh)

Tirthadipa Pradhan

Submitted for the degree of Masters of Philosophy (M.Phil)

March 2011

Centre for Biomedical and Developmental Genetics
Department of Biomedical Science
University of Sheffield

Acknowledgements

I would like to thank Professor David Strutt for his supervision, guidance and support throughout the two years of my study. Many thanks goes to Dr. Helen Strutt, Amy, Chloe, Sam, Liz and Jess for their help, love and warmth.

I am grateful to my advisors Professor Carl Smythe and Prof Steve Winder and my postgraduate tutor Dr. Andy Furley for their constant support and guidance.

My sincere thanks to all Fly lab members, and to the Biomedical Science department of the University of Sheffield.

I would also like to thank my friends Dhami, Asfarul, Kiran, Kavitha, Sarah B, Sarah J, Mariyam and Grinu for their trust, love and support which made my days in Sheffield happier.

Last but not the least I would like to thank my parents and my brothers for their unconditional love and constant encouragement.

Abstract

The noncanonical Frizzled signalling pathway regulates planar cell polarity (PCP) in both vertebrates and invertebrates. In the *Drosophila* wing, asymmetric subcellular localisation of PCP proteins specifies the production of a single distally pointing trichome in each cell. The localisation of core PCP proteins (Fz, Dsh, Dgo, Stbm, Pk and Fmi) at the proximal and distal cell edge acts as a cue for establishment of a polarisation event mediated by the effector proteins Inturned (In), Fuzzy (Fy), Fritz (Frtz), and Multiple wing hairs (Mwh).

Mwh, the most downstream effector protein known of the PCP pathway, localises at the apicoproximal membrane domain of each wing cell just before trichome formation. In its absence, ectopic actin bundle formation occurs over the entire apical surface of the cell, resulting in the formation of multiple trichomes with abnormal polarity.

There is limited understanding of how Mwh accumulates proximally in each wing cell and about its interaction with the cytoskeleton. To fill the gap in our knowledge I did an *in vivo* RNAi screen in the *Drosophila* wing, in order to search for novel regulators of Mwh. My screening has found several potential genes (such as *c12.1, Mo25, Rab23, staufen, sep2, cip4, Tsp29Fb, formin3*) that alter the distribution of Mwh protein and may therefore regulate it directly. Additionally, other genes were found which appears to have a potential role in regulating cell size, timing of trichome formation and trichome morphology.

Bioinformatic analysis has revealed the presence of a GBD/FH3 domain in Mwh, which is normally found in the Formin group of cytoskeletal regulatory proteins. In an *in vitro* study in mammalian fibroblast cells (3T3), the GBD domain of Mwh was found to induce cytoskeletal changes such as a significant reduction of stress fibres, suggesting a possible role for the GBD domain of Mwh in modulating the cell cytoskeleton.

Further investigation will provide better understanding of the pathway that leads to the formation of a single distally pointing trichome downstream of the core PCP cues, and also how Mwh regulates this pathway by modifying the actin cytoskeleton.

Contents

Chapter 3:- An *in vivo* UAS RNAi screen in the *Drosophila* wing to identify novel factors essential for a single trichome formation:

List of Figures:

List of Tables:

Chapter 1: General introduction

An overview of polarity:

What is polarity?

Polarity is a fundamental property of cells arising from various origins. Asymmetric organisation of cellular components and structures forms polarity within a cell. Most eukaryotic cells exhibit some kind of polarity within them.

Cell polarity is essential for differentiation, proliferation and morphogenetic processes exhibited by single and multicellular organisms. It also regulates axis formation, asymmetric cell division and cell migration in different organisms (Hertzog and Chavrier, 2011; Knoblich, 2008; Macara and Mili, 2008). Impaired polarity leads to different developmental disorders in many organisms. Different signalling cascades, membrane trafficking events and cytoskeletal dynamics are observed to play important roles in establishing cell polarisation.

Types of polarity:

Apical-basal polarity:

Polarisation of cells along the apical-basal axis is known as apical–basal polarity. This is the most frequent form of cell polarity exhibited by living organisms and is found in single layered epithelial cells (Van Aelst and Symons, 2002) to mediate the unidirectional transport of ions and nutrients (Cereijido *et al.,* 2004).

Three well-known protein complexes are known to regulate the apical basal polarity in different organisms: the Scribble complex (Scribble, DLG and LGL), the PAR complex (PAR3/PAR6/atypical protein kinase C [aPKC]) and PAR4/LKB1, and the Crumbs complex (Crumbs, PalS1 and PATj) (McCaffrey and Macara 2009). In the single layered epithelial cells, contacts between neighbouring cells provide spatial cues that activate these protein complexes to establish the initial cellular asymmetry which eventually leads to the development

of the apical and basolateral membrane domains (Suzuki and Ohno, 2006). These protein complexes are also known to regulate the activity of Cdc42 and Rac1 at the plasma membrane level (Nelson, 2009) to establish polarity.

Apical-basal polarity helps in the transport of molecules from the gut, kidney and/or glandular tissues across the cell membrane (Nelson, 2009). It also mediates selective secretion of extracellular components from the basal lamina (Eatons and Simons, 1995).

Planar cell polarity:

Along with the apical-basal polarity, most epithelial cells also show a secondary axis of polarity, perpendicular to the apical-basal axis. This is known as planar cell polarity (PCP) in which polarisation mostly takes place along the proximal and distal axis of the cell.

PCP was first reported in the cuticles of the moths *Rhodinus* and *Galleria* by various cuticle-grafting experiments (Wigglesworth ,1940; Piepho ,1955; Locke 1959). Later it was found in the eye and bristle patterns in an insect, known as the large milkweed bug (*Oncopeltus fasciatus*) (Lawrence and Shelton, 1975). It was also observed in the plant *Arabidopsis*. Here PCP helps in the positioning of the root hairs along the epidermal cells to coordinate towards the high concentration of auxin gradient at the root tip (Grebe 2004; Ikeda *et al.,* 2009).

Katherine Nubler-Jung first coined the term ‘Planar Polarity’ in the 1980s to define the polarisation of cells along the plane of an epithelium in various insects. Subsequently *Drosophila* became the ideal model to study PCP due to the presence of various adult tissues (such as wing, eye, and notum) displaying excellent manifestation of PCP (Gubb and Garcia Bellido, 1982).

Drosophila wing and eye tissues are the most studied organ systems used to understand the mechanism of PCP. In the *Drosophila* eye, PCP is required for

the proper orientation of ommatidia (specifies the R3/R4 photoreceptors in ommatidia) and in the absence of PCP proteins, misrotation and orientation defects occur in the eye (Strutt and Strutt, 2005) (Fig 1.1).

In the *Drosophila* wing, as a result of asymmetric subcellular localisation of core PCP proteins, a single trichome or wing hair forms from the distal vertex of each wing cell. In the *Drosophila* leg, bristles orient themselves distally, (Fig 1.1) and in the *Drosophila* notum hairs orient themselves in the anterior-posterior axis with the help of PCP (Strutt and Strutt, 2008).

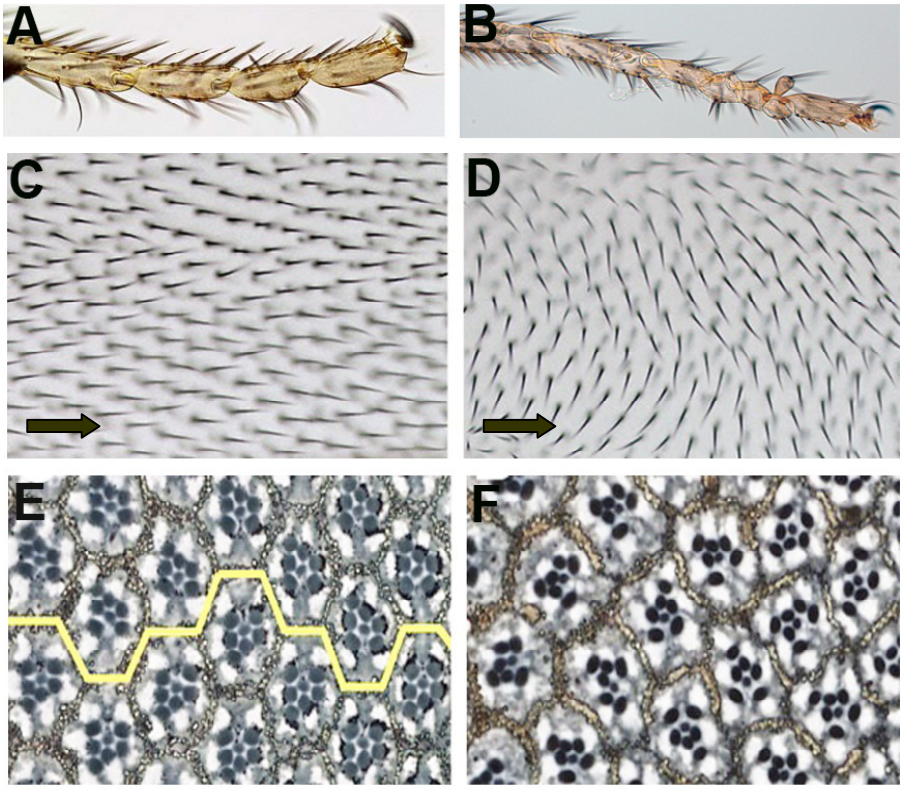

Figure1.1: PCP in *Drosophila* leg, wing and eye. (A-B) PCP in the *Drosophila* leg: distally pointed bristles in a wild type *Drosophila* leg (A) and disrupted bristles in a Fz mutant *Drosophila* leg (B). (C-D) PCP in the *Drosophila* wing: Distally pointed wing hairs in a Wild type *Drosophila* wing (arrow indicating towards the distal direction) (C) and loss of distal polarity in trichomes of a Fz mutant wing (D). (E-F) PCP in the *Drosophila* eye: Wild type *Drosophila* eye (histological section showing the ommatidia); Yellow line in E shows the equator which separates the two chiral forms of ommatidia and in a Fz mutant the ommatidial polarity is lost (F). Image taken from Strutt. D, 2008.

In vertebrates, the PCP pathway regulates the orientation of inner ear hair stereocilia (Montcouquiol *et al*., 2003), organisation of hairs in the skin (Guo *et*

al., 2004), neural tube closure (Kibar *et al.,* 2001), eyelid closure (Montcouquiol *et al*., 2003), and convergent extension mechanism (Djiane *et al.,* 2000; Heisenberg *et al.,* 2000; Wallingford *et al.,* 2000) which is involved in the gastrulation process of vertebrate embryos (Montcouquiol 2007; Wang and Nathans 2007) and development of various organ systems (Karner *et al.,* 2006; Wang and Nathans , 2007). Additionally, PCP has been found to regulate directed cell migration in some vertebrates, such as movement of zebrafish neurons in the developing hindbrain (Jessen *et al.,* 2002).

***Drosophila* as a model system:**

The fruit fly *Drosophila melanogaster* has been used as a model system to study genetic and developmental processes during the last 100 years. Thomas Hunt Morgan and his students first made *Drosophila* a successful model for genetic analysis and since then it has been routinely used in a number of cytogenetic, developmental and cell biological studies.

Several features of *Drosophila* make it an amenable and powerful model system for studying various biological processes. Firstly, *Drosophila* is very easy to maintain as well as cheap to rear in laboratory conditions with simple handling methods. Secondly, the life cycle of *Drosophila* is very short, completing in around 10 days at 25ºC, making it favourable for developmental genetics studies. Thirdly, it has only four pairs of chromosomes, one X/Y pair, two autosomes (second and third chromosome) and a very small fourth chromosome comprising of only a few genes; the *Drosophila* genome consists of around 14000 genes making it relatively simple (as compared to humans with 23000 genes) for various genetic and developmental studies. Although it has only 4 chromosomes, the fly genome shares a good percentage of similarity with different human disease related genes (around 75%), which is another hallmark of *Drosophila* system. Finally, the availability of interesting and powerful genetic tools for genetic analysis establishes *Drosophila* as one of the most successful models for different biological studies.

The developmental stages of *Drosophila*:

Drosophila development consists of several stages. On average, the full life cycle of *Drosophila* takes around 10 days to complete at 25ºC. The first stage is the embryonic development, which takes place during the first 24 hours of development. At this stage cleavage, cellularisation, gastrulation, dorsal closure and finally formation of imaginal disc cells take place.

After embryogenesis, the embryo hatches as the first instar larva and subsequently to second and third instar stages after one to two days each. During all these instar stages, the larvae feed extensively and undergo growth and proliferation by the process of endoreplication. Later on all the larval tissues are destroyed except for the imaginal disc cells, which are predetermined to become adult tissues.

The next step is the pupal stage, the final phase of development in which by the secretion of ecdysterone hormone the larva covers itself in a puparium case and undergoes metamorphosis at the pre pupal and pupal stages. Specification of wing veins, wing and leg inversions and elongations, disc fusions take place during this stage. Also during the pupal stage wing hair formation and eye pigmentation occurs. Then finally the adult fly ecloses from its pupal case.

Planar cell polarity and proteins of PCP pathway:

The upstream and core group of PCP proteins:

Based on phenotypic analysis and genetic epistasis experiments, the proteins known to be involved in the PCP pathway, can be divided into several groups (Adler, 1992; Wong and Adler, 1993). The upstream factors consist of two atypical cadherins, Fat (Ft) and Dachsous (Ds) and the Golgi-kinase Four-jointed (Fj), which together act as a cue for core PCP protein accumulation in the eye and wing cells of *Drosophila* (Strutt and Strutt, 2005). However, core proteins can

act independently of upstream factors as well, as seen in the *Drosophila* abdomen (Casal *et al.,* 2006).

The core group of PCP proteins is essential for establishing and maintaining polarity in different organisms. In *Drosophila*, the Core PCP proteins consist of the seven pass transmembrane receptor protein Frizzled (Fz) (Vinson and Adler, 1987; Vinson *et al.,* 1989; Adler *et al.,* 1990), the cytoplasmic protein Dishevelled (Dsh) (Adler, 1992) and the ankyrin rich protein Diego (Dgo) (Feiguin *et al.,* 2001; Das *et al.,* 2004) which localise at the apico-distal wing cell edges and the four pass transmembrane protein Strabismus (Stbm, also known as Van Gogh) (Wolff and Rubin, 1997; Taylor *et al.,* 1998; Bastock *et al.,* 2003) and the cytoplasmic protein Prickle (Pk) (Tree *et al.,* 2002) are found at the proximal end of each wing cell. Flamingo (Fmi) a seven pass transmembrane cadherin (Usui *et al.,* 1999) also belongs to the core group of PCP proteins and is found to localise at both the proximal and distal cell ends. As a result of this asymmetric subcellular localisation of core proteins a distal trichome or wing hair formation takes place in each *Drosophila* wing cell (Fig: 1.2,1.3) (Gubb and Garcia Bellido, 1982; Wong and Adler, 1993).

Perturbation of core protein localisation results in the disruption of polarity resulting in the generation of the trichome from the centre of each wing cell rather than distally (Gubb and Garcia Bellido, 1982; Wong and Adler, 1993). Among the core proteins, Fz and Stbm possess nonautonomous effects *i.e*. some mutant clones can affect the polarisation of neighbouring wild type cells (Taylor *et al.,* 1998). None of the other core proteins were found to elicit cell nonautonomous effects (Axelrod 2001; Bastock *et al.,* 2003; Das *et al.,* 2004; Jenny *et al.,* 2003; Strutt *et al.,* 2002; Tree *et al.,* 2002; Strutt and Strutt, 2007).
Although Fmi does not have a cell nonautonomous effect, in the Fmi null background Fz and Stbm lose their nonautonomy, suggesting Fmi localisation is required for the cell nonautonomous effects of Fz and Stbm (Strutt and Strutt, 2007).

PCP effector proteins:

Downstream of the core group of proteins, tissue specific PCP effector proteins are required to help in the establishment of PCP by regulating both the number and the direction of wing hairs/trichomes formed in the *Drosophila* wing. The role of core PCP proteins is suggested to be in restricting the action of the downstream effector proteins to the correct locality (Krasnow and Adler, 1994), such as higher level of Fz in the distal vertex of the wing cell (Strutt D, 2001) is observed to help in the formation of trichome distally by locally inhibiting activities of downstream effector proteins in that region (Wong and Adler, 1993).

The cytoplasmic protein Inturned (In) (Yun *et al.,* 1999; Adler *et al.,* 2004), the WD40 repeat containing protein Fritz (Frtz) (Collier *et al.,* 2005), the four pass transmembrane protein Fuzzy (Fy) (Collier and Gubb, 1997) and the GBD-FH3 domain containing formin-like protein Multiple wing hairs (Mwh) (Strutt and Warrington, 2008; Yan *et al.,* 2008) act as PCP effectors in the *Drosophila* wing. Genetic epistasis experiments revealed that these proteins act downstream of PCP signalling (Adler *et al.,* 2004) and their localisation is dependent on the core PCP proteins (Adler *et al.,* 2004; Strutt and Warrington, 2008; Yan *et al.,* 2008). In, Frtz and Fy act together and mutations in them result in the formation of more than one trichome (mostly two wing hairs /wing cell) with abnormal polarity (Adler *et al.,* 2004). Although *in* mutation affects ommatidial rotation and sensory bristle polarity, other effectors do not seem to have any effects in eye or bristle polarity (Adler, 2002).

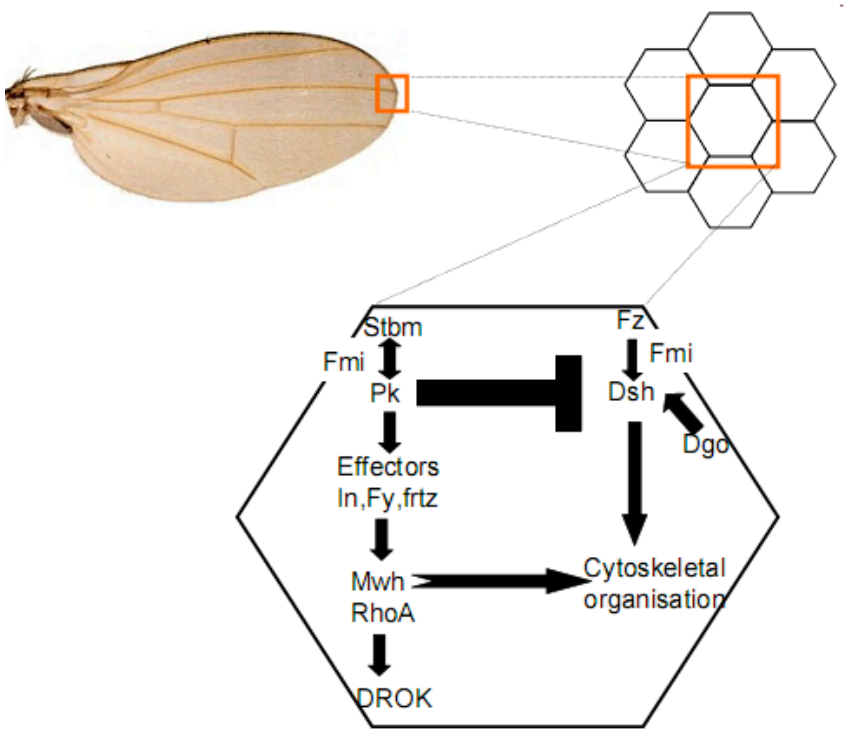

Figure 1.2: Schematic view of Planar cell polarity in the *Drosophila* wing. The *Drosophila* wing consists of numerous hexagonal cells and in each cell PCP proteins localises asymmetrically to establish the polarisation. The proximal complex (stbm, Pk) antagonises the distal complex (Fz, Dsh, Dgo) and Fmi localises at both the ends thereby stabilising both the proximal and the distal complex. The effector proteins localises at the proximal end with the help of the proximal core proteins. As a result of this subcellular asymmetric localisation a trichome forms from the distal vertex of each wing cell.

There are other tissue specific effectors, such as the Nemo (Nmo), Roulette (Rlt) (Choi and Benzer, 1994), Scabrous (Sca) (Chou and Chien, 2002), LamininA (LamA) (Henchecliffe *et al.,* 1993), RhoA (Winter *et al.,* 2001; Yan *et al.,* 2009) and *Drosophila* Rho associated kinase (DROK) (Winter *et al.,* 2001), which regulate the PCP pathway in the *Drosophila* eye (the latter two are also reported in the wing; detailed report in later section).

Upstream Factors of PCP	Core PCP proteins	Effector PCP proteins
Fat (Ft), Dachsous (Ds), Four-jointed (Fj)	Frizzled (Fz), Dishevelled (Dsh), Diego (Dgo) Strabismus (Stbm), Prickle (Pk), Flamingo (Fmi)	Inturned (In), Fuzzy (Fy), Fritz (Frtz) ---------- Multiple wing hairs (Mwh)

Table 1.1:Subdivisions of PCP proteins :PCP proteins in *Drosophila* can be divided into three groups; the first one is upstream factors of PCP, then the core group of proteins followed by PCP effectors which was based on genetic epistasis experiments and phenotypic analyses.

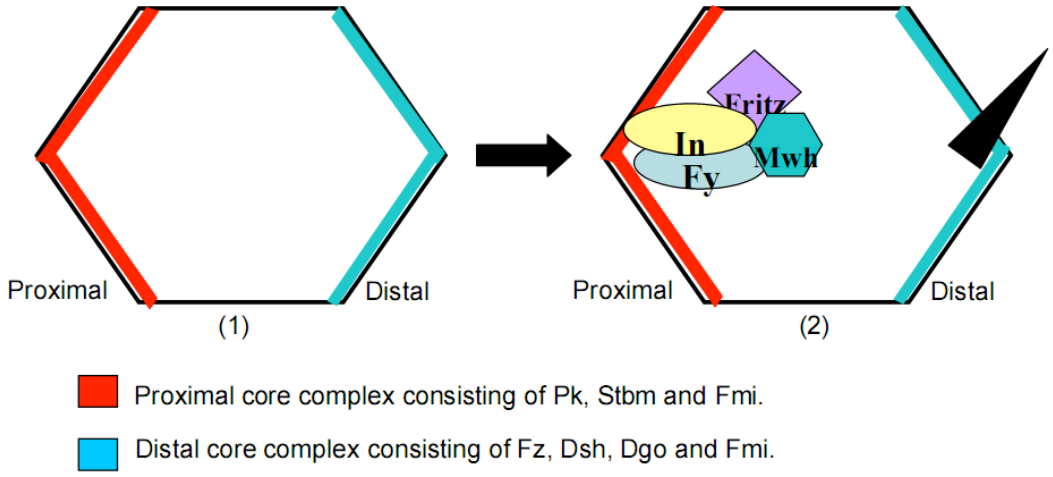

Figure 1.3: Schematic view of asymmetric localisationof PCP proteins in the Drosophilawing cell. The proximal complex (stbm,Pk; shown in red) localisesat the apicoproximal region of a wing cell and the distal complex (Fz,Dsh,Dgo; shown in blue) localisesthe apicodistal end. Fmilocalisesat both the both the proximal and the distal end thereby stabilising the core complex at both ends (1). The effectorproteins (In, Fy, Frtzand Mwh) then localisesat the proximal end with the help of the core proteins (2). As a result of this subcellularasymmetric localisationof PCP proteins a distally pointed trichome forms fr om the distal vertex of each wing cell.

Molecular detail of the effector proteins in *Drosophila*:

In is a cytoplasmic protein (Yun *et al.,* 1999), and is found to be required in all regions of the *Drosophila* wing (Park *et al.,* 1996). It acts cell autonomously (Park *et al.,* 1996) and functions prior to wing hair morphogenesis (Krasnow and Adler, 1994). During wing hair formation In interacts with the actin cytoskeleton to promote a single actin rich prehair (trichome) distally (Yun *et al.,* 1999) by localising at the apico proximal membrane region of the wing (Adler *et al.,* 1994).

In the absence of *in*, multiple trichomes form with disrupted polarity and the multiple hairs phenotype in the *in* mutant is stronger at 18ºC than at 29ºC indicating its cold sensitivity (Krasnow and Adler, 1994). This suggests that either *in* is inherently a cold sensitive gene or *in* dependent processes in *Drosophila* require the microtubule cytoskeleton, which is a cold sensitive structure.

Genetic analysis revealed that *in* is epistatic to *fz* group of core PCP genes as mutations in core PCP genes affect In localisation but not vice versa (Adler *et al.,* 2004). It was observed that domineering nonautonomy of the Fz group of PCP proteins depends on the presence of In and Mwh in the responding cells exhibiting nonautonomy (Lee and Adler 2002). It was also found that both an increase and a decrease in the activity of the Fz group of PCP proteins surprisingly cause enhancement of the phenotype of hypomorphic *in* and *fy* mutants (Lee and Adler 2002). Along with the core PCP proteins, Fy and Frtz are also required for the proper localisation of In in the *Drosophila* wing (Adler *et al.,* 2004).

Although In acts as a downstream epistatic factor to the Fz core group of proteins in the *Drosophila* wing and abdomen, in the eye a similar relationship is not seen, which suggests presence of tissue specificity in the transduction of PCP signalling (Lee and Adler, 2002).

Along with wing, eye and bristles, In protein was also found in the arista laterals of *Drosophila*, which are the terminal segments of the antennae. Mutation in *in* produce multiple and split laterals although there are no PCP defects present (He and Adler, 2002).

Finally, it was recently found that In physically interacts with the most downstream effector protein Mwh and the fusion protein of In::Mwh was able to perform the functions of both proteins (Qiuheng *et al.,* 2010).

Frtz, another downstream effector protein of the PCP pathway is a novel but evolutionarily conserved coiled coil protein with WD40 domain (Collier *et al.,* 2005). Frtz acts together with the other known effector proteins, In and Fy in a cell autonomous manner (Collier *et al.,* 2005) and mutation of *frtz* has the same phenotypic defect as that of *in*, producing multiple trichomes in each wing cell with abnormal polarity (Collier *et al.,* 2005). Frtz has also been found to regulate Mwh localisation and phosphorylation (Strutt and Warrington, 2008) in the *Drosophila* wing. Although the exact mechanism by which Frtz regulates Mwh still remains elusive, it suggests that Frtz may play an important role in the regulation of Mwh activity (Strutt and Warrington, 2008).

Another *Drosophila* downstream effector protein known as Fuzzy (Fy) is a cytoplasmic protein which also exhibits a similar mutant phenotype in the wing similar to other effector proteins i.e. presence of more than one trichome with disrupted polarity (Collier and Gubb, 1997). Fy, In and Frtz localisation and function in the wing is dependent on each other suggesting they may all interact together (Adler *et al.,* 2004). Fy can also act cell autonomously and the localisation of Fy is also dependent on the core as well as other effector proteins (Adler *et al.,* 2004; Strutt and Warrington, 2008).

The most downstream effector protein Multiple wing hairs (Mwh):

Mwh, the most downstream effector protein known in the PCP pathway, localises at the apico-proximal region of a wing cell prior to wing morphogenesis in a punctate zig- zag pattern (Strutt and Warrington, 2008; Yan *et al.,* 2008) and in its absence, multiple hairs (3-5 wing hairs/ wing cell) forms with abnormal polarity across the cell boundary (Gubb and Garcia Bellido, 1982; Strutt and Warrington 2008, Yan *et al.,* 2008). The multiple trichome phenotype observed in *mwh* mutants is phenotypically stronger than phenotypes exhibited by mutations in other effector proteins (Gubb and Garcia Bellido, 1982), suggesting a direct interaction between Mwh and the cytoskeleton in modulating trichome formation (Strutt and Warrington 2008; Yan *et al.,* 2008). Overexpression of *mwh* causes a

delay in trichome formation (Yan *et al.,* 2008) and loss of function causes ectopic multiple hair formation (Gubb and Garcia Bellido, 1982; Strutt and Warrington, 2008; Yan *et al.,* 2008). These phenotypes suggest that Mwh is involved in repressing multiple trichome formation across the wing cell boundary by restricting hair formation to the distal vertex of each wing cell (Gubb and Garcia Bellido, 1982; Strutt and Warrington, 2008; Yan *et al.,* 2008).

Mwh localisation is dependent on the other effector proteins In, Fy and Frtz. It was found that in either in, *fy* and *frtz* mutant backgrounds localisation of Mwh is impaired (Strutt and Warrington, 2008; Yan *et al.,* 2008), although in the case of the core group mutants (e.g. Stbm mutant background) Mwh was found to be reduced proximally but the apical punctate labeling was unaltered, suggesting that core proteins help in the localisation of the Mwh protein, but not on its activity (Strutt and Warrington, 2008).

Unlike other PCP effector proteins, Mwh localises at the base of the wing hair after the trichome formation (Yan *et al.,* 2008). Thus Mwh is considered to have two temporally different functions: the early function is to restrict wing hair formation distally by localising at the apicoproximal wing region and the later function is to resist endogenous wing hair formation by localising at the base of the wing hair (Yan *et al.,* 2008).

Like other effector proteins, Mwh also functions cell autonomously (Gubb and Garcia Bellido, 1982; Strutt and Warrington, 2008; Yan *et al.,* 2008) and *mwh* mRNA levels were found to be increased before wing hair formation (Ren *et al.,* 2005), suggesting its role in wing hair formation in *Drosophila*.

Other PCP effectors:

Among other effectors downstream of the PCP pathway, the Rho GTPases (RhoA, Cdc42 and Rac1) are most widely studied. In *Drosophila,* RhoA was found to be involved in PCP (Strutt *et al.,* 1997) as mutations in RhoA result in

multiple hairs in the wing and ommatidial rotation defects in the eye (Strutt *et al.,* 1997). A later report (Winter *et al.,* 2001) suggested that RhoA mutants produce multiple hairs in the wings but with normal polarity. Along with PCP defects, RhoA also regulates cell shape changes, F actin localisation and changes in cellular junctions (Yan *et al.,* 2009).

Along with the *Drosophila* eye, RhoA was also found to regulate the localisation of PCP core proteins such as Stbm in the wing due to its indirect effects on cell shape and adherens junction regulation (Yan *et al.,* 2009). Although RhoA is known to interact with Mwh in regulating PCP, it was found to have Mwh independent function in regulation of wing hair development in *Drosophila* (Yan *et al.,* 2009). All these observations suggest that RhoA is involved in PCP downstream of the Fz pathway (Strutt *et al.,* 2007) and it acts parallel to or upstream of Mwh to control wing hair formation (Yan *et al.,* 2008).

Drosophila Rho mediated kinase (DROK), which is a RhoA effector protein, is also known to regulate a subset of PCP responses in the eye and wing. In the eye, DROK is involved in the proper rotation of ommatidial clusters (Winter *et al.,* 2001) and in the wing it helps in formation of a single distally pointed trichome as loss of DROK causes multiple trichomes with abnormal polarity (Winter *et al.,* 2001). It is believed to regulate the actin cytoskeleton by phosphorylating nonmuscle myosin Ⅱ regulatory light chain (MRLC) and thereby maintains polarity (Winter *et al.,* 2001).

Rac1 and Cdc42 were initially found to have a role in the PCP pathway (Eaton *et al.,* 1996). In the *Drosophila* wing a dominant negative form of Rac1 (Rac1N17) caused multiple hair formation and dominant negative Cdc42 caused disruption in actin polymerization, thereby affecting hair growth (Eaton *et al.,* 1996). But a later report of loss of function mutant analysis of Rac1 and Cdc 42 argues against this role (Munoz Descalzo *et al.,* 2007) suggesting either they have a mild role in PCP generation or the function of Rho GTPases are redundant in this

process (Munoz Descalzo *et al.,* 2007).

Recent literature reports the effect of a putative vesicle trafficking protein Rab23 (Pataki *et al.,* 2010) in the coordination of PCP in *Drosophila*. *Drosophila* Rab23 interacts with the PCP core protein Pk and in its absence multiple trichome or wing hairs forms in the wing, leg and abdomen with distorted polarity (Pataki *et al.,* 2010). Rab23 was found to increase the multiple hair phenotypes of PCP core mutants and the homozygous form of it was found to be sensitive to the effects of gene dosage of PCP effectors (Pataki *et al.,* 2010). These findings suggest that along with other effector proteins, Rab23 also contributes in the maintenance of PCP in *Drosophila*.

Other genes involved in single trichome formation in *Drosophila*:

There are some other putative downstream proteins that have been found to regulate the wing hair formation in the *Drosophila* wing. Those proteins are listed in Table 2 with their effects on trichome formation:

Gene Name	Ontology (Based on Fly base)	Role in wing hair formation
slingshot (ssh)	phosphatase	Causes increased level of F actin which makes thick, twisted or splited wing hair .
singed (sn)	Actin binding protein	Multiple hairs, defects in hair and bristle morphology.
forked (f)	Actin binding protein	Multiple hairs, defects in hair and bristle morphology
tricornered (trc)	NDR kinase	Multiple hairs, defects in hair and bristle found to interact with Mwh
furry (fry)	Protein binding	Multiple hairs, defects in hair and bristle morphology

Table 1.2: Other factors involved in the regulation of wing hair formation in the *Drosophila* wing.

Other vertebrate PCP proteins:

There are a number of vertebrate specific PCP proteins, which have not been found to have a role in regulating PCP in *Drosophila.* Wnt5 and Wnt11 are members of the Wnt signalling pathway, which regulates noncanonical PCP signalling in vertebrates. Wnt5 regulates the inner ear hair cell orientation (Qian *et al.,* 2007) and both Wnt5 and 11 were found to be involved in convergent extension mechanism in vertebrates (Heisenberg *et al.,* 2000; Tada and Smith 2000; Kilian *et al.,* 2003).

Receptor serine threonine kinase protein PTK7 is another protein that was found to regulate the PCP pathway in vertebrates. Mutants of *PTK7* had inner ear hair orientation defects and neural tube defects (Lu *et al.,* 2004). Among other vertebrate PCP proteins, Scribble and Discs Large are especially interesting. They are generally known to be involved in apical basal polarity (Dow and Humbert 2007; Assemat *et al.,* 2008; Martin-Belmonte and Mostov 2008; Yamanaka and Ohno 2008), but in vertebrates they also regulate neural tube closure and hair cell orientation in the inner ear (Montcouquiol *et al.,* 2003).

The role of effector proteins in vertebrates:

Among the effector proteins of PCP pathway, the most downstream protein Mwh does not have any vertebrate homologs (Strutt and Warrington 2008, Yan *et al.,* 2008), but other effectors such as Frtz, In and Fy were found to regulate various aspects of vertebrate development (Park *et al.,* 2006; Gray *et al.,* 2009; Heydeck *et al.,* 2009; Zeng *et al.,* 2010).

In (Intu in vertebrates) and Fy (Fuz in vertebrates) are widely studied in vertebrates and are reported to play a wider role in different developmental processes. Studies in the *Xenopus* and mouse model over last few years have revealed that Intu and Fuz are essential for a range of organ development processes such as development of the neural tube, eye formation, skeletal morphogenesis, dorsoventral patterning of the spinal cord and anterior posterior

patterning of the limb bud in vertebrates (Park *et al.,* 2006; Gray *et al.,* 2009; Heydeck *et al.,* 2009; Zeng *et al.,* 2010). Absence of Intu and Fuz caused severe defects along with lethality at embryonic stage suggesting their importance in development (Park *et al.,* 2006; Zeng *et al.,* 2010).

Along with embryonic lethality mutant embryos were also seen to have defects in the neural tube, abnormal dorso-ventral patterning of the central nervous system (CNS), malformation of the anterior posterior patterning of the limbs resulting in severe polydactyly, craniofacial and ocular defects, defects in brain ventricles, hyperplastic lungs and abnormal anterior posterior patterning of the limb bud (Park *et al.,* 2006; Gray *et al.,* 2009a, Heydeck *et al.,* 2009b, Zeng *et al.,* 2010).

In *Drosophila,* In and Fy act together in a common pathway to maintain polarity and the phenotypes seen in vertebrates also suggest a similar scenario in higher organisms (Park *et al.,* 2006).

Both Intu and Fuz also caused defective ciliogenesis and reduction in total number of cilia in the *Xenopus* and mouse embryos. Also the other developmental defects in those mutants were similar to defects associated with ciliogenesis formation. Cilia are microtubule-based organelles, which are present at the surface of all cells of vertebrate origin and play a variety of roles in embryonic and postnatal development (Gerdes *et al.,* 2009). Defects in cilia formation cause a number of diseases in vertebrates such as retinal dystrophy, polydactyly, renal malformation, neural tube closure defects, hydrocephalus and mental retardation (Gerdes *et al.,* 2009). Human diseases such as Bardet-Biedl syndrome (BBS), Meckel-Gruber Syndrome (MKS), Kartagener's syndrome and Polycystic kidney disease occur due to cilia malformation (Ross *et al.,* 2005, Smith *et al.,* 2006, Nachury *et al.,* 2007, Sharma *et al.,* 2008).

Cilia are known to play an essential role in the transduction of the Hedgehog signalling, which regulates development of multiple organ system in vertebrates

(Jiang and Hui, 2008). When examined both in *Xenopus* and mouse embryos, the Hh target genes (such as *Nkx2.2*, *Netrin*, *FoxD1* and *Vax1*) were found to be reduced in an Intu and Fuz mutant background suggesting the role of the role of these effector proteins in controlling Hh signalling in vertebrates (Park et al., 2006; Gray *et al.,* 2009a; Heydeck *et al.,* 2009b; Zeng *et al.,* 2010).

Along with various developmental defects, *fuz* mutant embryos also exhibit PCP defects such as a curly or kinky tail (a phenotype which is normally seen when core PCP proteins are mutated) and severe cardiac malformation (Gray *et al.,* 2009).

Bioinformatic analysis and physical interaction studies revealed a novel interaction of Fuz with a small GTPase similar to REM2 and the vesicle targeting Rab proteins RSG1 (Rem/Rab–Similar GTPase 1) (Gray *et al.,* 2009). With the help of mGENETHREADER (Gray *et al.,* 2009) analysis of the protein domain structure of fuz was also analysed. This predicted its interaction with CLAMP (CaLponin homology and microtubule-associated protein), which is a microtubule-bundling protein present in cilia and flagella (Gray *et al.,* 2009). When tested Fuz as well as RSG1 were found to regulate the localisation of CLAMP at the apical tips of cilia and also in apical trafficking, defining a novel role of Fuz in membrane trafficking during ciliogenesis (Gray *et al.,* 2009). Furthermore Fuz was found to regulate the secretion of mucous secreting goblet cells suggesting a broader role of Fuz in membrane trafficking machinery (Gray *et al.,* 2009).

Fritz, a secreted Fz related protein with WD40 domain was found to antagonize the functions of Wnt in mouse and human cells in a non cellautonomous manner (Mayr *et al.,* 1997). Among the Wnt family proteins, Wnt8 and Wnt11 (Mili and Taira, 2009), (the latter being involved in PCP signalling in vertebrates) (Heisenberg *et al.,* 2000; Tada and Smith 2000; Kilian *et al.,* 2003) were found to be negatively affected by Fritz. It was also reported to have a role in the primary

development of mouth in vertebrates by suppressing the Wnt signalling, suggesting its importance in vertebrate development (Dickinson and Sive, 2009).

Thus accumulating evidence based on recent research has revealed that PCP effector proteins play a remarkable role in a number of developmental processes in vertebrates. It also reveals the novel function of PCP in the regulation of fundamental cellular systems such as membrane trafficking machinery. Although no such role of effector proteins in membrane trafficking has been reported in *Drosophila,* this data hints at such type of connection. The widespread requirement of effector proteins in cilia formation and function also depicts a role in regulating the cytoskeleton network in different organisms and hopefully it will begin to clarify the human diseases associated with cilia malformation.

Mwh is a formin like protein:

Genetic analysis of the *mwh* locus has revealed its cytological position as 61E-F (Strutt and Warrington 2008) and subsequently *CG13913* has been found to be the candidate gene encoding *mwh*. Further observations like phenocopying of the *mwh* phenotype through the expression of an RNAi hairpin of the *CG13913* transcript (Dietzl *et al.,* 2007) in *Drosophila* and rescuing the mutant phenotype either by overexpression of *CG13913* under different *Gal4* promoters or by expression of EGFP tagged CG13913 protein in transgenic flies, confirmed that *mwh* corresponds to *CG13913* (Strutt and Warrington 2008; Yan *et al*., 2008). The *mwh* gene is found to encode a 836 aa protein product.

Bioinformatic analysis of the *mwh* coding sequence for known protein domains revealed the presence of GBD (GTPase binding domain) and FH3 (Formin homology 3) domains at the N terminus and a C terminal domain of unknown function (Strutt and Warrington 2008; Yan *et al*., 2008)(Fig 1.2). The GBD and FH3 domains are normally found in formin group of proteins, which play a major role in actin nucleation process (Waller and Alberts, 2003) and thereby modulating the cytoskeleton.

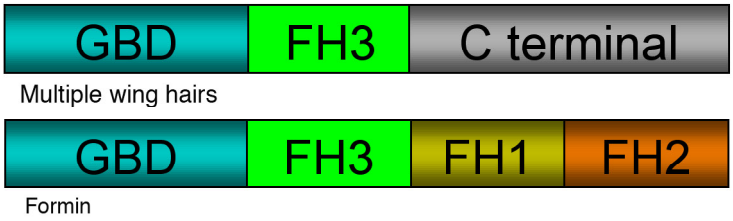

Figure1.3: A schematic representation of Mwh protein with its different domains compared to that of a conventional formin. GBD: GTPase binding domain, FH3: Formin homology 3 domain, FH1: Formin homology 1 domain and FH2: Formin homology 2 domain. FH1 and FH2 domains are responsible for actin nucleation, GBD domain has an autoinhibitory effect and binding with Rho GTPases reduces this autoinhibiton, FH3 domain helps in the subcellular localisation of the protein. C terminal end of Mwh is of unknown function and absence of FH1 and FH2 domains of a conventional formin makes it a formin like protein (Strutt and Warrington 2008; Yan *et al*., 2008).

Formins are highly conserved eukaryotic proteins with a wide range of roles in actin-based processes (Waller and Alberts, 2003). These are large, single polypeptide, multidomain proteins encoded by *Fmn* genes and mutations in mouse *Fmn* homologs gave rise to murine limb deformities and renal malformations (Wang *et al.,* 1997). Formins are involved in diverse processes like cytokinesis, hair cell stereocilia formation, cell polarization, sperm cell acrosome formation, as well as in normal embryonic development (limb and kidney morphogenesis)(Evangelista *et al.,* 2003, Otomo *et al.,* 2005). They are also found to have a role in *Drosophila* oocyte polarity regulation (Emmons *et al.,* 1995) and also in polarised cell growth in yeasts (Pruyne *et al.,* 2002).

The highly conserved feature of formins is the two juxtaposed formin homology domains FH1 and FH2 (Figure 1.3). Generally the FH2 domain of a formin is sufficient to mediate actin nucleation *in vitro* (Puryne *et al.,* 2002, Sagot *et al.,* 2002) and actin assembly *in vivo* (Copeland and Treisman 2002). The FH2 domain forms a tethered dimer and mutation that disrupt this dimer formation reduce its activity (Moseley *et al.,* 2003, Takeya and Sumimoto, 2003; Xu *et al.,* 2004). After actin nucleation, the FH2 domain remains bound to the barbed end of actin filament and moves forward as the actin filament elongates by preventing access of capping proteins to the filament (Shimada *et al.,* 2004). Subsequently the proline rich FH1 domain will interact with SH2 domains and the G actin binding protein profilin, thereby enhancing actin nucleation (Schwartzberg, 2007;

Covar 2006; Otomo 2005). No other interacting proteins have been identified for the FH2 domain of formin.

Studies of fission yeast Fus1 protein first identified the FH3 domain, which is required in subcellular localisation of the protein (Petersen *et al*., 1998), and the GBD domain is known to have an auto inhibitory effect (Wallar *et al.,* 2005). Binding of GTP bound RhoGTPases to the GBD domain causes the adjacent diaphanous (Dia) inhibitory domain (DID) to release the carboxyl-terminal dia autoregulatory (DAD) domain that flanks the FH1 and FH2 domains and makes it functionally active (Wallar *et al.,* 2006; Goode and Eck 2007).

Based on the phylogenetic analysis of the FH2 domain, formins are divided into different subtypes. Metazoans have seven different types of formin families: Dia, FMN, FHOD, delfilin, INP, FRL and Daam (Young and Copeland, 2008).

The GBD and FH3 domains are normally found together in the Dia family of formins, which plays a variety of roles in cell motility and membrane invagination (Afshar *et al.,* 2000, Minin *et al.,* 2006, Williams *et al.,* 2007). The absence of the more conserved FH1 and FH2 signature domains in Mwh suggests it is a formin like protein if not a true formin (Strutt and Warrington 2008; Yan *et al*., 2008).

The presence of only the GBD and FH3 domains were also found in some *Dictyostelium* RasGEFs, which lacks the FH1 and FH2 domains (Rivero *et al.,* 2005).

Homologs of Mwh are found in other arthropods such as *Pediculus humanus (*hemipteran), *Apis melifera (*hymenopteran)*, Tribolium castaneum* (coleopteran), *Bombyx mori (*lepidopteran) and *Daphnia pulex (*crustacean) (Yan *et al.,* 2008). However no homologs were identified in nematodes or vertebrates. The absence of any homologs of Mwh in vertebrates and its presence in insects suggests it is a part of an ancient morphogenesis-signalling network (Yan *et al.,* 2008).

Formins in *Drosophila*:

In *Drosophila* different formin proteins are present, which are involved in actin cytoskeleton regulation and various developmental pathways.

Daam (Dishevelled-associated activator of morphogenesis) is a novel formin subtype, which was found to have a role in planar cell polarity signalling during *Xenopus* gastrulation (Habas *et al.,* 1995) by regulating the convergent extension mechanism and acting as a "bridging factor " between Dsh and RhoA (Habas *et al.,* 1995). In *Drosophila, Daam* is maternally enriched in the embryo and was observed to regulate the actin cytoskeleton of different tissues including the tracheal system (Matusek *et al.,* 2006) but no role has been detected in the establishment of PCP, which could be masked due to redundancy (Matusek *et al.,* 2006).

In the trachea, branching morphogenesis of tubules produces an extensively interconnected tracheal network and *Daam* is found to regulate the branching mechanism by forming taenidial folds (Matusek *et al.,* 2006). In the absence of *Daam*, the actin filament network gets disrupted resulting in abnormal taenidial folds (Matusek *et al.,* 2006).

Daam was also found to have a role in the *Drosophila* embryonic central nervous system (CNS) function (Matusek *et al.,* 2008) and the absence of *Daam* led to defects in neurite growth.

Diaphanous (dia), another well-characterised formin protein in *Drosophila*, is primarily required during cytokinesis of mitotic and meiotic cell divisions (Castrillon and Wasserman, 1994). Mutations in *dia* cause sterility in both sexes of *Drosophila* (Castrillon and Wasserman, 1994). *dia* is also responsible for actin cytoskeleton organization in various tissues and membrane invagination of the cytoskeletal structure (Afshar *et al.,* 2000). It also regulates the formation and function of contractile rings (Castrillon and Wasserman, 1994; Afshar *et al.,* 2000).

dia interacts with Rho GTPases (RhoA) in various contexts. In the mitochondria, RhoA was shown to affect mitochondrial movement by its downstream effectors *dia* in *Drosophila* and *mdia1* in mouse cells (Minin *et al.,* 2006). Overexpression of the constitutively active mutant form of *dia* causes reduction in mitochondrial motility by disrupting their actin filaments, whereas knocking down the endogenous *dia* by RNAi stimulates the mitochondrial movements (Minin *et al.,* 2006).

Another widely known *Drosophila* formin is *Capuccino (Capu)*, which is a unique maternal–effect locus required for the formation of anterioposterior and dorsoventral pattern of *Drosophila* egg and embryo (Manseau and Schupbach 1989). Female mutants of C*apu* produce embryos lacking pole cells and polar granules suggesting its role in the oocyte-nurse cell complex formation.
Capu interacts (via its FH2 domain) with another actin nucleating protein Spire via its kinase noncatalytic C-lobe domain (KIND) and this interaction is conserved across the metazoan phyla (Quinlan *et al.,* 2007). Unlike other formins Capu family members lack the DAD and DID domains (Higgs 2005) and do not have N terminal autoinhibition over the FH2 domain (Rosales-Nieves *et al.,* 2006), suggesting Capu activity might be regulated by interaction with Spire in trans (Quinlan *et al.,* 2007).

Capu and *spire* were shown to have microtubule and microfilament crosslinking activity *in-vivo*. In this context SpireD binds to Capu and inhibits F-actin/microtubule crosslinking. Activated RhoA abolishes this inhibition suggesting that RhoA, *Capu* and *spire* are “elements of a conserved developmental cassette” and are capable of directly regulating the crosstalk between microtubules and microfilaments (Rosales-Nieves *et al.,* 2006).

Other formin proteins present in *Drosophila* are Formin 3, Fhos and CG 32138 (Table 1.3). Formin 3 possesses the FH1 and FH2 domain for actin nucleation

and an FH3 domain which normally helps in the subcellular localisation of the protein. The absence of the GBD domain suggests it does not have an autoinhibitory effect as that seen with dia (Tanaka *et al.,* 2004).

Formin 3 mRNA was found to be expressed in the trachea of a *Drosophila* embryo at around stage 11 (Tanaka *et al.,* 2004) and loss of *Formin 3* affects tracheal fusion process by inhibiting the F actin network assembly which is essential for cellular rearrangement during tracheal fusion (Tanaka *et al.,* 2004).

Fhos, another *Drosophila* formin gene was found to be expressed in subsets of *Drosophila* muscles and at the midline of the ventral nerve cord from stage 15 (by RNA *in situ* hybridization) (Tanaka *et al.,* 2004). Other formin proteins were not found to be expressed during the time of embryogenesis, although a weak level of expression could not be ruled out (Tanaka *et al.,* 2004). Very little information is known about the function of the remaining formins in *Drosophila.*

Although most of the metazoan formins are cytoplasmic, vertebrate formins are mostly nuclear (De la Pompa *et al.,* 1995, Trumpp *et al.,* 1992) and are observed to express during the kidney and limb development (Zeller *et al.,* 1989; Kleinebrecht *et al.,* 1982; Mass *et al.,* 1994). They are also involved in different morphogenetic signalling pathways, such as SHH signalling, which regulates the limb pattern formation in vertebrates (Chen *et al.,* 1995; Haramis *et al.,* 1995).

	Domains present (InterPro based)					
Name of the Formin (with CG number)	**FH1**	**FH2**	**FH3**	**GBD**	**Associated Rho GTPases**	**Cellular /Biological role**
Diaphanous (CG1768)	✓	✓	✓	✓	Rho1	Cell motility; mitochondrial motility; haemocyte activation; membrane invagination
Capuccino (CG3399)	✓	✓	✖	✖	Rho1	Cytoplasmic streaming in oocytes and cell polarity
Daam (CG14622**)**	✓	✓	✖	✓	RhoA	Tracheal development,
CG32138	✓	✓	✓	✓	Not known	Unknown function
Formin 3 (CG33556)	✓	✓	✓	✖	Not known	Not fully determined, but may be restricted to tracheal cells
Fhos (CG32030/CG5797)	✓	✓	✓	✓	Not known	Unknown function, present in trachea during embryogenesis
Mwh (CG13913) Formin like protein (ref: Strutt and Warrington 2008; Yan *et al.,* 2008)	✖	✖	✓	✓	RhoA	Planar cell polarity establishment in the *Drosophila* wing

Table1.3: List of Formin like proteins present in *Drosophila melanogaster.*

Formins and Rho GTPases:

The formin group of proteins act to regulate the actin cytoskeleton as downstream effectors of Rho GTPases, which are small G proteins involved in a number of signalling mechanisms (Dumontier *et al.,* 2000). Rho GTPases are found in almost all eukaryotes and play crucial roles in cell polarity, motility, membrane trafficking, cell adhesion and regulation of actin cytoskeleton (Etienne-Manneville and Hall, 2002; Sakumura *et al.,* 2005; Brock *et al.,* 1996).

These small G proteins bind to both GDP and GTP and have an intrinsic GTPase activity. Binding with GTP makes them functionally active and GTP bound Rho GTPases then interacts with a number of downstream effector genes. Rho GEFs regulate the binding of GTP subunits with Rho GTPases and modulate their interactions (Van Aelst and D'Souza-Schorey, 1997). There are a total of 22 Rho GTPases reported in mammals (Feltri *et al.,* 2008), but among them RhoA, Rac1 and cdc42 have been extensively studied. Rac1 and cdc42 induce plasma membrane protrusions such as filopodia and lamellipodia formation and RhoA affects vesicular trafficking across the membrane as well as actin stress fibre formation (Ridley and Hall, 1992; Ridley 1996; Hall 1998; Johnson, 1999).

Generally Rho GTPases bind to two downstream effectors to regulate the actin cytoskeleton, (i) WASP/WAVE complex which mediates actin polymerization by Arp2/3 complex (Millard *et al.,* 2004) and (ii) Diaphanous regulatory formins (DRFs) which mediates actin polymerization by its FH2 domain (Kovar, 2006; Pellegrin and Mellor, 2005).

Binding of Rho GTPases to the GBD domain of formins alleviates autoinhibiton of the GBD domain and causes the adjacent diaphanous (Dia) inhibitory domain (DID) to release the carboxyl-terminal Dia autoregulatory (DAD) domain that flank the FH1 and FH2 domains and makes it functionally active (Wallar *et al.,* 2005; Goode and Eck, 2007). The active FH2 domain then dimerises and binds to a growing actin chain. This binding of FH2 accelerates the elongation of the actin chain and prevents binding of capping proteins (Shimada *et al.,* 2004).

Rho GTPases are involved in a number of cell signalling and developmental processes in *Drosophila* (Xu *et al*., 2008; Hariharan *et al*., 1995; Paladi and Tepass, 2004; Fanto *et al*., 2000). RhoA (referred to Rho1 frequently) regulates PCP in the *Drosophila* eye and wing (Strutt *et al.,* 1997) as mentioned before.

Mwh was considered as a potential interacting partner of RhoA due to the

presence of the GBD domain (Strutt and Warrington, 2008; Yan *et al.,* 2008), which is known to interact with Rho GTPases (Wallar *et al.,* 2005; Goode and Eck, 2007). It was found that the accumulation of Mwh in the wing is dependent on RhoA, as dominant negative and constitutively active forms of RhoA resulted in reduction and increase respectively in the level of Mwh in the *Drosophila* wing (Yan *et al.,* 2009). A physical interaction between the two was further confirmed in a co immunoprecipitation assay in *Drosophila* wing cells where RhoA was found to bind with the full length and the GBD: FH3 domains of Mwh, but not with the C terminal domain (Yan *et al.,* 2009).

RhoA in mammalian cells regulates the formation of stress fibres, which are the contractile actin-myosin structures responsible for cell migration, contractility and adhesion (Langanger *et al.*, 1986). Stress fibres are normally found in non-muscle cells and can be categorized into three different types based on their subcellular localisation and interactions with focal adhesions; ventral stress fibres that are attached to focal adhesions at both ends, dorsal stress fibres that are attached to focal adhesions typically at one end and transverse arcs that are curved acto-myosin bundles, which do not directly attach to focal adhesions (Byers *et al.*, 1984).

A stress fibre is typically composed of actin filaments (which is the basic structural element of a stress fibre) and myosin II (which is responsible for producing contraction along the actin filament). Although myosin II does not comprise a bipolar structure, approximately 20-28 myosin molecules polymerises to produce the bipolarity required for contraction (Niederman and Pollard, 1975; Verkhovsky and Borisy, 1993). This myosin mediated contractility is important for the maintenance of the integrity of stress fibers, as inhibition or down regulation of myosin leads to loss of actin stress fibres (Chrzanowska-Wodnicka and Burrige, 1996; Bao *et al.*, 2005; Hotulainen and Lappalainen, 2006; Kolega, 2006).

Although actin filaments and myosins are the primary structural unit of a stress fibre, several other proteins are also present which are required to maintain its integrity. α actinin is amongst the best characterized proteins present in the actin stress fibre structure and it helps in crosslinkling F-actin filaments (Naumanen *et al.,* 2008).

Palladin is another actin cross-linking protein, which colocalises with α actinin and helps in the crosslinking of signalling proteins with the stress fibres. In the absence of palladin (either by RNAi knockdown or complete knockdown of the gene by loss of function allele) cells seem to lose the actin stress fibres (Parast and Otey, 2000; Luo *et al.*, 2005).

Numerous other proteins are also found to localise in the actin stress fibres with unknown functions or roles in stress fibre formation and regulation (Naumanen *et al.,* 2008).

The RhoA downstream effector proteins ROCK 1 and ROCK 2 have a role in phosphorylating the myosin regulatory light chains (MLC) and thereby increases myosin's ATPase- and filament-forming activities (Leung *et al.,* 1996; Kimura *et al.,* 1997). ROCK 1 and ROCK 2 also phosphorylates the myosin binding subunit of MLC phosphatase thereby inhibiting the activation of phosphatases and eventually causes dephosphorylation of MLC (Amano *et al.,* 1997). ROCK 1 was shown to have RhoA independent role in actin phosphorylation suggesting its role as a key mediator in the formation of stress fibres (Leung *et al.*, 1996).

dia1 is another well-characterized downstream effector of RhoA. The FH1 domain of dia1 binds to profilin, which is known to induce actin polymerisation by its interaction with actin binding protein VASP (Watanabe *et al.,* 1997). A truncated versions of dia1 retaining just the FH1 and FH2 domains induced an accumulation of actin filaments which suggests that the N terminal end of dia interacts with RhoA and this interaction releases the autoinhibition of dia which

ultimately leads to excessive actin polymerisation (Watanabe *et al.,* 1999).

Another signalling pathway which regulates actin stress fibres formation is the Ca2+ /calmodulin-dependent activation of myosin light chain kinase (MLCK) (Totsukawa *et al.,* 2000, Katoh *et al.,* 2001). MLCK also phosphorylates myosin light chains, which eventually leads to actomyosin contraction. Among these two signalling pathways MLCK causes more actin contractility as compared RhoA signalling (Totsukawa *et al.,* 2000). It was suggested that MLCK signalling is important for peripheral stress fibres formation whereas RhoA mediated signalling pathway regulates the central stress fibre formation of the actin cytoskeleton (Katoh *et al.,* 2001).

When RhoA is constitutively active excessive actin polymerization takes place and removal of the endogenous RhoA shows the opposite effect, resulting in reduction and eventually total loss of actin stress fibres, suggesting the ability of RhoA to induce stress fibres assembly and increased contractility in cells (Ridley and Hall, 1994).

Aim of the thesis:

As Mwh is the most downstream effector protein of PCP in *Drosophila* and since it is also known to directly interact with the actin cytoskeleton, I wanted to find out the mechanisms through which Mwh regulates the actin cytoskeleton and the distal restriction/orientation of wing hair/ trichome formation. Currently there is limited knowledge of the potential interactors of Mwh protein. To address these questions, I designed and performed an *in-vivo* RNAi screen in the *Drosophila* wing to identify novel interactors of Mwh.

The functions of different domains of Mwh were also investigated in a mammalian cell culture system in order to try to assign specific roles for the individual domains in the context of actin cytoskeleton regulation.

Chapter 2: Material and Methods

Fly Genetics:

Fly Stocks:

Fly strains used in various crosses were *w*; *ptc-Gal4* ; *UAS-Dcr 2* (Strutt Lab), *w; ptc-gal4*, *MS1096-Gal4*; *UAS -Dcr2* (Strutt Lab), *Daam1 /FM7; EGFP* (Bloomington Stock Centre), y^{1}; trc^{1}; *FRT 80 B kan* ^{2} ry^{566}/*TM6c ry* (Bloomington Stock Centre), *yw; Ubx Flip;p{w+,arm- lac Z} FRT 73.50/TM6C* (Bloomington Stock Centre), *p{w+, hs- fz- EGFP}* viable *on II* and *p{w+, hs- fz- EGFP}* viable *on III* (Strutt Lab).

RNAi lines:

All the RNAi lines used in this study were obtained either from the Vienna *Drosophila* RNAi Center (VDRC) (GD lines and KK lines) (Dietzl *et al.,* 2007) or from the National Institute of Genetics Fly Stock Center (NIG). For a complete list of the RNAi lines used, refer to Chapter 3.

GAL4/UAS system:

The *UAS/Gal4* system is a standard transgenic technique, originally adapted from yeast, and is widely used in flies for spatial and temporal gene expression studies. With the help of this system any gene placed downstream of a set of Upstream Activation Sequences (*UAS*) will express itself under the control of a promoter region placed upstream of the *Gal4* transcription factor, for example *ptc-GAL4*, which will drive the expression of the given gene under UAS control specifically in the *ptc* expression domains (Brand and Perrimon, 1993). *UAS* and *Gal4* constructs are integrated into separate fly lines and by crossing the two strains together the desired expression can be induced.

***Drosophila* adult wing dissection:**

Adult wings were removed at the hinge with a pair of sharp and clean forceps and were placed in a drop of isopropanol. After partial evaporation of the isopropanol, wings were mounted in 12 µl of 1:1 mix of methyl salicylate and canada balsam, which were applied to the coverslip. Approximately 6 wings were mounted on each slide.

Counting adult wing hairs in *Drosophila*:

RNAi lines were crossed with specific drivers (*ptc-Gal4; UAS-Dcr2* [2] and *MS 1096-Gal 4, UAS-Dcr2*) and raised in a 29˚C incubator until eclosion. Adult wings were then dissected and mounted as mentioned above. Number of cells with multiple trichomes were counted in each wing under a brightfield microscope and based on the total number of multiple trichomes per wing, RNAi lines were divided into 3 groups such as, weak (<10 multiple wing hairs /wing), medium (10-30 multiple wing hairs /wing), and strong (>30 multiple wing hairs /wing). Subsequently the RNAi lines with medium and strong multiple hairs were screened in the pupal wing by immunostaining.

***Drosophila* pupal wings dissection:**

Newly pupated white prepupae were collected and aged at 29˚C for 27 hours, for the trichomes (wing hairs) to form. For RNAi lines with a delay in trichome formation, lines were aged upto 28 hours at 29˚C.

Prepupae were removed from pupal case using a razor blade on top of a double-sided tape and fixed in 4% paraformaldehyde in PBS for 30-40 minutes. Wings were dissected from the pupae in a drop of paraformaldehyde, the wing cuticles removed and the wings washed in 0.2% Triton X 100 in PBS. They were then incubated in primary antibody with 0.2% Triton X 100 in PBS and 5% BSA overnight at 4˚C in microtitre plates, washed in 0.1% Triton X 100 in PBS for 10 times, incubated in secondary antibody in 0.1% Triton X 100 in PBS /0.5% BSA overnight, then washed again in 0.1% Triton X 100 in PBS. Wings were post-fixed in a 1:1 mix of 0.1% Triton X 100 in PBS and 4% paraformaldehyde in PBS

for 5-10 minutes at RT. Finally, wings were washed in PBS and then mounted in 10% glycerol and 2.5% Dabco anti-fade in PBS, and the edges of the coverslip sealed with nail varnish.

For actin staining, wings were incubated in Texas-red (TR)-phalloidin (1:100 of 6.6μM stock, Molecular Probes) for 30 minutes at room temperature followed by antibody treatments as mentioned above.

Antibodies:

The following primary antibodies were used

Antibody	**Concentration used**
Rabbit anti-Mwh	1:1000 (Strutt and Warrington, 2008)
Mouse anti-Armadillo	1:100 (DSHB)
Rabbit anti-Fritz	1:1000, (Strutt and Warrington 2008)
Mouse anti-Flamingo	1:50 (Usui *et al.,* 1998)
Mouse monoclonal anti-beta galactosidase	1:500, Promega
Mouse anti-GFP	1:250, Promega
Rat anti-Mwh	1: 100, (Strutt and Warrington, 2008).
Rabbit anti-GFP	1:4000, Molecular Probes
Rat anti-E cadherin	1:20, Sigma
DAPI (4′,6-diamidino 2 phenylindole)	1:10 of 0.2mg/ml stock (≈700nM/ml).

Secondary antibodies used were:

Antibody	**Concentration used**
rabbit Cy 2	1:500 (Jackson)
mouse Cy 5	1:500 (Jackson)
rabbit RRX	1:500 (Jackson)
preabsorbed mouse Cy2	1:500 (Jackson)
rat Cy5	1:500 (Jackson)

Phalloidin Texas Red (1:200, Molecular Probes)

Microscopy:

Drosophila adult wings were examined under a Leica DMR microscope and photographed using a ProgRes camera. Fluorescent staining was visualised using a Leica confocal microscope in the LMF facility. Images were processed using Image J and Adobe Photoshop V 7.0.

Tissue Culture:

3T3 cell culture:

3T3 cell culture was carried out according to the standard protocol. Briefly, cells were cultured in DMEM (GIBCO, cat no 11971) supplemented with 10% FCS (GIBCO). Cells were frozen with 15% FCS, 10% DMSO in cryo-container at -80°C – then shifted to liquid Nitogen.

3T3 cell transfection:

Cells were transfected using Lipofectamine 2000 (Roche). Cells were seeded 12 hours before transfection to attain 50% confluency in a 6-well dish with 4 x 13mm coverslips per well. Media was changed to Optimum (GIBCO) prior to transfection. Transformation mixer were prepared containing 2µg DNA + 100µl Optimum (A) and 6µl Lipofectamine + 100µl Optimum (B). A and B were then mixed and left for 20 minutes at room temperature and finally 800µl Optimum was added per tube and transfection mixture was added into each well. After incubation of 24 hrs, cells were fixed in 4 % paraformaldehyde and stained for proteins with various antibodies.

Immunohistochemistry of 3T3 cells:

Cells were fixed in 4% paraformaldehyde, blocked in 5% BSA and 0.1% Triton X 100 in PBS. Primary antibodies were added and incubated at 4°C overnight followed by three times rinse in 0.1% Triton X 100 in PBS. Secondary antibodies diluted in PBS containing 5%BSA were added and incubated. Cells were subsequently mounted in Vectashield mounting medium.

Primary antibodies used were Rabbit anti-GFP (1:4000, Molecular Probes), rat anti-Mwh (1: 100, Strutt and Warrington, 2008). Rabbit anti-Cy2 (1:500, Jackson) and rat anti-Cy5 (1:250, Jackson) were used as secondary antibodies.

Cell Imaging:

Images of 3T3 cells were taken under a Leica microscope. Fluorescent staining were also visualised using a Leica confocal microscope in the LMF facility. Images were processed using Image J and Adobe Photoshop V 7.0.

Actin phenotype rating:

Stress fibre formation and morphology of 3T3-transfected cells was rated blindly. Presence or absence of stress fibres, general cell shape and size and presence or absence of actin ruffles were scored in transfected cells. Each experiment was repeated 5 times, all the ratings were averaged and Student's t-test was performed each time to find out the significance of a particular phenotype.

Molecular Biology:

Constructs used in tissue culture assays:

In all 3T3 cell experiments the following constructs were used: The full length Mwh-GFP in pEGFPC-1 (Strutt and Warrington, 2008) and the pEGFPC-1 empty vector (CloneTech) were used as controls. Deletion mutant constructs of Mwh such as EGFP-N terminal Mwh, EGFP-GBD Mwh, EGFP-FH3 Mwh and EGFP-C terminal Mwh were made in pEGFPC-1 by PCR amplification and subcloning. Mwh protein is composed of 836 amino acids, with the GBD domain comprising 52 to 275 AA and the FH3 region extending from 290 to 492 AA, together making the N terminal domain of protein with 1-492 AA. The C terminal domain spans from 492 to 836 AA (Yan *et al.,* 2008). The amplified DNA fragments were inserted at the C terminus of EGFP in the construct.

Primers were designed with EcoRI and ApaI sites in them at the 5' and 3' ends respectively and covered from AA 50 to 277 for the GBD domain, 290 to 493 for

FH3 domain, 493 to 876 for C terminal domain and a total of 1 to 499 AA for the N terminal domain of Mwh.

Primers used to make the constructs:

Constructs	5'end primer	3'end primer	Restriction sites
N terminal Mwh-EGFP	GGCGAATTCATGG CTCCCAGTGTGTG CGAGATGGCC	GCATGGGCCCTTAGGATGC ACCCGTCCCGAACTGCTGA TGCC	EcoRI (5') and ApaI (3')
GBD Mwh-EGFP	GCGAATTCGGGC GGCTCCGAACAG AGTTGGCCTCAG	GCATGGGCCCTTATCCGAA GGGCTGGGATCGCAGGCG GAGGC	EcoRI (5') and ApaI (3')
FH3 Mwh-EGFP	GCGAATTCAGGAA GCGGCAGTGGTG GTCAGAAGATAGC C	GCATGGGCCCTTAGGATGC ACCCGCTCCGAACTGCTGA TGCC	EcoRI (5') and ApaI (3')
C terminal Mwh -EGFP	GCGAATTCGGGT GGCATCAGCAGTT CGGAGACGGGTG CATCC	GCATGGGCCCCTTAGTAGA GGCCGGATGGAGATCCGT GAC	EcoRI (5') and ApaI (3')

Chapter 3: Results

Title: An *in vivo* UAS-RNAi screen in the *Drosophila* wing to identify novel factors essential for the localization of PCP effector protein Mwh.

Introduction:

Although planar cell polarity pathway genes are well defined in *Drosophila*, the process by which PCP regulates cytoskeletal changes in the *Drosophila* wing and helps in the formation of a distally pointed trichome from each wing cell is not very well understood. PCP effector proteins are known to be associated with the process of cytoskeleton regulation and as Mwh is the most downstream effector protein known of this pathway (Strutt and Warrington, 2008; Yan *et al.,* 2008), it is supposed to be the key factor in this process possibly by interacting with novel genes associated with the cytoskeleton.

Mwh localises to the apicoproximal membrane domain of each wing cell just before the onset of trichome formation (Strutt and Warrington, 2008; Yan *et al.,* 2008). In the absence of Mwh, ectopic actin bundle formation occurs over the entire apical surface of the wing cell, resulting in the formation of multiple trichomes with disrupted polarity (Strutt and Warrington, 2008; Yan *et al.,* 2008).

When examined for its binding partner, Mwh was not found to colocalise with F-actin in the *Drosophila* bristles, larval muscles and salivary glands (by overexpressing it ectopically) suggesting there is no direct evidence of Mwh and F actin interaction (Yan *et al.,* 2008). It was then speculated that Mwh binds with one of the actin regulatory or binding components (myosin or another unknown component) and thereby regulates the actin cytoskeleton (Strutt and Warrington, 2008; Yan *et al.,* 2008), although no such novel interaction has been reported. There is also a limited understanding of how Frtz regulates the phosphorylation of

Mwh and the genes involved in this pathway. With these intriguing questions in mind, I did an *in vivo* RNAi screening in the *Drosophila* wing.

Previous RNAi screen in the lab have identified a number of genes involved in polarity defects, including genes which exhibit a phenotype of more than one wing hair per cell (H. Strutt, V. Thomas-McArthur, C. Thomas unpublished data). Further investigations have been carried out on selected RNAi lines that exhibited multiple hair phenotype in the adult wing screen by subjecting them to a pupal wing screen. Also, the interplay of effector proteins and other genes involved in recruiting Mwh had also been investigated in the screening.

RNAi screening as a method for identifying novel genes in a pathway:
After its first successful use in *C elegans* by Fire and Mello (Fire *et al* in 1998), RNAi has become a widely used reverse genetic tool to study the function of genes in different developmental and cell biological processes. In this technique, short double stranded RNA is expressed in the tissue of interest and the targeted homologous mRNA is degraded leading to silencing of the corresponding gene. This target specific degradation of mRNA by the cell is believed to be a defense response against infection by RNA viruses (Stram and Kuzntzova, 2006). It has gained wide popularity as a technique, which can be used in different organisms to characterize functions of known genes and/or can also be used at the whole genome level to perform reduced or complete loss-of-function screens on a large scale to identify novel genes and their functions.

Over the last few decades RNAi screen has gained more popularity as a genetic approach over classical forward genetic screening, as identifying a possible phenotype of a particular gene is more tedious and time consuming in forward genetic screens as compared to RNAi screens (Boutros and Ahringer, 2008). RNAi screening is easily quantifiable and both upregulators and downregulators can be obtained from a single screen. Since the dominant phenotype caused by a particular gene in forward genetic screening could be due to secondary

function of that gene or genetic redundancy (Boutros and Ahringer, 2008), currently genome wide screening by RNAi seems to be the ideal strategy.

Despite the advantages of RNAi there are some drawbacks such as requirement of robust statistical analysis for the quantitation of screening data in *in vitro* screening, possibility of false positive results due to off target effects, occurrence of false negatives due to resistance of some tissues to RNAi or unsusceptibility of some genes to RNAi and the effects of RNAi are also not inheritable in most cases (Boutros and Ahringer, 2008).

RNAi screens in *Drosophila*:

Drosophila melanogaster is one of the best-characterized model organisms in which RNAi screens have been previously used both at individual gene level and at the level of whole genome to study variety of developmental, genetic and cell biological processes *in vivo* and *in vitro* (Boutros and Ahringer, 2008). The first genome wide RNAi screen was done in *Drosophila* cells (Boutros *et al.,* 2004) and since then it is been routinely used in different genetic and developmental studies.

In the case of *in vivo* RNAi, genes are triggered either by injecting into the preblastoderm embryos or by the expression of transgenes encoding long double stranded hairpin RNAs of gene fragments cloned as inverted repeats (IRs). *in vivo* RNAi by injection method suffers from some limitations such as the study of gene function is restricted to embryonic development and can sometimes be masked by maternally loaded proteins. On the contrary, transgenic RNAi can be easily used to study function of genes in somatic tissues (Mohr *et al.,* 2010) Combined with *Gal4 UAS* expression system (Brand and Perrimon, 1993), the expression of the transgene can be driven in specific tissues and/or at particular developmental time points to get a more complete overview of a gene's function under desired developmental conditions (Dietzel *et al.,* 2007).

Utilizing the genome wide transgenic RNAi library of *UAS* driven IRs covering 97% of the protein coding genes constructed by Dietzel *et al.,* in 2007, *Gal4 UAS* expression system was employed in the lab (H. Strutt, V. Thomas-McArthur, C. Thomas unpublished data) to perform the screening *in vivo* in the *Drosophila* wing. These lines (GD lines) were made available by Vienna *Drosophila* Research Centre (VDRC), (http://stockcentre.vdrc.at/control/main). At the same time RNAi lines were also made commercially available at the National Institute of Genetics (NIG, http://shigen.nig.ac.jp) in Japan (although these lines covered fewer number of genes as compared to the VDRC stock centre). Recently VDRC started providing another type of RNAi collection known as KK lines (ref VDRC), which are designed to reduce off target effects by having the same insertion site for each gene.

Around 10000 lines were primarily screened (H. Strutt, V. Thomas-McArthur, C. Thomas unpublished data) in our lab with a wing specific driver (*MS1096-Gal4*). These lines were selected mostly based on levels of expression of respective genes during *Drosophila* wing morphogenesis and differentiation (Ren *et al.,* 2007). Along with these, RNAi lines were also ordered based on protein domain (Interpro) homology and gene ontology (Flybase) (D.Strutt, unpublished data).

Based on gene ontology (Flybase), genes involved in signaling mechanisms (like receptors, G protein coupled receptor (GPCRs), kinase/phosphatase, GTPase/GAP/GEF, G-proteins, cadherins, transmembrane secreted proteins), genes related to cytoskeleton (such as actin, tubulin/microtubule, dynein/myosin/kinesin), and genes/proteins involved in trafficking (such as ubiquitination, endocytosis, vacuolar proteins, vesicle proteins) were identified as positive selection criteria for the screen candidates(D.Strutt, unpublished data) .

Similarly, negative selection criteria was based on the genes involved in gene regulation/expression mechanisms (such as transcription, translation, chromatin modification), genes involved in essential maintenance of the cell and

metabolism (such as glycolysis, cell cycle, mitochondria genes), genes involved in sensory processes (such as neurotransmitters, channels, taste and smell receptors, and defence response genes), and miscellaneous gene families (such as glue proteins, salivary secretions, serine endopeptidases) (D.Strutt, unpublished data) .

Selection of drivers in the RNAi screen and the screening design:
The wing specific driver *MS1096-Gal4* was primarily used in the adult wing screen, as it expresses throughout the development of wings in *Drosophila*. The *MS1096-Gal4* insertion is on the X chromosome, which gives a stronger phenotype in males, and they were thus essentially used for the adult wing screen. Around 150 RNAi lines were selected based on previous screen data of the lab (H.Strutt, V Thomas McArthur, and C. Thomas, unpublished data) to cross to *MS1096-Gal4*. These lines were also crossed to *MS1096-GAl4; UAS-Dcr2* to check the increase in the strength of the phenotype by over expressing Dicer, an RNAse enzyme of RNAi machinery, which is reported to enhance the strength of the RNAi mechanism by 15% by cleaving the double stranded RNAi sequence and making it more efficient in binding with the target mRNA sequence (Dietzel *et al.,* 2007).

For screening in the pupal wing, the *ptc-GAl4; UAS-Dcr2* line was mainly used in as it exhibits a defined area of expression in the pupal wing (between the longitudinal veins 3 and 4) which facilitates the identification of mutant tissue easily and allows comparison with the adjacent wild type tissue.

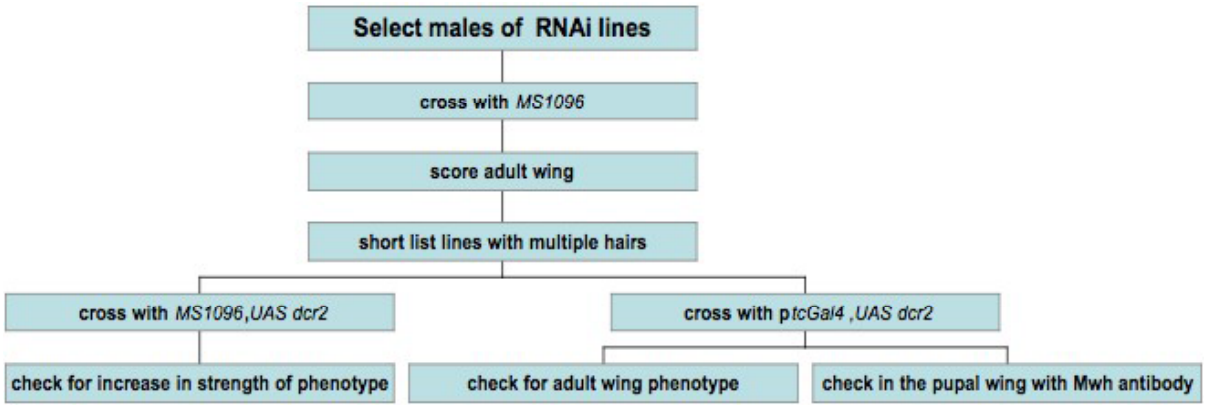

Figure 3.1: Outline of the RNAi screen design. Male flies of the RNAi lines were crossed with wing specific driver *MS1096-Gal4* and scored in the adult wing for multiple hairs phenotypes. Lines were short listed based on phenotypic strength. Those lines were then crossed to *MS1096-GAl4; UAS-Dcr2* to check for increase in the multiple hair phenotype. These lines were finally crossed to *ptc-GAl4; UAS-Dcr2* to determine Mwh antibody localisation in the *ptc-Gal4* expressing domain.

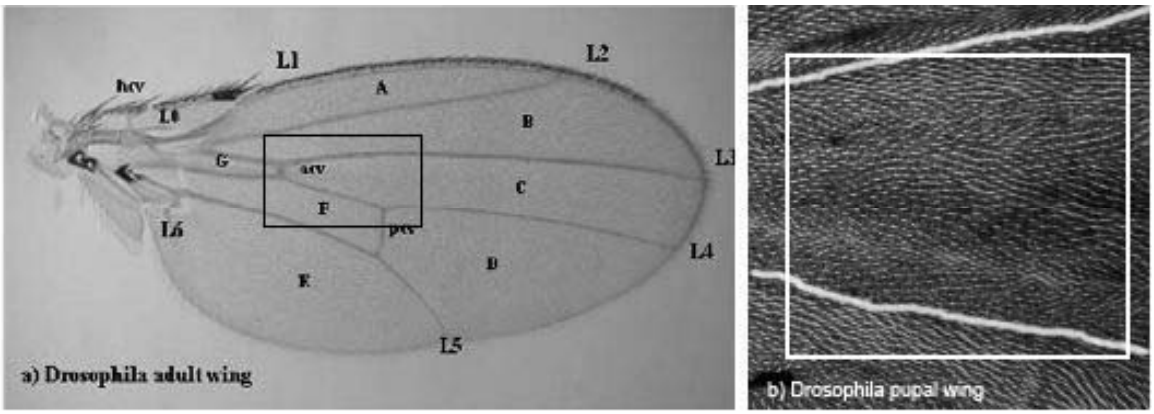

Figure 3.2: *ptc-Gal4* expression domain in the *Drosophila* wing. (a)*Drosophila* adult wing is marked with different veins (L1-L5) and cross veins (acv and pcv). *ptc-Gal4* expression is in between veins L3 and L4 and it is strongest proximally. The black box in (a) shows the region in which all adult wing images are taken (b) *Drosophila* pupal wing is marked with a white box to denote the strongest *ptc-Gal4* expressing domain similar to adult wing region. All adult and pupal wing images were taken at the same region of the wing.

Males of UAS RNAi lines were crossed to virgin females carrying wing specific driver *MS1096-GAl4*. The progeny was reared in 29ºC to get the maximum knockdown of the gene by RNAi (Brand and Perrimon, 1993) (Fig 3.1). Adult wings of the males of the F1 generation were then scored for multiple hairs and other polarity related phenotypes. Similarly UAS RNAi lines were crossed to *MS1096-GAl4; UAS-Dcr2* to check increase in the phenotype previously found and *ptc-GAl4; UAS-Dcr2* for the pupal wing screening under similar conditions (Fig 3.1).

Results:

Results of adult wing screen in *Drosophila*:

For the adult wing screen, I hypothesised that genes which interact with Mwh to form a single distal trichome should also mimic (although not necessarily) the multiple hairs phenotype in the wing. Lines which gave multiple hairs phenotype after crossing to *MS1096-GAl4* were identified. These lines vary in frequency of cells with the phenotype, number of hairs per cell, and the presence or absence of defects in cell size/number, which is likely to reflect a cell division defect, rather than a PCP defect (Adler, 1995).

Source of RNAi lines	Total number of RNAi lines screened in the adult wing	Total number of RNAi lines screened in the pupal wing
VDRC	125	85
NIG	100	55
KK (VDRC)	51	32

Table 3.1: The total number of RNAi lines (from various sources), which were screened in the adult and pupal wing of *Drosophila melanogaster*.

All these lines with multiple hairs were then scored under a bright field microscope to quantitate the number of multiple hairs present in them and categorised into three different groups, viz. lines exhibiting 1. Weak multiple hairs (<10 multiple wing hairs per wing), 2. Intermediate multiple hairs (10-30 multiple wing hairs per wing), and 3. Strong multiple hairs (>30 multiple wing hairs per wing) (Table 3.2, Figure 3.2).

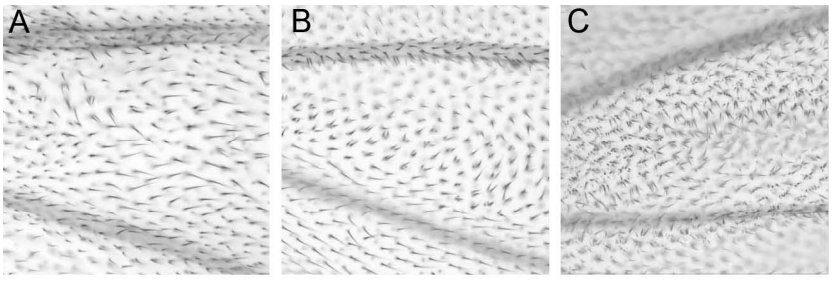

Figure 3.3: Classification of RNAi lines based on their multiple hairs phenotype found in the adult wing screening of *Drosophila*. Based on total number of multiple hairs present lines were categorised into (A) weak (containing <10 multiple wing hairs /wing), (B) medium (containing 10-30 multiple wing hairs /wing), and (C) strong (containing >30 multiple wing hairs /wing).

Phenotypes found	Number of each phenotype
Weak multiple hair phenotype	52
Medium multiple hair phenotype	21
Strong multiple hair phenotype	25
Hair morphology defects	18
No wing development	9
Nonscorable phenotype	20

Table3.2: Raw data of phenotypes found in the adult wing screening of *Drosophila.*

Additionally, some of the RNAi lines were found to give hair morphology defects such as thin and wavy trichomes compared to wild type trichomes as well as stumpy trichomes or trichomes with abnormal polarity (Table 3.2, Figure 3.4). A small percentage of the RNAi lines when crossed to either of the drivers gave non-scorable wings (curly or badly disrupted wing) or exhibited no wing development in my screen (Table 3.2, Figure 3.4) and were not considered for further analysis. The fly strain *MS1096> w^{1118}* was used as a negative control as each wing cell in *MS1096> w^{1118}* produces a single distally pointed trichome (Figure 3.3) and *MS1096> CG13913IR* (gene encoding *mwh*) was used as a positive control as wing cells in this line produce more than three to five trichomes with altered polarity (Figure 3.3).

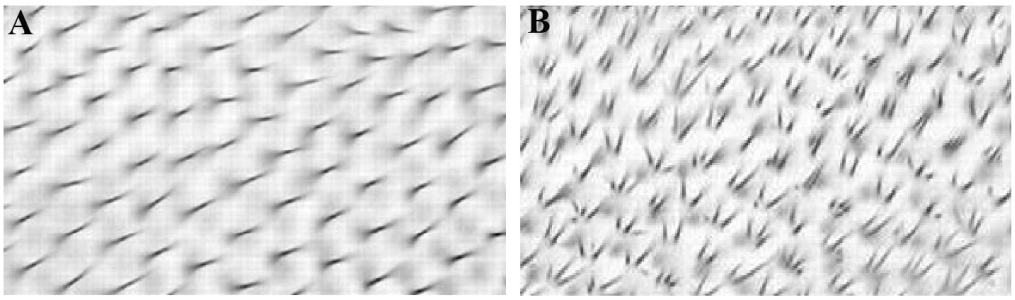

Figure 3.4: Controls used in the adult wing RNAi screening. A) w^{1118} where each wing cell produces a single trichome was used as a negative control and B) CG13113-IR (gene encoding Mwh) each wing cell produces more than three to five trichomes was used as a positive control.

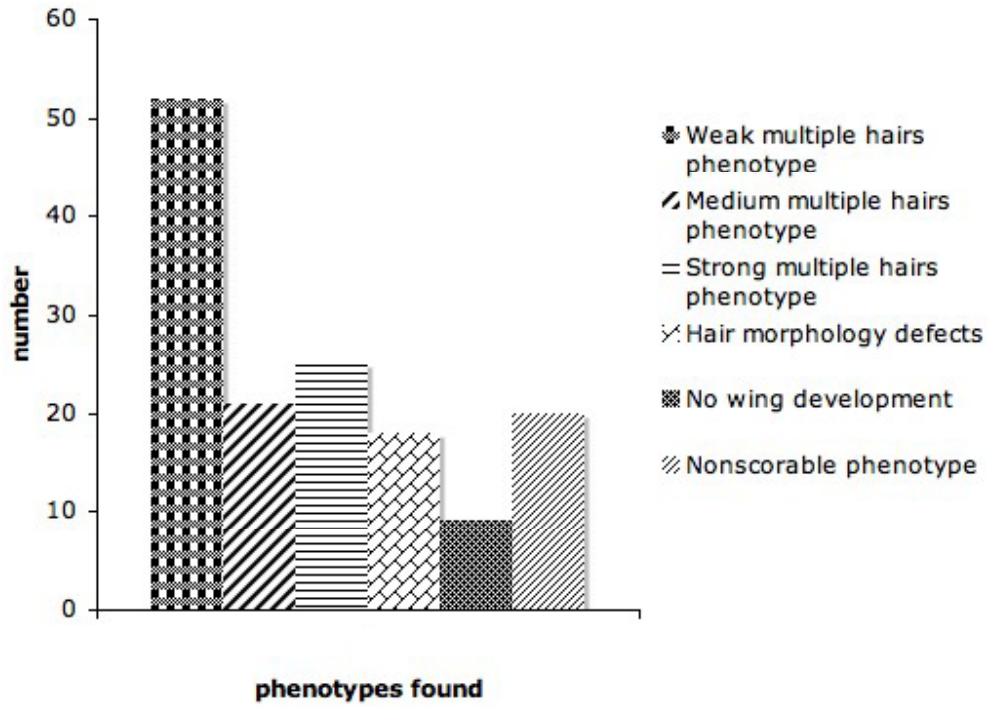

Figure 3.5: Bar graph representing the scores of different phenotypes found in the adult wing screening when RNAi lines were crossed with *ptcGal4, UAS dcr*^{2} and adult wings were scored for different phenotype. X-axis of the graph represents different types of phenotypes found and Y-axis of the graph represents number of total RNAi lines corresponding to each phenotype.

Line Name	Gene Name	CG number	Adult wing phenotype found
937	ed	CG12676	Weak mwh phenotype
938	ed	CG12676	Medium mwh phenotype
1021	Fur2	CG18734	Weak mwh phenotype, wings short and notching present
1128	CG31431	CG31431	Medium mwh phenotype
2824	Tsp29Fb	CG9496	Weak mwh phenotype
2907	aPKC	CG10261	Weak mwh phenotype
3336	SP1029	CG11956	Weak mwh phenotype
3339	MESR3	CG15162	Weak mwh phenotype
6168	CG15060	CG15060	Medium mwh phenotype
7769	cno	CG2534	Medium mwh phenotype
9210	CG7394	CG7394	Weak mwh phenotype
9241	dco	CG2048	Weak mwh phenotype, hair swirl
9265	ck	CG7595	Strong mwh phenotype
11791	pnut	CG8705	Strong mwh phenotype
12555	d	CG31610	Weak mwh phenotype, some hair swirling. Wings short
12830	CG14375	CG14375	Strong mwh phenotype
12834	ARP-like	CG7013	Medium mwh phenotype, weak hair swirls
13145	Rab23	CG2108	Strong hair swirls, medium mwh phenotype
13147	Rab23	CG2108	Strong hair swirls, medium mwh phenotype
13872	CG15650	CG15650	Strong hair swirls, medium mwh phenotype
14537	CG3588	CG3588	Weak mwh phenotype

Line Name	Gene Name	CG number	Adult wing phenotype found
15369	CG2016	CG2016	Medium mwh phenotype
15494	CG12416	CG12416	Medium mwh phenotype
15495	CG12416	CG12416	Medium mwh phenotype
15636	CG9772	CG9772	Strong multiple hairs
16434	CG16734	CG16734	Medium multiple wing hairs, wings uneven
17517	CG14395	CG14395	Medium mwh phenotype. Wings not flat enough to score polarity
17760	stg	CG1395	Strong multiple wing hairs. Wings small
18492	Cip4	CG15015	Strong mwh phenotype
18553	CG34401	CG34401	Weak multiple hairs, absent, small or misoriented hairs
18554	CG34401	CG34401	Weak multiple hairs, patchy loss of wing hairs.
18754	sub	CG12298	Weak mwh phenotype
19241	Mst36Fb	CG31791	Weak mwh phenotype
19529	l(1)G0237	CG1558	Weak mwh phenotype, also hair morphology defects.
19658	Spn	CG16757	Weak mwh phenotype, stronger swirl than normal below vein 4
20518	dia	CG1768	Strong mwh phenotype, cells large
20705	CG18818	CG18818	Medium mwh phenotype, also loss of some margin bristles
21177	CG30440	CG30440	Medium mwh phenotype
21178	CG30440	CG30440	Medium mwh phenotype
21344	CG31436	CG31436	Medium mwh phenotype, also hair morphology defect
21908	SCAR	CG4636	Weak mwh phenotype. Weak hair swirls with MS1096/29˚C
22207	Hem	CG5837	Medium mwh phenotype
22671	Rme-8	CG8014	Medium mwh phenotype, wings more swirly than normal below vein 4,
24107	l(1)G0222	CG8465	Strong multiple wing hairs and swirls
24253	CG8239	CG8239	Weak mwh phenotype
24254	CG8239	CG8239	Medium mwh phenotype
24740	E(bx)	CG32478	Medium mwh/hair morphology defect
25707	epsin-like	CG31170	Strong mwh phenotype
25709	epsin-like	CG31170	Strong mwh phenotype
26003	gish	CG6963	Strong mwh phenotype
26019	Src42A	CG6873	Weak mwh phenotype
26367	CG4030	CG4030	Medium mwh phenotype
26413	Sep2	CG4173	Medium mwh phenotype
26548	Arpc3A	CG4560	Strong mwh phenotype
26549	Arpc3A	CG4560	Strong mwh phenotype
27566	Lrr47	CG6098	Strong mwh phenotype
27503	stau	CG5753	Strong mwh phenotype
27578	fl(2)d	CG6315	Weak mwh phenotype
27984	CG7371	CG7371	Weak mwh phenotype
28243	Cam	CG8472	Strong mwh phenotype
28347	Kul	CG1964	Strong mwh phenotype
28971	CG8878	CG8878	Strong mwh phenotype
29239	pncr003:2L	CR31696	Weak mwh phenotype
29943	Arp14D	CG9901	Strong mwh phenotype
29944	Arp14D	CG9901	Strong mwh phenotype
30046	CG14135	CG14135	Weak mwh phenotype
31120	CG12065	CG12065	Medium mwh phenotype
31121	CG12065	CG12065	Medium mwh, cells larger
31329	neb	CG10718	Weak mwh phenotype

Line Name	Gene Name	CG number	Adult wing phenotype found
31330	neb	CG10718	Weak mwh phenotype
33486	Myo10A	CG2136	Weak mwh phenotype
33968	CG31559	CG31559	Strong Multiple/split hairs, hair morphology defect
34788	Mo25	CG4083	Strong Multiple wing hairs, hair morphology defect?
34789	Mo25	CG4083	Strong Multiple/split hairs, hair morphology defect
34908	Sra-1	CG4931	Strong mwh phenotype
35029	ari-1	CG5659	Scattered cells with weak multiple wing hairs
35132	CG6897	CG6897	Strong mwh phenotype
35212	CG7358	CG7358	Weak mwh phenotype
35772	CG34401	CG17757	Patchy loss of trichomes
35794	SIP1	CG30173	Strong mwh phenotype
35988	trc	CG8637	Strong mwh phenotype
36424	CG6434	CG6434	Weak mwh phenotype
37530	Myo10A	CG2136	Medium Mwh, also hair morphology defect
37534	jar	CG5695	Some multiple wing hairs/hair morphology defect (hairs wavy).
39166	CG32235	CG32235	Medium mwh, not flat enough to score polarity
39591	ari-1	CG5659	Scattered cells with multiple wing hairs
39864	CG15072	CG15072	Weak hair swirls
39893	CG1890	CG1890	Weak mwh phenotype
39894	CG1890	CG1890	Weak mwh phenotype
41854	CG6945	CG6945	Medium Multiple wing hairs/hair morphology defect
41875	dlt	CG32315	Strong Multiple wing hairs, mostly posterior to L5
41876	dlt	CG32315	Strong mwh phenotype
42677	CG3655	CG3655	Medium multiple wing hairs
42978	CG12124	CG12124	Scattered multiple wing hairs on 1 wing, rare mwh on other wings
4312	ds	CG17941	Proximal hair swirls in some wings. Wings broad/short, some loss of cross veins
43987	CG6327	CG6327	Weak mwh phenotype
45013	Arc-p34	CG10954	Weak mwh phenotype
45257	CG8260	CG8260	Mwh and swirls in some wings? Or wings not flat
45402	sub	CG12298	Medium mwh phenotype
45550	CG5360	CG5360	Weak mwh phenotype
45939	CalpC	CG3692	Weak multiple wing hair phenotype, second hair often short
47000	qm	CG8593	Weak multiple wing hair phenotype, some loss of margin bristles
47001	qm	CG8593	Strong multiple wing hair phenotype, some loss of margin bristles
47274	CG17754	CG17754	Very weak mwh phenotype
47298	sls	CG1915	Hair swirling and multiple wing hairs (poorly viable, only 1 wing)
48042	CG8924	CG8924	Very weak mwh phenotype
48631	CG11555	CG11555	Strong Multiple wing hairs/hair morphology defect
48653	CG1518	CG1518	Proximal mwh/some split hairs, also some swirling?
50780	CG13802	CG13802	Weak mwh phenotype
10105R-2	Sin1	CG10105	Medium mwh phenotype
10105R-3	Sin1	CG10105	Weak mwh phenotype
10336R-4	CG10336	CG10336	Weak mwh phenotype
10591R-4	CG10591	CG10591	Weak multiple wing hair phenotype
10954R-1	Arc-p34	CG10954	Weak mwh phenotype
10667R-1	Orc1	CG10667	Multiple wing hairs, also loss or duplication of margin bristles

Line Name	Gene Name	CG number	Adult wing phenotype found
10667R-3	Orc1	CG10667	Multiple wing hairs, also loss or duplication of margin bristles
11084R-1	pk	CG11084	Strong swirls, especially on ventral wing surface
11084R-2	pk	CG11084	Strong swirls, especially on ventral wing surface
11207R-1	feo	CG11207	Strong mwh phenotype
11207R-2	feo	CG11207	Weak mwh phenotype
11448R-4	CG11448	CG11448	Weak mwh phenotype
11621R-2	Pi3K68D	CG11621	Weak mwh phenotype
11753R-1	CG11753	CG11753	Strong mwh phenotype
11753R-3	CG11753	CG11753	Moderate mwh phenotype
11895R-1	stan	CG11895	Strong swirls
11895R-3	stan	CG11895	Strong swirls
12091R-3	CG12091	CG12091	Strong mwh phenotype
12135R-2	c12.1	CG12135	Strong mwh phenotype
12135R-4	c12.1	CG12135	Strong mwh phenotype
12298R-2	sub	CG12298	Weak mwh phenotype
12298R-3	sub	CG12298	Weak mwh phenotype
12306R-3	polo	CG12306	Some multiple wing hairs, wings small (loss of anterior)
1288R-2	CG1288	CG1288	Medium mwh phenotype
1288R-3	CG1288	CG1288	Weak mwh phenotype
12964R-1	CG12964	CG12964	Scattered cells with multiple wing hairs
13436R-2	CG13436	CG13436	Weak mwh phenotype
1395R-1	stg	CG1395	Strong mwh phenotype. Wings small
1395R-2	stg	CG1395	Strong mwh phenotype. Wings small
1463R-2	CG1463	CG1463	Weak mwh phenotype
15015R-2	Cip4	CG15015	Strong mwh phenotype
15015R-3	Cip4	CG15015	Strong mwh phenotype
15064R-2	Him	CG15064	Weak mwh phenotype
1512R-3	cul-2	CG1512	Weak mwh phenotype
16734R-2	CG16734	CG16734	Medium Mwh phenotype
16734R-3	CG16734	CG16734	Medium mwh phenotype
16757R-2	Spn	CG16757	Strong mwh in 1/6 wings
16894R-1	CG16894	CG16894	Weak mwh phenotype
16894R-2	CG16894	CG16894	Weak mwh phenotype
17282R-3	CG17282	CG17282	Proximal hairs swirl, and multiple wing hairs
17299R-1	SNF4Agamma	CG17299	Swirls, particularly distal to pcv
17565R-2	CG17565	CG17565	Strong swirl distally below vein 4
1768R-1	dia	CG1768	Strong mwh phenotype. Wings small
17985R-4	CG17985	CG17985	Weak mwh phenotype
18468R-3		GA14945	Weak mwh phenotype
1964R-2	Kul	CG1964	Strong mwh phenotype
1964R-3	Kul	CG1964	Strong mwh phenotype, also hair morphology defect
2048R-1	dco	CG2048	Hair swirls on vein 3
2136R-1	Myo10A	CG2136	Strong Mwh phenotype, also hair morphology defect
2160R-3	Socs44A	CG2160	Weak mwh phenotype
2534R-2	cno	CG2534	Medium mwh phenotype
2615R-1	ik2	CG2615	Weak hair swirls
2621R-1	sgg	CG2621	Medium mwh phenotype
2837R-1	CG2837	CG2837	Small wings with multiple wing hairs
31049R-1	Doa	CG33553	Medium mwh phenotype
31559R-3	CG31559	CG31559	Some mwh, also hair morphology defect
31960R-1	CG31960	CG31960	Weak multiple wing hair phenotype
32087R-1	CG32087	CG32087	Weak mwh phenotype

Line Name	Gene Name	CG number	Adult wing phenotype found
32087R-3	CG32087	CG32087	Strong mwh phenotype
3492R-2	CG3492	CG3492	Weak mwh phenotype in some wings
3533R-3	uzip	CG3533	Medium mwh phenotype
3588R-3	CG3588	CG3588	Medium mwh phenotype
4083R-1	Mo25	CG4083	Strong mwh phenotype.
4083R-4	Mo25	CG4083	Medium mwh phenotype
4129R-1	l(1)G0045	CG32763	Weak multiple wing hair phenotype between v3 and v4.
4140R-2	CG4140	CG4140	Proximal mwh in some wings, also swirls?
4140R-3	CG4140	CG4140	Proximal mwh in some wings, also swirls?
4173R-3	Sep2	CG4173	Medium mwh phenotype
4636R-2	SCAR	CG4636	Medium mwh phenotype
4931R-1	Sra-1	CG4931	Weak mwh phenotype
4931R-2	Sra-1	CG4931	Strong mwh phenotype
5360R-1	CG5360	CG5360	Wings small and uneven. Multiple wing hairs
5360R-3	CG5360	CG5360	Some cells with mwh, margin bristle defects
5514R-1	CG5514	CG5514	Weak multiple wing hairs
5543R-2	CG5543	CG5543	Multiple wing hairs. Wings too Cy to tell if hairs swirl
5854R-2	CG5854	CG5854	Weak multiple wing hair phenotype. Wings slightly crumpled/blistered
5973R-1	CG5973	CG5973	Weak mwh phenotype
6163R-2	CG6163	CG6163	Multiple wing hairs, hairs thin/spindly, may also swirl?
6434R-1	CG6434	CG6434	Weak multiple wing hair phenotype, hairs also short
6963R-1	gish	CG6963	Strong mwh phenotype
6963R-3	gish	CG6963	Strong mwh phenotype
7058R-3	CG7058	CG7058	Weak mwh phenotype
7305R-2	Rim	CG33547/ CG7305	Most wings blistered/crumpled. Mounted females - in most severe see wing margin defects and swirls below vein 4
7830R-1	CG7830	CG7830	Weak mwh phenotype
7830R-3	CG7830	CG7830	Weak mwh phenotype
7838R-1	Bub1	CG7838	Weak mwh phenotype, also hair morphology defect
7855R-2	timeout	CG7855	Weak mwh phenotype
8569R-2	CG8569	CG8569	Weak multiple wing hair phenotype. Wings uneven
8637R-1	trc	CG8637	Strong mwh phenotype
8637R-2	trc	CG8637	Strong mwh phenotype
8683R-1	CG8683	CG8683	Weak multiple wing hair phenotype.
8683R-2	CG8683	CG8683	Moderate multiple wing hair phenotype
8929R-2	CG8929	CG8929	Weak multiple wing hair phenotype.
9210R-2	Ac13E	CG9210	Weak multiple wing hair phenotype, hairs not straight
9699R-2	CG9699	CG9699	5 wings wild type, one wing fluid-filled with some mwh
9774R-3	rok	CG9774	Strong mwh phenotype. Wings too short/ballooned to score polarity
9819R-1	CanA-14F	CG9819	Swirls and medium multiple wing hairs
Baz xMax	baz	CG5055	Weak hair swirls

Table 3.3: Result of adult wing screening in the *Drosophila*. RNAi lines were crossed with *MS1096-Gal4; UASDdcr2* and scored for multiple hairs.

The RNAi lines, which were found to produce intermediate to strong, multiple hairs were cross-referenced in Fly Base (FB2011_02, released February 18th, 2011) for their corresponding gene ontologies and were classified into different

categories (Figure 3.5). A considerable percentage of RNAi lines that gave a multiple hair phenotype were categorized into the cell division and cytoskeleton related categories (Figure 3.5). Previous study indicates that a large cell can also produce multiple hairs, independent of PCP function (Adler *et al.,* 2000). These multiple hairs normally arise due to splitting of a single hair early in development or due to cytokinesis defects. A large number of RNAi lines were found to belong in actin binding and cytoskeleton regulation. Along with these various other categories of RNAi lines were also found. Some of the genes were found to belong in different overlapping categories, which are shown in the bargraph of proportion below (Figure 3.5).

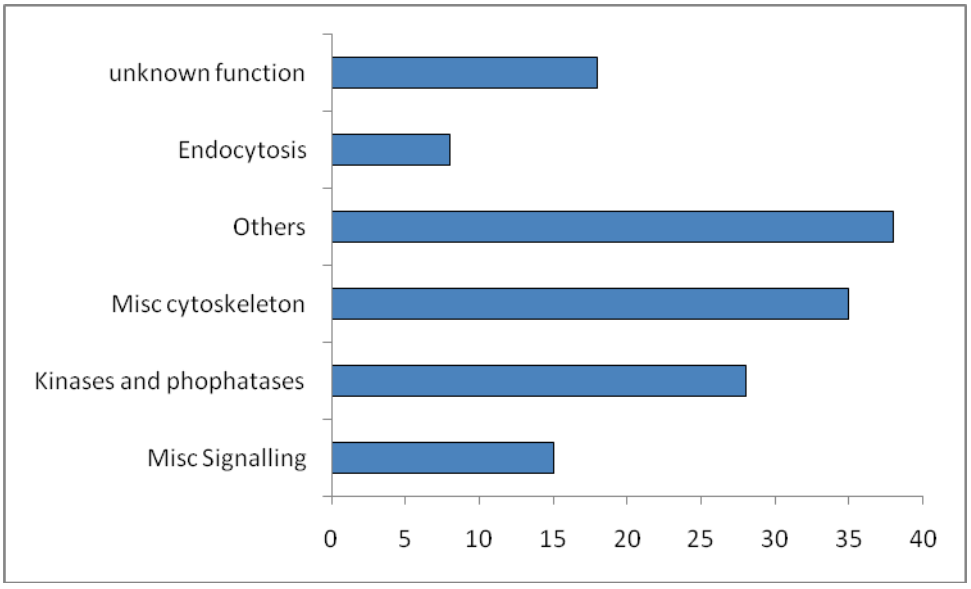

Figure 3.6: Bar chart of proportion representing gene ontologies found (Fly Base) for each RNAi line causing multiple hair phenotypes. Some of the genes overlap to more than one category. X-axis of the graph represents % of RNAi lines belonging to each category and Y-axis of the graph represents different categories found.

Drosophila pupal wing screening:

RNAi lines exhibiting intermediate to strong multiple hair phenotypes in the adult wing were short listed for pupal wing screening. I hypothesised that if a gene interacts with Mwh, knock down of its mRNA/protein by RNAi may be able to produce a change in Mwh protein level (either by increasing or by decreasing it) or

its localisation in the *ptc-Gal4* expressing region which can be easily seen in the pupal wing by immunostaining.

As Mwh protein localises to the apicoproximal region of the wing cell immediately before trichome formation (27 hrs APF at 29ºC) (Strutt and Warrington, 2008; Yan *et al.,* 2008), I tried to look at Mwh localisation in the wing at 27 hrs APF. RNAi lines were crossed with *ptc-Gal4, UAS- Dcr2* and immunostained for Mwh to monitor effects of the knockdown of different mRNAs and the corresponding proteins using different inverted repeats (IRs) on Mwh protein localisation. Along with Mwh, phalloidin and Armadillo were also done to observe the trichomes and the adherens junctions respectively. *ptc> w*^{1118} and *ptc>CG13913* (gene encoding Mwh) were used as negative and positive controls respectively (Figure 3.6).

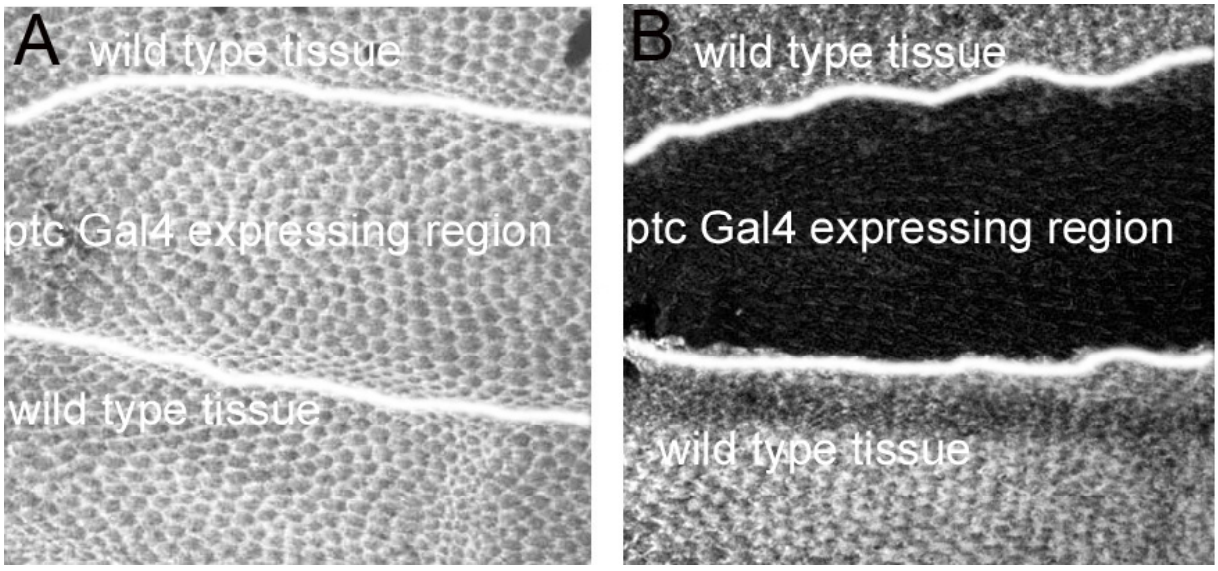

Figure 3.7: Controls used in the pupal wing RNAi screen. A) *w*^{1118} was crossed with *ptc-Gal4, UAS-Dcr2* and stained with Mwh antibody. Mwh protein localisation was looked at in the region of L3 and L4 (marked by white line) and no change in Mwh protein localisation was found as compared to wild type tissue (marked) above and below the *Gal4* expressing region and B) *CG13113* (gene encoding Mwh) was crossed with *ptc- gAl4, UAS-Dcr2* and stained with Mwh antibody. Mwh protein localisation was looked at in the region of L3 and L4 (marked by white line), and it was found to be reduced as expected.

Line Name	Gene Name	CG number	Pupal wing phenotype found
937	ed	CG12676	Wild type phenotype
938	ed	CG12676	In some wings large cells are present near the vein 4 with patchy loss of Mwh
1021	Fur2	CG18734	Normal distribution of Armadillo and Mwh antibody, trichomes normal
1128	CG31431	CG31431	Normal distribution of Armadillo and Mwh antibody, trichomes normal
2824	Tsp29Fb	CG9496	Reduction of Mwh antibody, trichomes formation delayed proximally
2907	aPKC	CG10261	Normal distribution of Armadillo and Mwh antibody, trichomes normal
3336	SP1029	CG11956	Normal distribution of Armadillo and Mwh antibody, trichomes normal
3339	MESR3	CG15162	Normal distribution of Armadillo and Mwh antibody, trichomes normal
6168	CG15060	CG15060	Cells are sick near the ptc region, no trichome development.
7769	cno	CG2534	Trichome morphology defect
9210	CG7394	CG7394	Normal distribution of Armadillo and Mwh antibody, trichomes normal
9241	dco	CG2048	Delay in trichome formation, Mwh appears normal at later time point
9265	ck	CG7595	Trichome morphology defect, trichomes are short and stumpy
11791	pnut	CG8705	Cells are slightly larger, Mwh seems to be increased
12555	d	CG31610	Inconsistent results, sometimes showing a delay in trichome formation; not reproducible
12830	CG14375	CG14375	Large cells with multiple hairs
12834	ARP-like	CG7013	Slight reduction of Mwh antibody localisation.
13145	Rab23	CG2108	Slight reduction of Mwh antibody localisation.
13147	Rab23	CG2108	Strong reduction of Mwh antibody localisation.
13872	CG15650	CG15650	Results are variable, sometimes *ptc* region looks a bit sick, and multiple hairs.
14537	CG3588	CG3588	Not done as multiple hair phenotype was very weak
15369	CG2016	CG2016	Normal distribution of Armadillo and Mwh antibody
15494	CG12416	CG12416	Not done
15495	CG12416	CG12416	Normal distribution of Armadillo and Mwh antibody
15636	CG9772	CG9772	Large cells with multiple hairs
16434	CG16734	CG16734	Cells look sick and larger at the ptc region
17517	CG14395	CG14395	Delay in trichome formation, Mwh appears normal
17760	stg	CG1395	Large cells with multiple hairs
18492	Cip4	CG15015	Normal distribution of Armadillo and Multiple wing hairs antibody, trichomes normal
18553	CG34401	CG34401	Delay in trichome formation and Mwh reduction
18554	CG34401	CG34401	Delay in trichome formation and Mwh reduction
18754	sub	CG12298	Not done.
21177	CG30440	CG30440	Normal distribution of Armadillo and Mwh antibody
21178	CG30440	CG30440	Normal distribution of Armadillo and Mwh antibody
21344	CG31436	CG31436	Normal distribution of Armadillo and Mwh antibody
21908	SCAR	CG4636	Normal distribution of Armadillo and Mwh antibody, trichomes normal
22207	Hem	CG5837	Very weak reduction of Mwh antibody
22671	Rme-8	CG8014	Mwh localisation to the cell is abnormal
24107	l(1)G0222	CG8465	Large cells with multiple hairs
24253	CG8239	CG8239	Normal distribution of Armadillo and Mwh antibody, trichomes normal
24254	CG8239	CG8239	Normal distribution of Armadillo and Mwh antibody
24740	E(bx)	CG32478	Large cells with multiple hairs
25707	epsin-like	CG31170	Weak reduction of Mwh, slightly larger cells
25709	epsin-like	CG31170	weak reduction of Mwh, slightly larger cells
26003	gish	CG6963	Normal distribution of Armadillo and Mwh antibody, trichomes multiple
26019	Src42A	CG6873	Normal distribution of Armadillo and Mwh antibody
26367	CG4030	CG4030	Normal distribution of Armadillo and Mwh antibody
26413	Sep2	CG4173	Variable result, occasionally stripe of large cells, normal distribution of Mwh antibody.

Line Name	Gene Name	CG number	Pupal wing phenotype found
26548	Arpc3A	CG4560	Delay in trichome formation, abnormal morphology of trichomes
26549	Arpc3A	CG4560	Delay in trichome formation, abnormal morphology of trichomes
27566	Lrr47	CG6098	Large cells with multiple hairs
27503	stau	CG5753	Increase in Mwh antibody in the ptc expressing region, slightly large cells
27578	fl(2)d	CG6315	Not done.
27984	CG7371	CG7371	Not done.
28243	Cam	CG8472	Not done.
28347	Kul	CG1964	Normal distribution of Armadillo and Mwh antibody
28971	CG8878	CG8878	Large cells with multiple hairs
29239	pncr003: 2L	CR31696	Not done.
29943	Arp14D	CG9901	Normal distribution of Armadillo and Mwh antibody
29944	Arp14D	CG9901	Delay in trichome formation and Mwh reduction
30046	CG14135	CG14135	Not done.
31120	CG12065	CG12065	Large cells with multiple hairs
31121	CG12065	CG12065	Not done.
31329	neb	CG10718	Not done.
31330	neb	CG10718	Not done.
33486	Myo10A	CG2136	Normal distribution of Armadillo and Mwh antibody
33968	CG31559	CG31559	More images needed
34788	Mo25	CG4083	More images needed
34789	Mo25	CG4083	More images needed
34908	Sra-1	CG4931	Slightly larger cells with multiple hairs
35029	ari-1	CG5659	More images needed
35132	CG6897	CG6897	Large cells with multiple hairs
35212	CG7358	CG7358	Not done.
35772	CG34401	CG17757	Need more images
35794	SIP1	CG30173	Need more images
35988	trc	CG8637	Slight reduction of Mwh antibody localisation.
36424	CG6434	CG6434	Not done.
37530	Myo10A	CG2136	Trichome morphology defect, trichomes are extremely thin and wavy
37534	jar	CG5695	Normal distribution of Armadillo and Mwh antibody
39166	CG32235	CG32235	Need more images
39591	ari-1	CG5659	Slight increase of Mwh in some wings
39864	CG15072	CG15072	Slight increase of Mwh
39893	CG1890	CG1890	Need more images
39894	CG1890	CG1890	Not done.
41854	CG6945	CG6945	Normal distribution of Armadillo and Mwh antibody, trichomes normal
41875	dlt	CG32315	Increase in Mwh antibody in the ptc expressing region, slightly large cells
41876	dlt	CG32315	Large cells with multiple hairs and some increase of Mwh slightly
42677	CG3655	CG3655	Delay in trichome formation, Mwh appears normal at later time point
42978	CG12124	CG12124	Large cells with multiple hairs
4312	ds	CG17941	Not done.
43987	CG6327	CG6327	Normal distribution of Armadillo and Mwh antibody
45013	Arc-p34	CG10954	Normal distribution of Armadillo and Mwh antibody, trichomes normal
45257	CG8260	CG8260	Normal distribution of Armadillo and Mwh antibody, trichomes normal
45402	sub	CG12298	Cells occasionally look sick, normal Mwh localisaion
48631	CG11555	CG11555	Normal distribution of Armadillo and Mwh antibody, trichomes normal
48653	CG1518	CG1518	Large cells with multiple hairs
50780	CG13802	CG13802	Not done.
10105R-2	Sin1	CG10105	Normal distribution of Armadillo and Mwh antibody, trichomes normal
10667R-1	Orc1	CG10667	Large cells with multiple hairs
10667R-3	Orc1	CG10667	Need more images
11207R-1	feo	CG11207	Large cells with multiple hairs

Line Name	Gene Name	CG number	Pupal wing phenotype found
11207R-2	feo	CG11207	Large cells with multiple hairs
11753R-1	CG11753	CG11753	Delay in trichome formation and Mwh reduction
11753R-3	CG11753	CG11753	Normal distribution of Armadillo and Mwh antibody, trichomes normal
11895R-3	stan	CG11895	Not done.
12091R-3	CG12091	CG12091	Normal distribution of Armadillo and Mwh antibody, trichomes normal
12135R-2	c12.1	CG12135	Slight reduction of Mwh antibody localisation.
12135R-4	c12.1	CG12135	Slight reduction of Mwh antibody localisation.
12298R-2	sub	CG12298	Need more images
12298R-3	sub	CG12298	Need more images
12306R-3	polo	CG12306	Normal distribution of Armadillo and Mwh antibody, trichomes normal
1288R-2	CG1288	CG1288	Normal distribution of Armadillo and Mwh antibody, trichomes normal
1288R-3	CG1288	CG1288	Not done.
12964R-1	CG12964	CG12964	Normal distribution of Armadillo and Mwh antibody
13436R-2	CG13436	CG13436	Not done.
1395R-1	stg	CG1395	Large cells with multiple hairs
1395R-2	stg	CG1395	Large cells with multiple hairs
1463R-2	CG1463	CG1463	Not done.
15015R-2	Cip4	CG15015	Normal distribution of Armadillo and Mwh antibody, trichomes normal
15015R-3	Cip4	CG15015	Normal distribution of Armadillo and Mwh antibody, trichomes normal
15064R-2	Him	CG15064	Not done.
1512R-3	cul-2	CG1512	Not done.
16734R-2	CG16734	CG16734	Need more images
16734R-3	CG16734	CG16734	Need more images
16757R-2	Spn	CG16757	Normal distribution of Armadillo and Mwh antibody, trichomes normal
16894R-1	CG16894	CG16894	Not done.
16894R-2	CG16894	CG16894	Not done.
17282R-3	CG17282	CG17282	Large cells with multiple hairs
17299R-1	SNF4Agamma	CG17299	Not done.
17565R-2	CG17565	CG17565	Not done.
1768R-1	dia	CG1768	Large cells with multiple hairs
17985R-4	CG17985	CG17985	Not done.
18468R-3		GA14945	Not done.
1964R-2	Kul	CG1964	Slight reduction of Mwh antibody localisation.
1964R-3	Kul	CG1964	Slight reduction of Mwh antibody localisation.
2048R-1	dco	CG2048	Cells are sick and inconclusive.
2136R-1	Myo10A	CG2136	Trichome morphology defect, trichomes are extremely thin and wavy
2160R-3	Socs44A	CG2160	Normal distribution of Armadillo and Mwh antibody, trichomes normal
2534R-2	cno	CG2534	Cells are abnormal in shape in the ptc expressing region
2615R-1	ik2	CG2615	Normal distribution of Armadillo and Mwh antibody, trichomes normal
2621R-1	sgg	CG2621	Normal distribution of Armadillo and Mwh antibody, trichomes normal
2837R-1	CG2837	CG2837	Normal distribution of Armadillo and Mwh antibody, trichomes normal
31049R-1	Doa	CG33553	Weak reduction of Mwh antibody, occasional large cells
31559R-3	CG31559	CG31559	Need more images
31960R-1	CG31960	CG31960	Not done.
3533R-3	uzip	CG3533	Need more images
3588R-3	CG3588	CG3588	Crossed now
4083R-1	Mo25	CG4083	Reduction of Multiple wing hair antibody localisation.
4083R-4	Mo25	CG4083	Need more images
4129R-1	l(1)G0045	CG32763	Not done.
4140R-2	CG4140	CG4140	Normal distribution of Armadillo and Multiple wing hairs antibody, trichomes normal
4140R-3	CG4140	CG4140	Need more images

Line Name	Gene Name	CG number	Pupal wing phenotype found
4173R-3	Sep2	CG4173	Not done.
4636R-2	SCAR	CG4636	Normal distribution of Armadillo and Mwh antibody, trichomes normal
4931R-1	Sra-1	CG4931	Normal distribution of Armadillo and Mwh antibody, trichomes normal
4931R-2	Sra-1	CG4931	Normal distribution of Armadillo and Mwh antibody, trichomes normal
5360R-1	CG5360	CG5360	Normal distribution of Armadillo and Mwh antibody, trichomes normal
5360R-3	CG5360	CG5360	Normal distribution of Armadillo and Mwh antibody, trichomes normal
5514R-1	CG5514	CG5514	Not done.
5543R-2	CG5543	CG5543	Normal distribution of Armadillo and Mwh antibody, trichomes normal
5854R-2	CG5854	CG5854	Not done.
5973R-1	CG5973	CG5973	Not done.
6163R-2	CG6163	CG6163	Normal distribution of Armadillo and Mwh antibody, trichomes normal
6434R-1	CG6434	CG6434	Not done.
6963R-1	gish	CG6963	Normal distribution of Armadillo and Mwh antibody, trichomes multiple
6963R-3	gish	CG6963	Normal distribution of Armadillo and Mwh antibody, trichomes multiple
7058R-3	CG7058	CG7058	not done.
7305R-2	Rim	CG33547 / CG7305	Not done
7830R-1	CG7830	CG7830	Normal distribution of Armadillo and Mwh antibody, trichomes normal
7830R-3	CG7830	CG7830	Not done.
7838R-1	Bub1	CG7838	Normal distribution of Armadillo and Mwh antibody, trichomes normal
7855R-2	timeout	CG7855	Not done.
8569R-2	CG8569	CG8569	Not done.
8637R-1	trc	CG8637	Slight reduction of Mwh antibody localisation.
8637R-2	trc	CG8637	Slight reduction of Mwh antibody localisation.
8683R-1	CG8683	CG8683	not done.
8683R-2	CG8683	CG8683	Normal distribution of Armadillo and Mwh antibody, trichomes normal
8929R-2	CG8929	CG8929	not done.
9210R-2	Ac13E	CG9210	Large cells with multiple hairs in only two wings others are normal
9699R-2	CG9699	CG9699	Normal distribution of Armadillo and Mwh antibody, trichomes normal
9774R-3	rok	CG9774	Large cells with multiple hairs
9819R-1	CanA-14F	CG9819	Normal distribution of Armadillo and Mwh antibody, trichomes normal

Table 3.4: Result of pupal wing screening in the *Drosophila*. RNAi lines were crossed with *MS-1096 Gal4;UAS-Dcr2* and stained with Mwh, Phalloidin and armadillo to examine changes in Mwh localisation.

From the pupal wing screening RNAi lines were classified and put into different categories based on their respective phenotypes. The lines which were able to change the Mwh protein localisation either by increasing or by decreasing the total amount of Mwh protein in the *ptc-Gal4* expressing region were classified correspondingly as potential up regulators or down regulators of Mwh. However, these RNAi lines mostly gave a weak phenotype which could be due to incomplete knockdown of the gene by RNAi. It is also possible that the genes are not really having a strong effect in regulating Mwh localisation in the pupal wing. They were further validated with second set of independent RNAi lines from KK sources.

Besides these, I found some additional phenotypes such as abnormal trichome morphology, large cell phenotype and delay in the timing of trichome formation in this screen. Also a large number of RNAi lines produced wild type phenotype in the screen, which could be due to those lines being nonfunctional or having no effect in Mwh regulation. Redundancy of the gene corresponding the RNAi lines is also possible.

RNAi lines regulating Mwh localisation:

A) **Lines with reduced apical Mwh:**

Rab23, c12.1, kul, Tsp29Fb, Mo25, trc, CG14375, Manf, and *cip4* were able to reduce apical Mwh localisation in the pupal wing in the *ptc* expressing region (Table 3.5 and Figure 3.8). Lines that showed a reduction in Mwh amount are tabulated below (Table 3.5) along with their molecular function (based on Flybase), involvement in biological processes (based on Flybase) and phenotypes found.

Gene Name	**Line Name**	**Molecular function (Based on Flybase)**	**Involved in biological process (Based on Flybase)**	**Phenotypes seen in each line**
c12.1	12135R2/R3(NIG)	Unknown function	Mitotic spindle organization	Strongly reduces Mwh antibody localisation in the *ptc* expressing domain. Cells are variable in size.
kul	1964R2/R3(NIG)	metalloprotease	proteolysis	Weak decrease of Mwh antibody localisation in the *ptc* expressing domain. Strong multiple hairs phenotype seen.
Tsp29Fb	2824(GD)	unknown	unknown	Strongly reduces Mwh antibody localisation in the *ptc* expressing domain. Delay in trichome formation was also noted.

Gene Name	**Line Name**	**Molecular function (Based on Flybase)**	**Involved in biological process (Based on Flybase)**	**Phenotypes seen in each line**
Mo25	4083R1(NIG)	binding	Embryonic development via syncitial blastoderm	Strongly reduces Mwh antibody localisation in the *ptc* expressing domain. There was also a reduction of armadillo when crossed to *ptc-Gal4, UAS- Dcr2*
trc	8637R1/R2(NIG)	protein binding	bristle development; regulation of dendrite morphogenesis; dendrite morphogenesis; antennal morphogenesis; imaginal disc-derived wing morphogenesis; signal transduction; imaginal disc-derived wing hair organization.	Reduces Mwh antibody localisation in the *ptc* expressing domain. Strong multiple hairs phenotype seen
CG14375	12830(GD)	G-protein-coupled receptor binding.	Unknown	Reduces Mwh antibody localisation in the *ptc* expressing domain weakly.
Manf	12834(GD)	Unknown	neuron homeostasis; neuron projection development	Weak decrease of Mwh antibody localisation in the *ptc* expressing domain
Rab23	13147(GD)	GTPase activity	morphogenesis of a polarized epithelium	Strongest reduction of Mwh antibody localisation in the *ptc* expressing domain. Strong multiple hairs phenotype seen
Cip4	18492(GD)	Rho GTPase binding	wing hair organization; mesoderm	Weak decrease of Mwh antibody localisation in

			development	the *ptc* expressing domain. Strong multiple hairs phenotype seen

Table 3.5: Tabular representation of the genes which showed reduction in Mw localisation in the RNAi screening. Along with the genes, their CG number, ontology, function and phenotype found is also tabulated here..

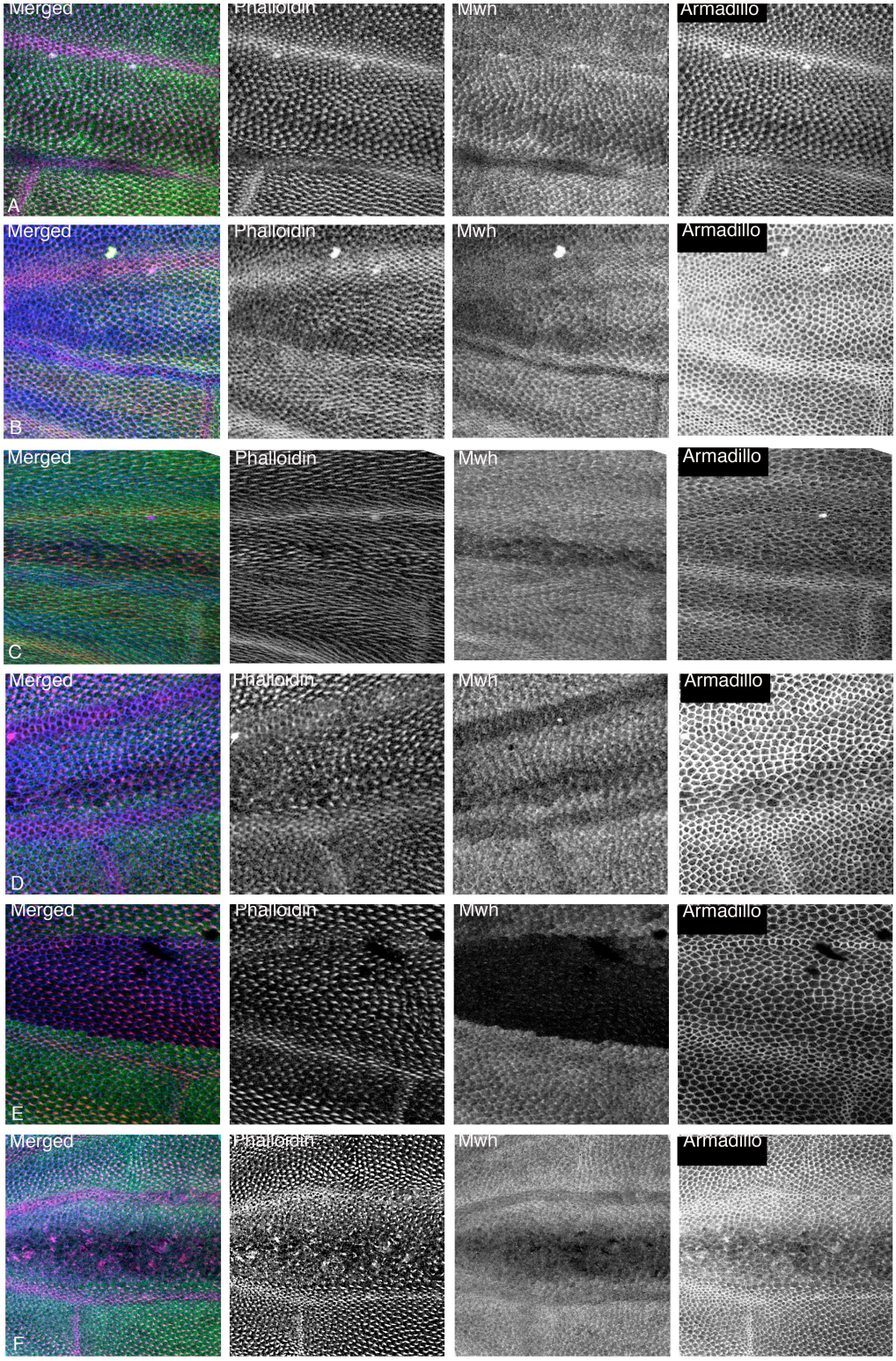

Figure 3.7: RNAi lines showing a reduction of Mwh localisation in the pupal wing in the *ptc* expressing region. Lines were crossed with *ptc-Gal4; UAS- Dcr2* and stained with phalloidin (first channel, red), Mwh (second channel, green) and Armadillo (third channel, blue) the region expressing RNAi and wild type tissues are marked in the Mwh channel. A) *ku*l B) *Tsp29F*b C) *c12.1,* D) *CG14375* E) *Rab23* and F) *Mo25* RNAi lines.

B) **Lines with increased apical Mwh:**

Similarly, I have found that *Formin3 (form3), staufen (stau), pnut, CanA14F, Rim, Furin 2(Fur2), CG12964, septin 2 (sep2), microtubule star (mts*), *dlt* and *CG8860* were able to increase the apical Mwh accumulation in the pupal wing in the *ptc* expressing region (Table 3.6, Figure 3.9-10). Lines that showed an increase in Mwh amount are tabulated below (Table 3.6) along with their molecular function (based on Flybase), involvement in biological processes (based on Flybase) and phenotypes found.

Gene Name	**Line Name**	**Molecular function (Based on Flybase)**	**Involved in biological process (Based on Flybase)**	**Phenotypes seen in each line**
Rim	7305R2(NIG)	small GTPase regulator activity	Regulation of exocytosis; synaptic vesicle exocytosis	Weak increase of Mwh antibody localisation in the *ptc* expressing domain
CanA14F	9819R1(NIG)	protein serine/threonine phosphatase activity	Positive regulation of NFAT protein import into nucleus	Increases Mwh antibody localisation in the *ptc* expressing domain. Trichomes gave a swirly phenotype.
CG12964	12964R1(NIG)	Unknown	Unknown	Weak increase of Mwh antibody localisation in the *ptc* expressing domain
Fur2	1021(GD)	serine-type endopeptidase activity	proteolysis	Weak increase of Mwh antibody localisation in the *ptc* expressing domain. Delay in trichome formation.

Gene Name	**Line Name**	**Molecular function (Based on Flybase)**	**Involved in biological process (Based on Flybase)**	**Phenotypes seen in each line**
pnut	11791(GD)	actin binding; ubiquitin protein ligase binding; microtubule binding; GTPase activity	cytokinesis; positive regulation of apoptosis	Increases Mwh antibody localisation in the *ptc* expressing domain. Cell size large.
Sep2	26413(GD)	protein binding; GTPase activity	cytokinesis	Strongly increases Mwh antibody localisation in the *ptc* expressing domain. Multiple trichomes.
stau	27503(GD)	mRNA 3'-UTR binding	pole plasm protein localization; regulation of pole plasm oskar mRNA localization; long-term memory; anterior/posterior axis specification,	Strongly increases Mwh antibody localisation in the *ptc* expressing domain. Multiple trichomes are also present.
mts	37917(GD)	phosphatase regulator activity; protein serine/threonine phosphatase activity	cell cycle; organelle organization; cell cycle process; biological regulation; anatomical structure development; microtubule cytoskeleton organization; regulation of developmental process; chromosome segregation;	Strongly increases Mwh antibody localisation in the *ptc* expressing domain. Multiple hairs and large cells are also seen.

			response to light stimulus; macromolecule modification; establishment or maintenance of cell polarity; localization; reproductive process in a multicellular organism; signaling pathway; actin based process	
CG8260	45257(GD)	Unknown	Unknown	Increases Mwh antibody localisation in the *ptc* expressing domain
dlt	41875/41876(GD)	Unknown	S phase of mitotic cell cycle; olfactory behavior; cellular process; imaginal disc morphogenesis; regulation of cell proliferation	Increases Mwh antibody localisation in the *ptc* expressing domain
Formin3	28437(GD)	actin binding	Branch fusion, open tracheal system	Increases Mwh antibody localisation in the *ptc* expressing domain, although no multiple hairs were seen.

Table 3.6: Tabular representation of the genes which showed increase in Mwh localisation in the RNAi screening. Along with the genes, their CG number, ontology, function (Fly base) and phenotype found is also tabulated here.

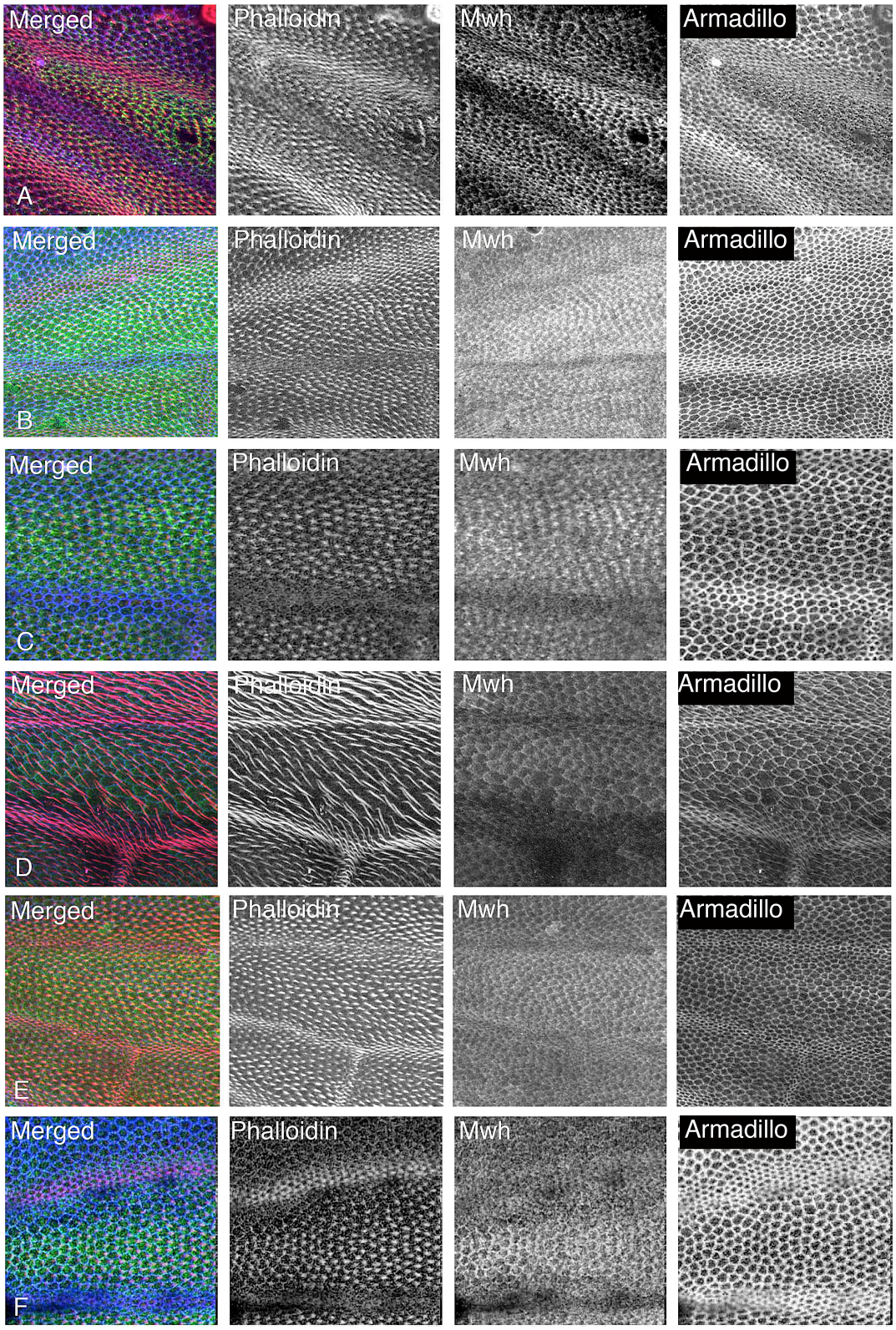

Figure 3.8: RNAi lines showing an increase of Mwh localisation in the pupal wing in the *ptc* expressing region. Lines were crossed with *ptc-Gal4;UAS -Dcr2* and stained with phalloidin (first channel), Mwh (second channel) and Armadillo (third channel). A) *Rim* B) *Fur2* C) *CanA14F* D) *pnut* E) *CG12964* and F) *septin* RNAi lines. RNAi expressing tissue is marked by white lines in the Mwh channel.

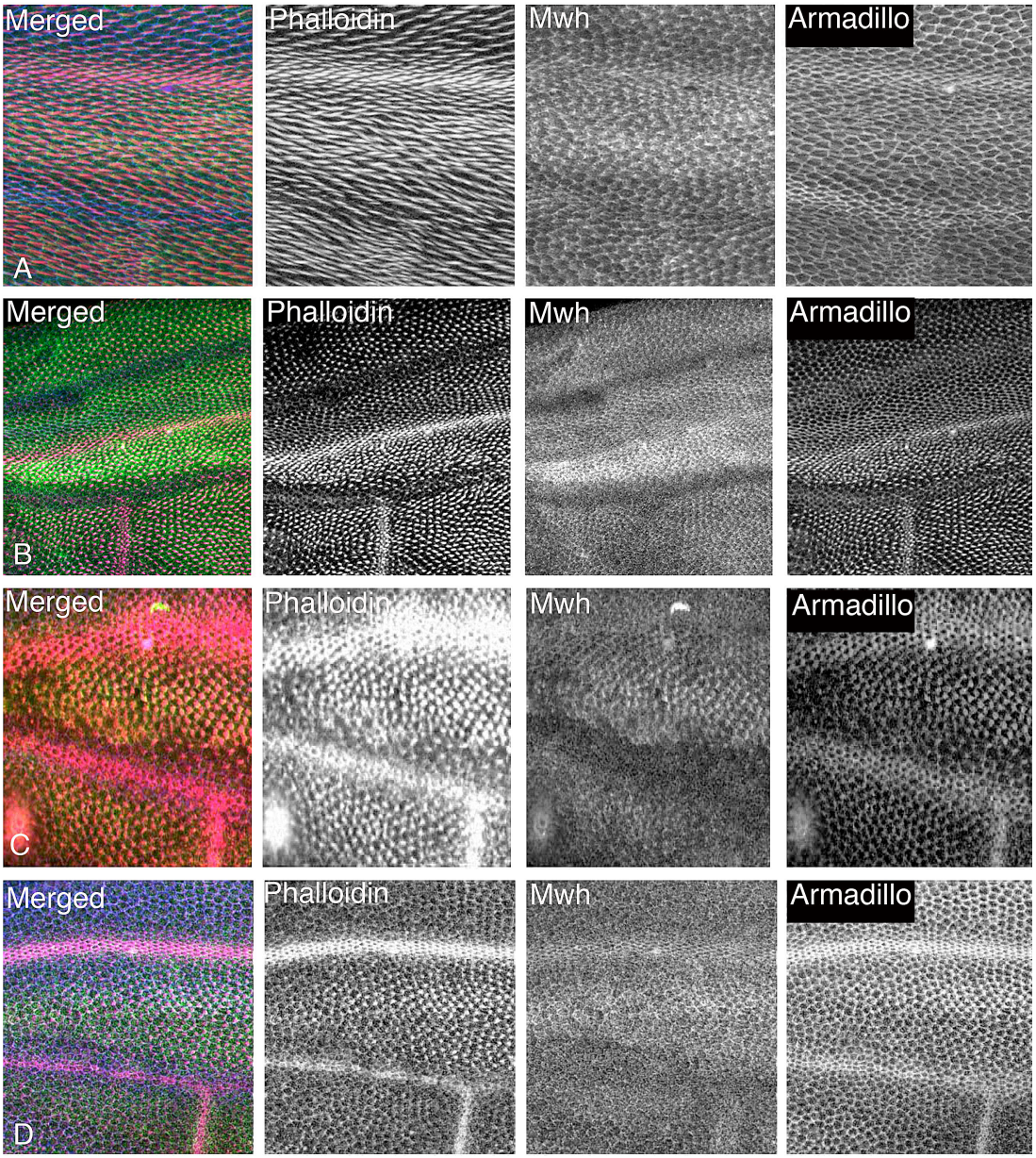

Figure 3.9: RNAi lines showing an increase of Mwh localisation in the pupal wing in the *ptc* expressing region. Lines were crossed to *ptc-Gal4;UAS-Dcr2* and stained with phalloidin (first channel), Mwh (second channel) and Armadillo (third channel). A) *mts* B) *dlt* C) *stau* D) *CG8260* RNAi lines. RNAi expressing tissue is marked with white lines and wild type tissue below is also marked.

Validation of hits by KK lines:

Genes such as *c12.1, cip4, kul, staufen, septin2* and *formin3* gave the same phenotype (although the degree of strength varies) when rescreened with kk lines (Figure 3.11 and 3.12). Although I tried to validate all the hits found in the pupal wing screen, some of the genes did not have another RNAi line from other sources.

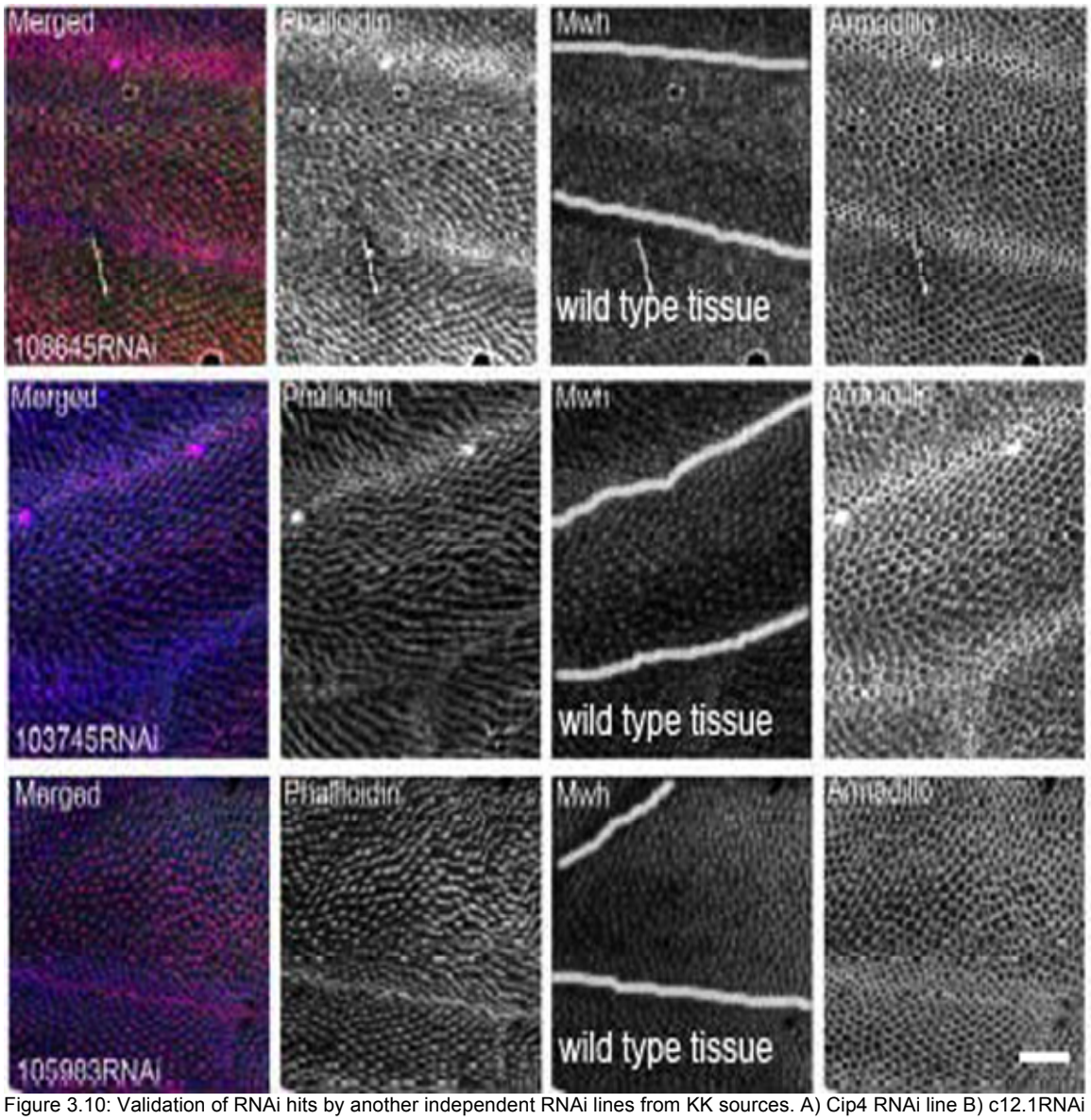

Figure 3.10: Validation of RNAi hits by another independent RNAi lines from KK sources. A) Cip4 RNAi line B) c12.1RNAi line and c) Kul RNAi line were crossed to with *ptc-Gal4; UAS-Dcr2 Dcr2* and stained with phalloidin (first channel), Mwh (second channel) and Armadillo (third channel). Mwh staining reveals very weak loss of Mwh in the ptc expressing region. RNAi expressing tissue is marked by white lines in the Mwh channel. Scale bar is 8 um.

Additional phenotypes found in the pupal wing screen:

RNAi lines with delayed trichome formation:

Some of the RNAi lines in the screen showed a delay in trichome formation as compared to controls and other wild type lines, and trichomes were found to form one to two hours late in them (Figure 3.13 to 17). Two different time points were

selected for dissecting and immunostaining of these lines, one at the normal time of trichome formation (27 hrs APF at 29ºC) and another later time point to find out the exact timing of trichome formation (28 hrs APF at 29ºC).

Lines showing a delay in trichome formation sometimes associated with other additional phenotypes such as trichome morphology defects (Figure 3.13, 3.17) and reduction in Mwh localisation (Figure 3.13, 3.15, 3.17). Although the reductions in Mwh are most likely to be due to a developmental delay of the RNAi expressing tissue since at a later time point (when trichomes were formed) Mwh localisation was found to be normal. Lines that showed a delay in trichome formation are tabulated below (Table 3.7) along with their Flybase ontology and function.

Gene Name	**Line Name**	**Molecular function (Based on Flybase)**	**Involved in biological process (Based on Flybase)**	**Phenotypes seen in each line**
dco	9241(GD)	kinase activity	biological regulation; anatomical structure development; regulation of biological process; phosphorus metabolic process; establishment of planar polarity; signaling pathway; macromolecule modification; growth; response to cocaine; rhythmic process	Causes delay in trichome formation in the ptc expressing domain
CG14395	17517(GD)	Unknown	Unknown	Causes delay in trichome formation in the ptc

				expressing domain
CG34401	18553/18554(GD)	Zinc ion binding	Unknown	Causes delay in trichome formation in the ptc expressing domain
Arpc3A	26548/26549(GD)	actin binding	regulation of actin filament polymerization	Causes delay in trichome formation in the ptc expressing domain
Gene Name	**Line Name**	**Molecular function (Based on Flybase)**	**Involved in biological process (Based on Flybase)**	**Phenotypes seen in each line**
Arp14D	29943/29944(GD)	structural constituent of cytoskeleton; actin binding	cytoskeleton organization	Causes delay in trichome formation in the ptc expressing domain

Table 3.7: Tabular representation of the genes which showed a delay in trichome formation in the RNAi screening. Along with the genes, their CG number, ontology (Fly base), function (Fly base) and phenotype found is also tabulated here

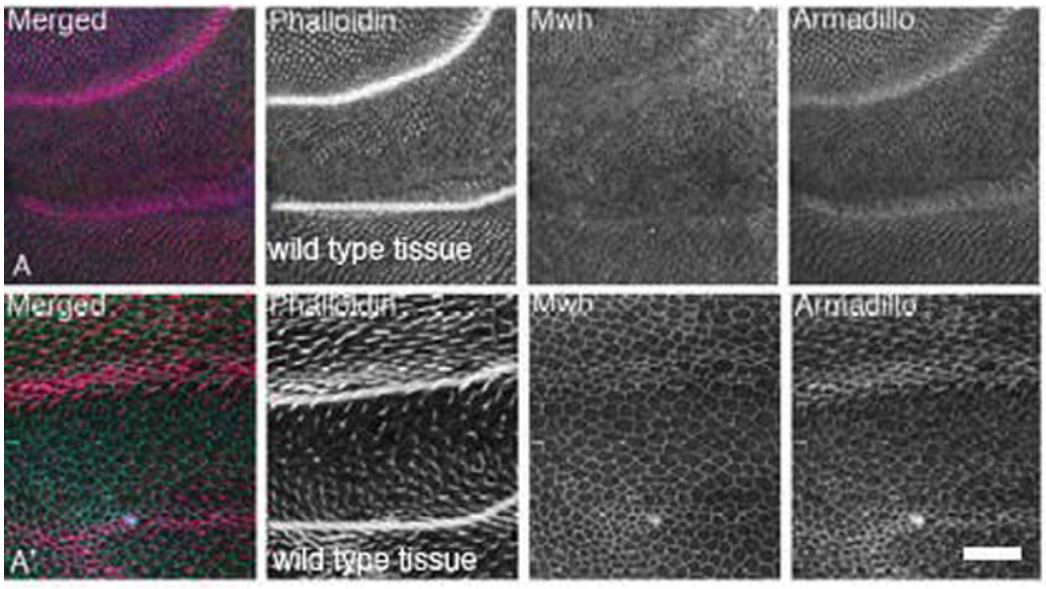

Figure 3.11: RNAi lines showing a delay in trichome formation in the pupal wing in the *ptc* expressing region. Lines were crossed with *ptc-Gal4; UAS-Dcr2* and stained with phalloidin (first channel), Mwh (second channel) and Armadillo (third channel). A) *dco* RNAi crossed with *w; ptc-Gal4; UAS-Dcr2 and* dissected after 27 hrs APF, phalloidin staining (first channel) shows delay in trichome formation, A') *dco* RNAi crossed with *w; ptc-Gal4; UAS-Dcr2 and* dissected after 28 hrs APF, phalloidin staining (first channel) shows trichomes have started forming. RNAi expressing tissue is marked by white lines in the phalloidin channel. Scale bar is 8 um.

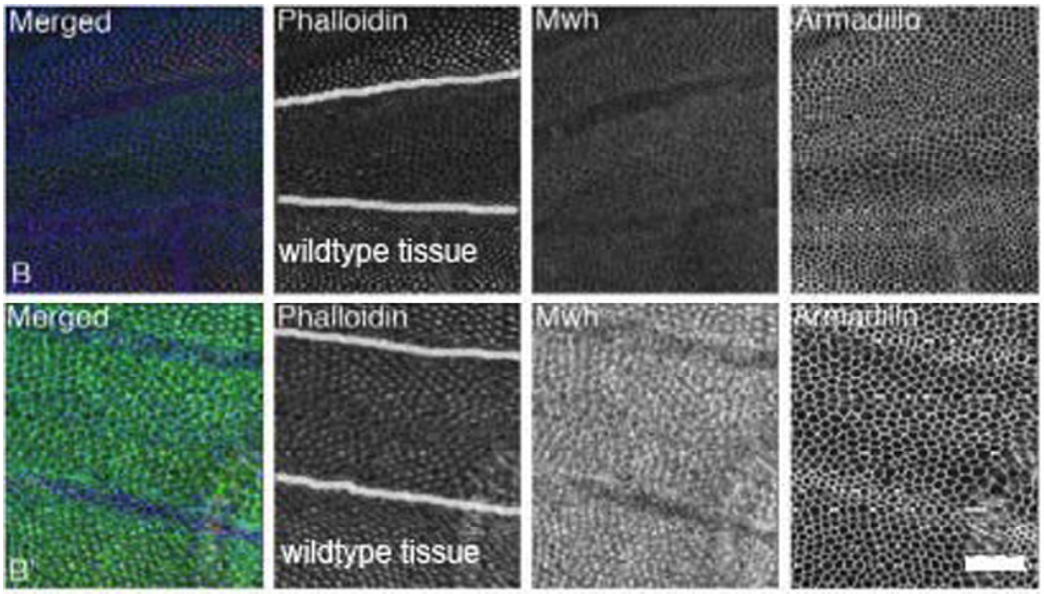

Figure 3.12: RNAi lines showing a delay in trichome formation in the pupal wing in the *ptc* expressing region. Lines were crossed with *ptc-Gal4; UAS-Dcr2* and stained with phalloidin (first channel), Mwh (second channel) and Armadillo (third channel). B) *17517* RNAi crossed with *w; ptc-Gal4; UAS-Dcr2 and* dissected after 27 hrs APF, phalloidin staining (first channel) shows delay in trichome formation, B') *17517* RNAi crossed with *w; ptc-Gal4; UAS- Dcr2 and* dissected after 28 hrs APF, phalloidin staining (first channel) shows trichomes have started forming. RNAi expressing tissue is marked by white lines in the phalloidin channel. Scale bar is 8 um.

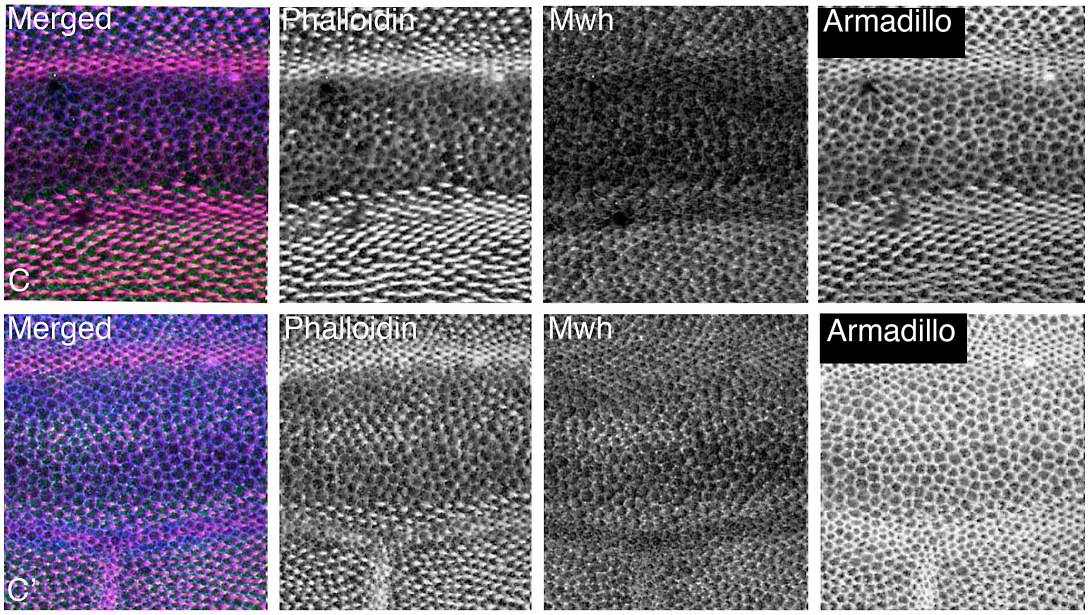

Figure 3.13: RNAi lines showing a delay in trichome formation in the pupal wing in the *ptc* expressing region. Lines were crossed with *ptc-Gal4; UAS-Dcr2* and stained with phalloidin (first channel), Mwh (second channel) and Armadillo (third channel). C) *CG34401* RNAi crossed with *w; ptc-Gal4; UAS-Dcr2 and* dissected after 27 hrs APF, phalloidin staining (first channel) shows delay in trichome formation, B) A) *CG34401* RNAi crossed with *w; ptc-Gal4; UAS-Dcr2 and* dissected after 28 hrs APF, phalloidin staining (first channel) shows trichomes have started forming. RNAi expressing tissue is marked by white lines in the phalloidin channel. Scale bar is 8 um.

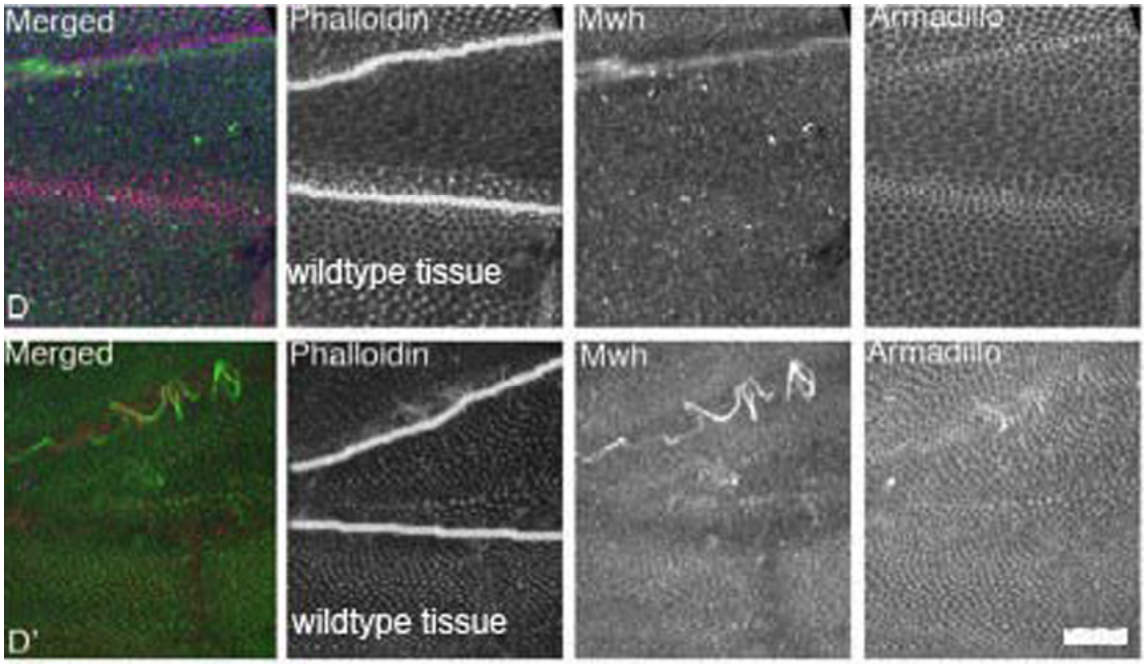

Figure 3.14: RNAi lines showing a delay in trichome formation in the pupal wing in the *ptc* expressing region. Lines were crossed with *ptcGal4; UAS Dcr2* and stained with phalloidin (first channel), Mwh (second channel) and Armadillo (third channel). D) *Arpc14D* RNAi crossed with *w; ptcGal4; UAS Dcr2 and* dissected after 27 hrs APF, phalloidin staining (first channel) shows delay in trichome formation, D') *Arpc14D* RNAi crossed with *w; ptc-Gal4; UAS-Dcr2 and* dissected after 28 hrs APF, phalloidin staining (first channel) shows trichomes have started forming. RNAi expressing tissue is marked by white lines in the phalloidin channel. Scale bar is 8 um.

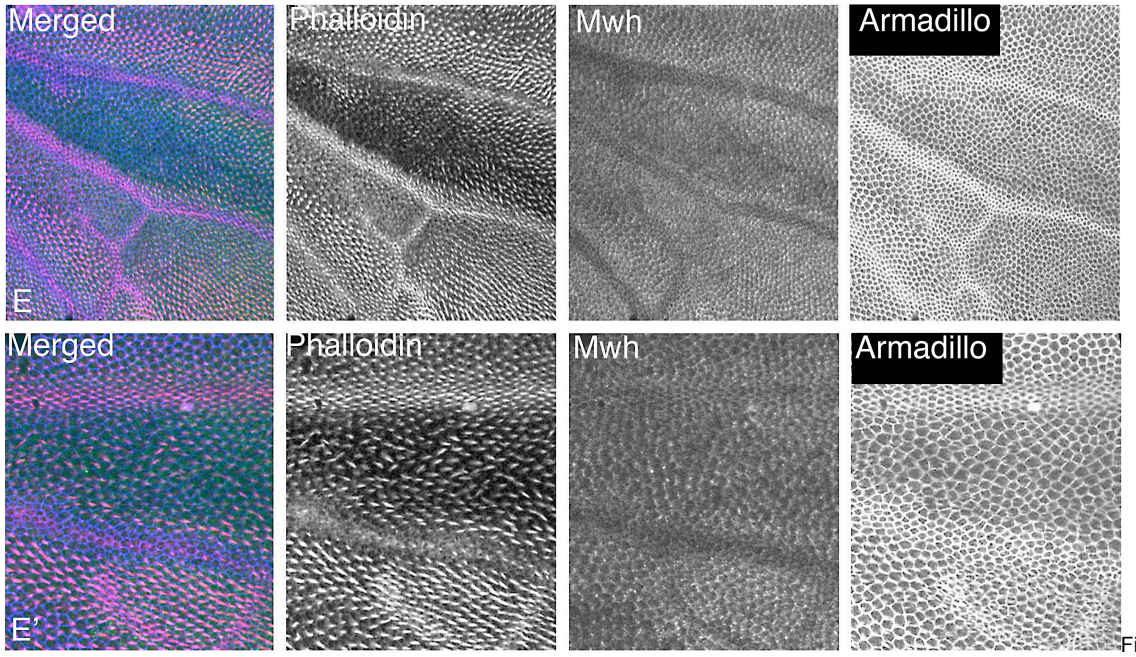

Figure 3.15: RNAi lines showing a delay in trichome formation in the pupal wing in the *ptc* expressing region. Lines were crossed with *ptc-Gal4; UAS-Dcr2* and stained with phalloidin (first channel), Mwh (second channel) and Armadillo (third channel). E) *Arpc3A* RNAi crossed with *w; ptc-Gal4; UAS-Dcr2 and* dissected after 27 hrs APF, phalloidin staining (first channel) shows delay in trichome formation, B) A) *Arpc3A* RNAi crossed with *w; ptc-Gal4; UAS-Dcr2 and* dissected after 28 hrs APF, phalloidin staining (first channel) shows trichomes have started forming. RNAi expressing tissue is marked by white lines in the phalloidin channel. Scale bar is 8 um.

RNAi lines with large cell morphology:

A large number of RNAi lines in the screen showed a typical large cell phenotype with multiple hairs (Fig: 3.19-20). When immunostained with Mwh antibody, some of these lines also showed a reduction of Mwh which could be due to large cells and thus an increase in the total area at each cell as compared to the total Mwh protein available. However an effect on Mwh localisation could not be ruled out .

To differentiate between the two-above mentioned possibilities of Mwh reduction, these RNAi lines were crossed with *UAS CyclinE,* which is a cell cycle regulator (CyclinE binds with cdk2 and helps in the transition from G1 to S phase; Stain *et al.,* 2006). I hypothesized that if the RNAi lines causing large cells are coexpressed with CyclinE, the cell division defect can be rescued. *mwh* and *string (stg)* RNAi lines were taken as negative and positive controls in this experiment as mwh RNAi does not give large cells and string is a known regulator of cell cycle which produces cells larger than normal in the *Drosophila* wing (Edgar *et al.,* 2001).

Although instead of rescuing the cell size defect, these RNAi lines when crossed with *UASCyclinE* produced larger cells than before (Figure 3.18). Therefore I conclude that it is possible that RNAi knockdown of these genes can regulate Mwh localisation independently of the cell division regulation, but I was unable to characterize that further using my experimental conditions. Lines that showed a large cell phenotype are tabulated below (Table 3.8) along with their Flybase ontology and function.

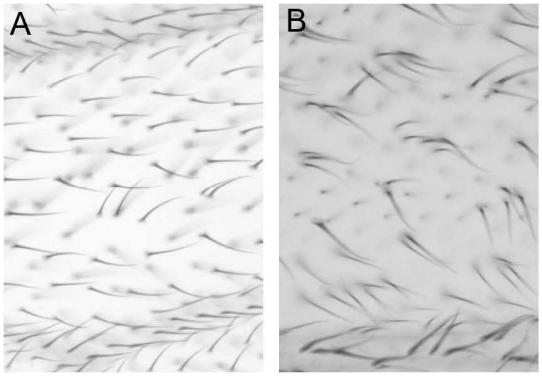

Figure 3.18: 17760 RNAi line when crossed to *ptc-Gal4; UAS-Dcr2* caused multiple hairs and large cells (A) and when expressed along with UAS cyclinE (B) the large cell phenotype got stronger (trichomes are more far apart than a).

Gene Name	**Line Name**	**Molecular function (Based on Flybase)**	**Involved in biological process (Based on Flybase)**	**Phenotypes seen in each line**
string	1395R1/R2(NIG)	protein tyrosine phosphatase activity	protein amino acid dephosphorylation; regulation of mitotic cell cycle; gastrulation; centriole replication; G2/M transition of mitotic cell cycle	Causes large cells with multiple hairs in the *ptc* expressing domain. Reduction of Mwh was also found.
diaphanous	1768R1(NIG)	protein binding	cell cycle; cell division; anatomical structure development; localization; cell cycle process; biological regulation; reproductive process in a multicellular organism; multicellular organismal process; actin filament-based process;	Causes large cells with multiple hairs in the *ptc* expressing domain. Reduction of Mwh was also found.
CG2837	2837R1(NIG)	Unknown	Unknown	Causes large cells with multiple hairs in the *ptc* expressing domain
minus	5360R1(NIG)	Unknown	cyclin catabolic process; ovarian nurse cell to oocyte transport; positive regulation	Causes large cells with multiple hairs in the *ptc* expressing domain

			of cell proliferation; endomitotic cell cycle; regulation of cell cycle; positive regulation of multicellular organism growth; positive regulation of mitotic cell cycle	
CG7830	7830R1(NIG)	Unknown	Unknown	Causes large cells with multiple hairs in the *ptc* expressing domain
Adenylyl cyclase 35C Ac13E	9210R2(NIG)	adenylate cyclase activity	cAMP biosynthetic process	Causes large cells with multiple hairs in the *ptc* expressing domain
DROK	9774R2/R3(NIG)	GTPase binding; protein binding; protein serine/threonine kinase activity.	biological regulation; localization; cell cycle; ovarian nurse cell to oocyte transport; multicellular organism reproduction; cell cycle process; gamete generation; organelle organization; post-embryonic organ morphogenesis; establishment of planar polarity	Causes large cells with multiple hairs in the *ptc* expressing domain. Cells look sick also.
CG9772	15636(GD)	Unknown	ubiquitin-dependent protein catabolic process	Causes very large cells with multiple hairs in the *ptc* expressing

				domain. Reduction of Mwh
Lrr47	27566(GD)	Unknown	Ras protein signal transduction	Causes large cells with multiple hairs in the *ptc* expressing domain
CG8878	28971(GD)	protein serine/threonine kinase activity	protein amino acid phosphorylation	Causes large cells with multiple hairs in the *ptc* expressing domain. Reduction of Mwh.
CG14375	12830(GD)	G-protein-coupled receptor binding	Unknown	Causes large cells with multiple hairs in the *ptc* expressing domain
CG12065	31120/31121(GD)	catalytic activity	nucleoside metabolic process	Causes large cells with multiple hairs in the *ptc* expressing domain
ariadne (ari1)	35029(GD)	ubiquitin-protein ligase activity	negative regulation of transcription	Causes large cells with multiple hairs in the *ptc* expressing domain. Reduction of Mwh was also found.
CG6897	35132(GD)	protein binding	asymmetric protein localization involved in cell fate determination; activation of protein kinase activity;.	Causes large cells with multiple hairs in the *ptc* expressing domain
multi sex combs	42978(GD)	DNA binding	hemocyte differentiation; hemocyte proliferation	Causes large cells with multiple hairs in the *ptc* expressing domain

CG1518	48653(GD)	oligosaccharyl transferase activity	protein amino acid glycosylation	Causes large cells with multiple hairs in the *ptc* expressing domain
Origin recognition complex subunit 1 (ORC1)	10667R1(NIG)	DNA binding	DNA amplification; DNA-dependent DNA replication initiation;	Causes large cells with multiple hairs in the *ptc* expressing domain

Table 3.8: Tabular representation of the genes which showed large cells in the RNAi screen. Along with the corresponding genes, their CG number, ontology, function and phenotype found is also tabulated here.

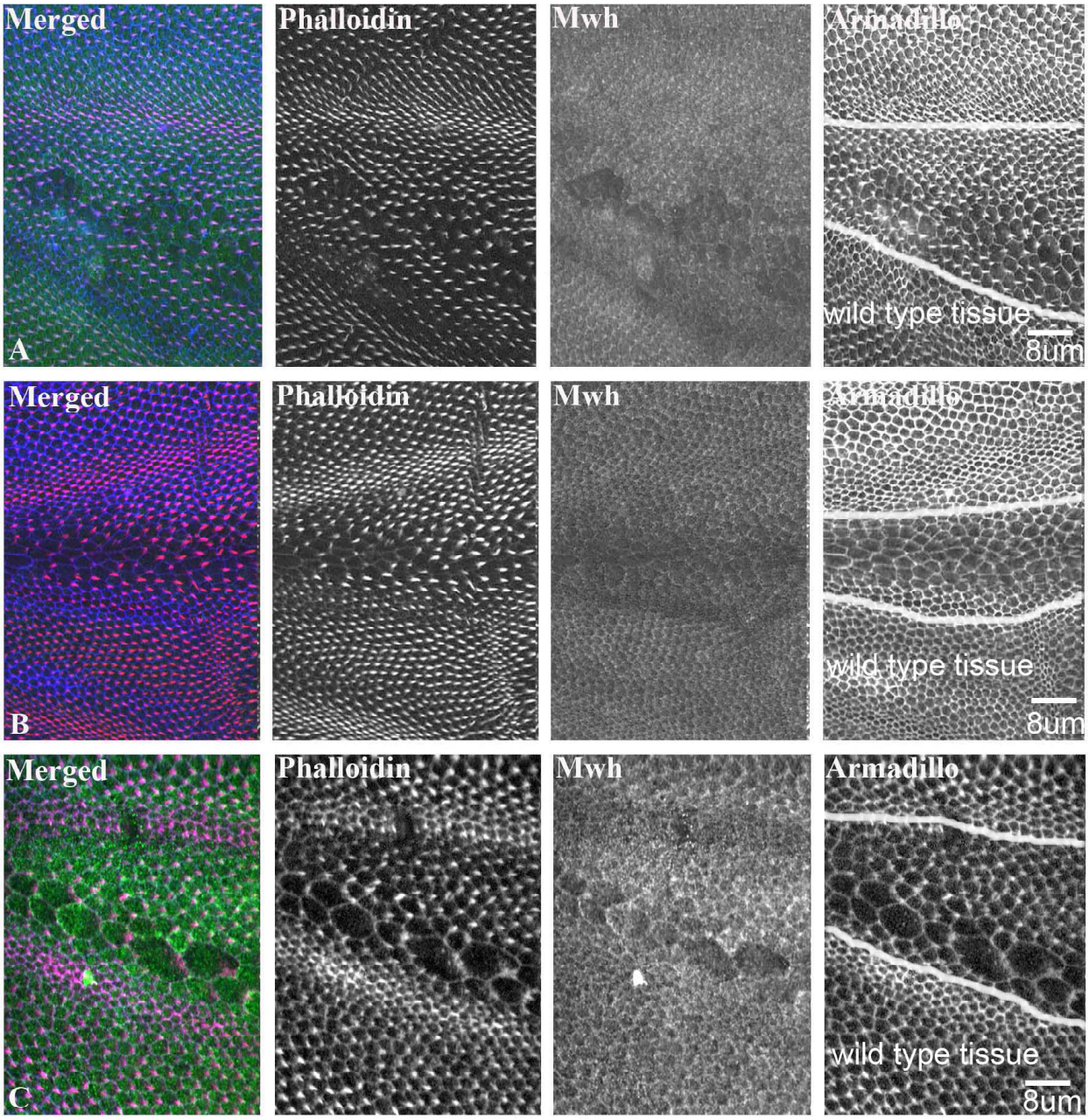

Figure 3.19: RNAi lines showing large cells in the pupal wing in the *ptc* expressing region. Lines were crossed with *ptc-Gal4; UAS-Dcr2* and stained with phalloidin (first channel, red), Mwh (second channel, green) and Armadillo (third channel, blue). A) CG9772 B) 15636 C) 12830 RNAi lines which shows large cells. RNAi expressing tissue is marked by white lines in the armadillo channel. The size of each scale bar is mentioned in the image.

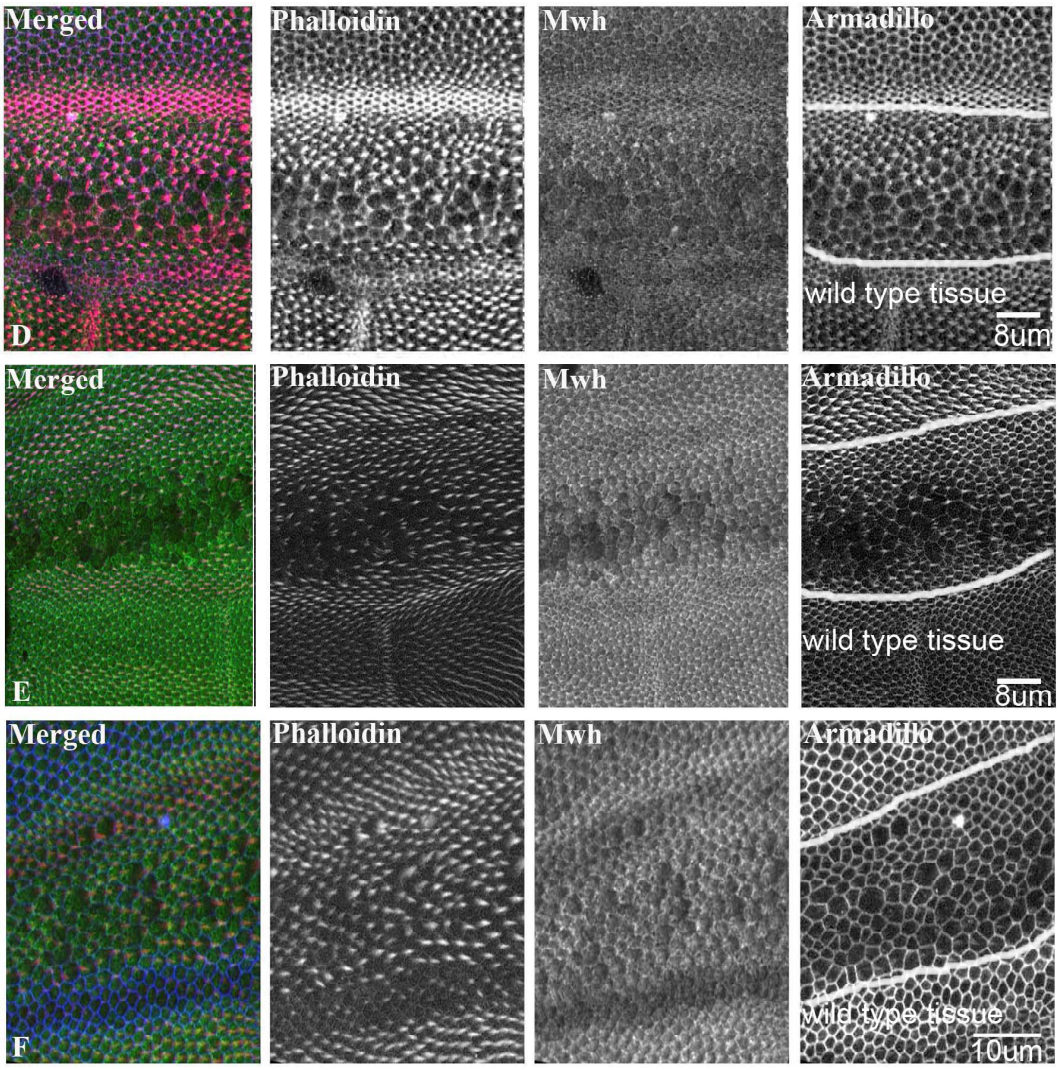

Figure 3.20: RNAi lines showing large cells in the pupal wing in the *ptc* expressing region. Lines were crossed with *ptc-Gal4; UAS-Dcr2* and stained with phalloidin (first channel, red), Mwh (second channel, green) and Armadillo (third channel, blue). D) 31120 E) 28907 and F) DROK RNAi lines which shows large cells. RNAi expressing tissue is marked by white lines in the armadillo channel. The size of each scale bar is mentioned in the image.

RNAi lines with abnormal trichome morphology:

A small number of RNAi lines were found to be involved in regulating the morphology of trichomes. These lines were further fixed and stained for actin (phalloidin) to study the actin phenotype. Along with trichome morphology defects some of the RNAi lines also had associated additional phenotypes such as delay in trichome formation (Figure 3.21). Lines that showed abnormal trichome

morphology are tabulated below (Table 3.9) along with their Flybase ontology and function.

Gene Name	**Line Name**	**Molecular function (Based on Flybase)**	**Involved in biological process (Based on Flybase)**	**Phenotypes seen in each line**
Canoe (cno)	7769(GD)	Actin binding	embryonic morphogenesis; dorsal closure; regulation of JNK cascade; epidermis morphogenesis; compound eye development; ommatidial rotation	Trichome morphology defect
Crinkled (ck)	9265(GD)	Actin dependent ATPase activity	antennal morphogenesis; imaginal disc-derived wing vein morphogenesis; bristle morphogenesis; sensory organ development; actin filament-based movement;	trichome morphology defect, trichomes are short and stumpy
Arp3A	26548/26549(GD)	actin binding	regulation of actin filament polymerization	Trichome morphology defect,
Myo10A	37530(GD)	Protein binding	dorsal closure; filopodium assembly; intracellular protein transport	trichome morphology defect, trichomes are extremely thin and wavy

Table 3.9: Tabular representation of the genes which showed abnormal trichome morphology in the RNAi screen. Along with the genes, their CG number, ontology, function and phenotype found is also tabulated here.

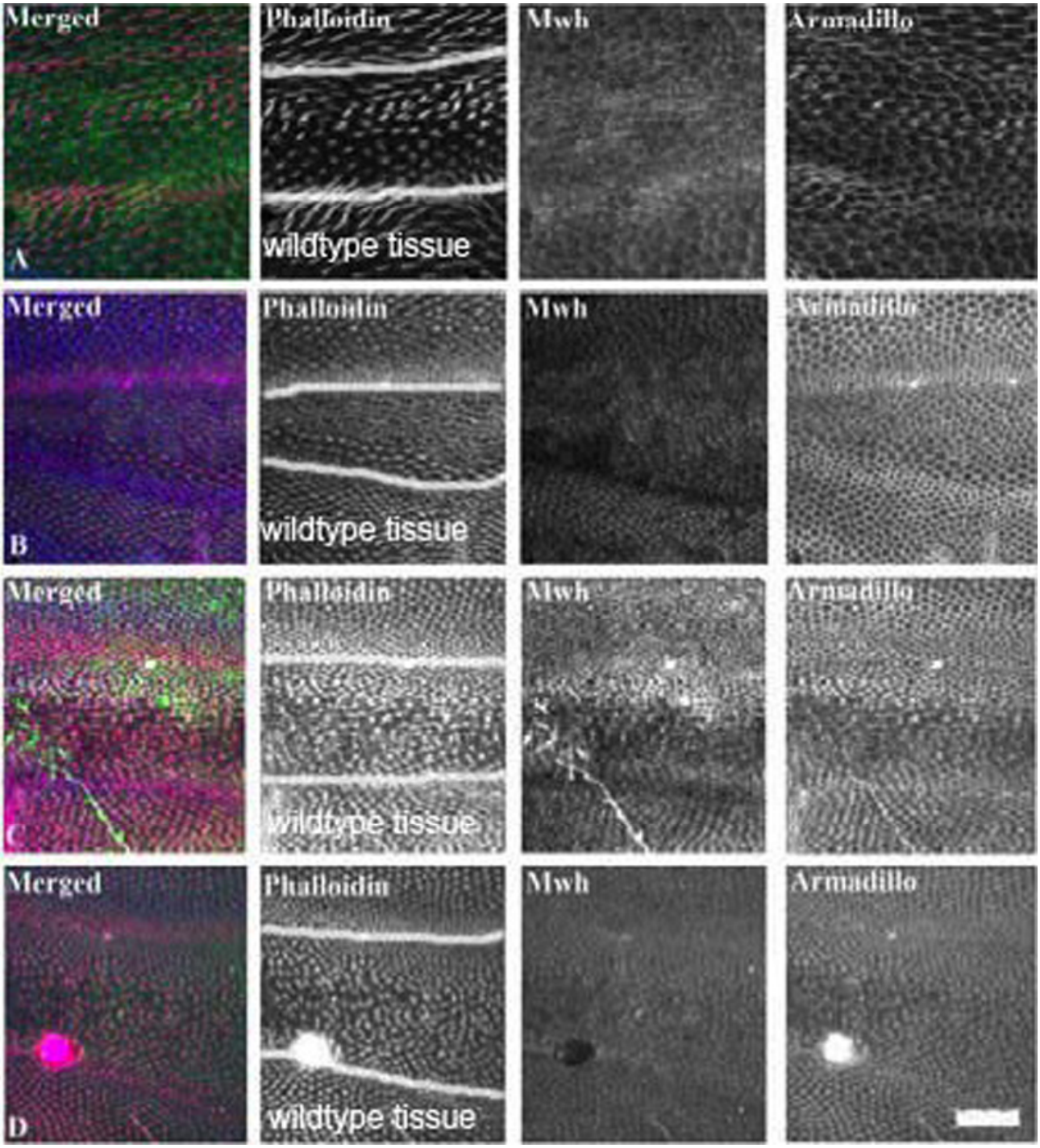

Figure 3.21: RNAi lines showing actin morphology defects in the pupal wing at the *ptc* expressing region. Lines were crossed with *ptcGal4; UAS-Dcr2* and immunostained with phalloidin (first channel, red), Mwh (second channel, green) and Armadillo (third channel, blue). A) *ck* B) Myo10A C) Arp3A, D) Arp3A. RNAi lines are shown here with trichome morphology defects. RNAi expressing tissue is marked by white lines in the phalloidin channel..

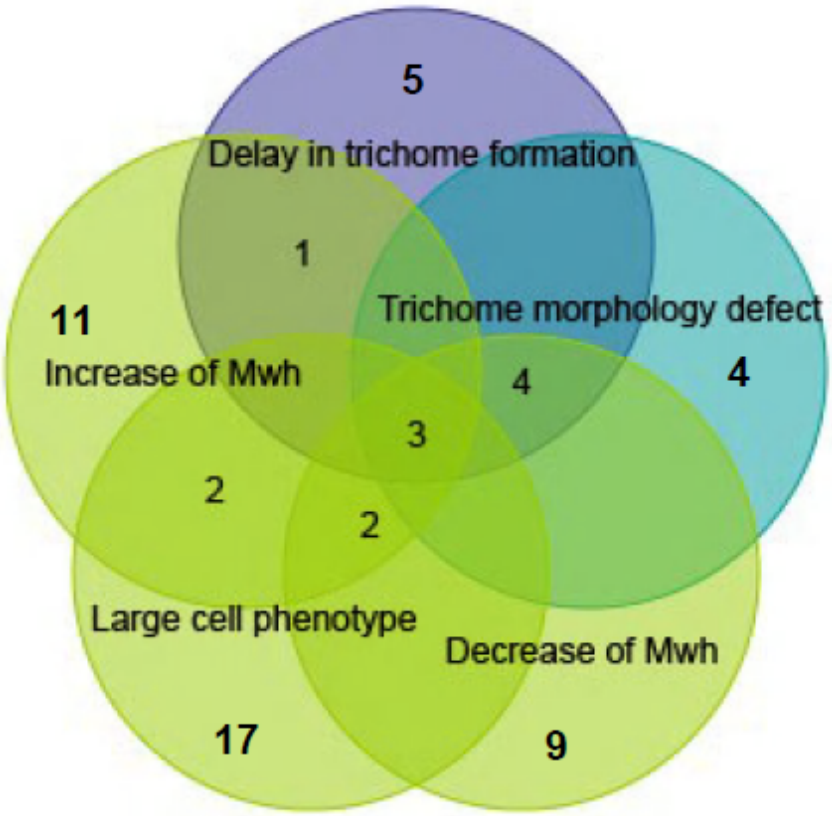

Figure 3.22**:** Venn diagram showing the different phenotypes found in the pupal wing RNAi screen. Some of the categories were overlapping with each other. The number inside the circles shows the overlapping phenotypes and the numbers outside of the circles showing the nonoverlapping phenotypes found in each category.

Advantages of our RNAi screen:

This *in vivo* RNAi screen in the *Drosophila* adult and pupal wings had several advantages such as the multiple hair phenotype in the adult wing was easy to score and quick to perform. In the pupal wing screening as the RNAi lines were crossed with *ptc-Gal4* driver, it was easy to compare the mutant phenotype with the adjacent wild type tissue in the same wing. The crossing scheme of the pupal screen was quite straightforward devoid of several steps of genetic crosses. Further validation of the phenotype was possible by using another independent set of RNAi line with different hairpin structure. Finally, interpretation of the data was straightforward and was not dependent on robust statistical calculations or rigorous downstream analysis.

Disadvantages of our RNAi screen:

Although RNAi screening was the most straightforward approach to identify novel genes, there were still some disadvantages. As with any other RNAi screen, my assay had picked up lines with false positive effects caused by off target genes and false negative results due to incomplete or weak knockdown of genes. To solve the issue of false positive phenotypes, independent RNAi lines with different hairpins (KK) were used to confirm the observed phenotypes. However RNAi lines with very weak multiple hair phenotypes were not taken into consideration for further investigation, meaning that I may have missed some interesting lines. Also, in my screen a large number of RNAi lines produced multiple hairs along with large cells.

As previously mentioned large cells can produce multiple hairs independent of a PCP defect and this is likely to be due to a cell division defect (Adler *et al.,* 2000). But I was not able to distinguish between cells producing multiple hairs due to cell division (cytokinesis) defects and those exhibiting multiple wing hair formation independent of cytokinesis defects. Also I could not explain no change in Mwh localisation of some lines which exhibited a strong multiple hairs phenotype in the adult wing.

Hits found in the screen:

In the pupal wing screen, hits were found to regulate Mwh localization by either causing a decrease or an increase in Mwh localization. Among the genes which caused a decrease in Mwh localization, *Rab23*, which belongs to the Rab family of small GTPases caused strong reduction of Mwh when crossed to *ptc-Gal4, UAS-Dcr2* (Fig 3.8). Rab23 is involved in a number of signalling and intercellular transportation machinery. It plays an important role in the Hedgehog signalling pathway in vertebrates by its interaction with smoothened (Smo) (Wang *et al.,* 2006).

A recent study suggests it has a role in the regulation of the planar cell polarity pathway in *Drosophila* (Pataki *et al.,* 2010). Mutation in *Rab23* causes accumulation of excess apical actin in the pupal wing resulting in the formation of multiple trichomes with distorted polarity (Pataki *et al.,* 2010), a phenotype which is also observed in PCP effector mutants (Strutt and Warrington, 2009). It was also found to interact with the PCP core protein Pk in the *Drosophila* wing (Pataki *et al.,* 2010). However, they did not look at Mwh localisation.

As Rab23 is involved in membrane trafficking and in its absence Mwh is reduced, I think that the trafficking of Mwh is important for its proper localisation and activity. However no clear link between endocytosis and Rab23 was found in the mammalian system (Evans *et al.,* 2003, Eggenschwiler *et al.,* 2006, Wang *et al.,* 2006).

Although the genetic hierarchy between *mwh* and *Rab23* is not known yet, this novel function of Rab23 in regulating Mwh accumulation in the *Drosophila* wing suggests a link between PCP and Rab23. Another interesting phenomenon is the involvement of Rab23 and PCP effector proteins (In, Fy, Frtz) in primary ciliogenesis (Park *et al.,* 2006; Gray *et al.,* 2009; Heydeck *et al.,* 2009; Zeng *et al.,* 2010), which suggests that PCP effectors and Rab23 possibly interacts together in regulating actin cytoskeleton in different organisms.

Mo25 in *Drosophila* is a member of the Mob family of proteins, which play an essential role in the formation of buds in yeast (Nelson *et al.,* 2003). There are 4 Mob genes in *Drosophila,* which are related to the yeast Mob family and apart from Mo25 (He et al., 2005) all the others can physically interact with tricornered (trc), a protein which belongs to the NDR family of serine threonine kinase (Mah *et al.,* 2001; Hou *et al.,* 2003). Homozygous Mo25 causes thickening of wing veins, loss of wing margin, multiple wing hairs and bristles in *Drosophila* (Hu *et al.,* 2005). In the RNAi screen I have found that knocking down of Mo25 by RNAi causes reduction of Mwh accumulation in the pupal wing and a multiple hairs phenotype

(Fig 2.7). These data suggest that Mo25 regulates the accumulation of Mwh in *Drosophila* wing. As Mo25 is known to interact with a number of kinase families, it could regulate Mwh accumulation by interacting with a kinase/s in the *Drosophila* wing, although other modes of regulation also cannot be ruled out.

Tricornered itself was also found to regulate Mwh accumulation in our screen. Along with regulating Mwh accumulation, it also had an effect in trichome formation as the timing of trichome formation was found to be delayed in a *trc* mutant background (Fang *et al.,* 2010). NDR kinases are widely known for their role in cell polarisation events in different organisms (Hergovich *et al.,* 2006). *trc* is involved in epidermis and sensory neuron formation and in its absence, multiple hairs and split bristles occur (Geng *et al.,* 2000). Reduction of Mwh accumulation (Fang *et al.,* 2010) suggests that this NDR kinase plays a role in Mwh activity and localisation possibly by phosphorylating it. Although the role of *trc* in Mwh phosphorylation still remains elusive, this suggests a link between the effectors of PCP pathway and NDR kinases in *Drosophila*.

Among other genes that were found to regulate Mwh accumulation in the *Drosophila* pupal wing by reducing its amount, *c12.1, cip4* and *Tsp29Fb* are worth mentioning. The precise molecular function of both the genes are yet unknown. *c12.1* was reported to regulate the mitotic spindle organisation in *Drosophila* S2 cells (Goshima *et al.,* 2007). As mitotic spindle organisation is essential for microtubule formation, which is known to be an essential component of wing hairs, it is possible that in its absence, Mwh cannot properly localise to the wing hair, resulting in its reduced accumulation (Fig 3.8). This phenotype was further confirmed by another independent RNAi line from the KK source.

Cip4, which was found to reduce Mwh localisation in the *Drosophila* wing, helps in actin nucleation complex formation by interacting with WASP/WAVE complex. *Cip4* mutants cause multiple hairs in the *Drosophila* wing (Fricke et al., 2009). It was also found to be involved in membrane invagination and vesicle trafficking

(Fricke et al., 2009). As it is directly involved in actin assembly and cytoskeleton regulation, Mwh localisation might gets affected when *cip4* is not present in the membrane.

Tsp29Fb belongs to an evolutionarily conserved tetraspanin group of proteins. Tetraspanins are known to form multidomain complexes with the surface proteins of the membrane (Tordes *et al.,* 2000). Out of 23 tetraspanins only one of them Late bloomer (Lbl) is molecularly characterized in *Drosophila* (Kopczynski *et al.,* 1996). Lbl is involved in embryonic synapse formation and has been associated with mental disorders in flies and humans (Fradkin *et al.,* 2002). Although nothing is known about the function of Tsp29Fb, being a member of tetraspanin group of proteins, which acts as a scaffold protein in bringing multiple proteins to one area of the cell membrane, it may play a role in Mwh localisation (Fig 2.7) to the cell membrane.

CG14375, a gene with an unknown function; Kul, a metalloprotease and Arp-like, an actin binding protein were also found to affect Mwh accumulation weakly. Pnut, a gene involved in cell cytokinesis (Neufield and Rubin, 1994) produced an increase in Mwh accumulation along with a large cell phenotype (Fig 3.8). It is a member of the septin family of proteins, which regulate polarisation events in yeast (Neufield and Rubin, 1994). It is also known as an ubiquitin ligase protein which binds to microtubules and GTPases (Wong *et al.,* 2010). Another Septin (Septin 2) was also found in our screen to regulate the accumulation of Mwh by increasing its total amount (in our pupal wing immunostaining assay) (Fig 3.9). It is possible that similar to the yeast model system where all the septin proteins function as part of a complex, in *Drosophila* they could also be working together and accumulation of Mwh may become disrupted in the absence of these complexes.

Staufen, which plays a role in pole granule formation (Raff *et al.,* 1990), actin mediated mRNA transport (Micklem *et al.,* 2000), mRNA processing and positive

regulation, was found to regulate Mwh localisation. This phenotype was further confirmed by another independent RNAi line from the KK source. Although the exact role played by Staufen in regulating Mwh still remains elusive, it is possible that in the absence of Staufen, Mwh is either not transported properly or as Staufen is a member of the RNAi machinery, it somehow down regulates a second gene which in turn causes accumulation of Mwh.

Microtubule star (mts) is a serine threonine phosphatase. It plays a role in cell cycle regulation (Snaith *et al.,* 1996) and microtubule organisation in the cytoskeleton (Snaith *et al.,* 1996). As it is involved in cell cycle regulation, the knockdown of the gene by RNAi caused large cells, but in addition multiple hairs and accumulation of Mwh was evident (Fig 3.10). mts could regulate Mwh assembly by various methods; firstly, being a phosphatase, it could reduce the activity of kinase/s involved in the regulation of Mwh activity thereby increasing its total amount. Secondly, as it is a regulator of the microtubule cytoskeleton, its absence could disrupt the microtubule dynamics.

The only *Drosophila* formin, which was found to be involved in Mwh regulation in our screen was formin3 (Fig 3.9). Although the effect was weak, formin3 knockdown by RNAi caused an increase in Mwh accumulation in the pupal wing suggesting a novel interaction between Mwh and Formin3. It is possible that Mwh, which is a formin like protein (due to the presence of its GBD and FH3 domains), acts with formin3 in regulating the cytoskeleton possibly with its GBD domain and in the absence of the latter, Mwh cannot interact and accumulates in the pupal wing.

Along with the above-mentioned proteins, Rim, CanA14F, CG12964, Fur2 and CG8260 were also found to cause increased accumulation on Mwh in the wing. As the effect of these genes was really weak (in the pupal wing immunostaining assay), they were not considered for further validation and future experimentation.

Significance of the additional phenotypes found in the screening:

Although the additional phenotypes found in my screening are not exclusively related to PCP pathway and regulation of Mwh, these finding are important in the process of the wing and wing hair development in *Drosophila* as a whole. Further validation and characterization of the genes would be useful in understanding the development of *Drosophila* wing structure.

Future experiments:

All the hits that were found in our screen need to be validated by either independent sets of RNAi lines of the same gene which have a different hairpin structure or through various genetic mutation analyses such as loss of function clonal analysis or rescue of the RNAi phenotype by overexpressing the transgene impervious to the RNAi. The underlying concept in using an independent hairpin to the same gene is that it will be able to reduce the off target effect as it would target the mRNA corresponding to the RNAi line at a different location.

Further confirmatory genetic analysis such as loss of function and overexpression studies may provide insight about the function of the gene corresponding the RNAi lines. Finally and more conclusively if the phenotype caused by a particular RNAi line can be rescued by expression of a transcript that can confer the activity of the gene without evading the RNAi treatment such as by expressing 3' UTR of that particular gene (Stieloe *et al.,* 2004; Perrimon *et al.,* 2010), it would confirm the effect.

Together, my results have identified a putative new set of genes in the *Drosophila* wing that are probable novel interactors of Mwh protein as knockdown of these genes were found to cause either an increase or a decrease in its total amount in the wing and Mwh may regulate the actin cytoskeleton machinery of the wing by its interaction with these genes. Further experimentation and research will confirm the putative functional roles of these genes in regulation of Mwh and also will give us a

clue to how PCP is established and maintained downstream of effector proteins in the *Drosophila* wing.

My screening has found several genes (such as *Rab23, Tsp29Fb, Mo25, c12.1, staufen, microtubule star, septin 2, pnut*) that alter the distribution of Mwh protein and may therefore regulate it directly. Additionally, other genes were found which appeared to have a role in regulating cell size, timing of trichome formation and trichome morphology.

Further study will provide better understanding of the pathway that leads to the formation of a single distally pointing trichome downstream of the core PCP cues, and also how Mwh regulates this pathway by modifying the actin cytoskeleton.

Chapter 4: Results

Title: The GBD domain of Mwh causes stress fibre reduction when expressed *in vitro* in mammalian 3T3 cells.

Introduction:

What is the molecular Function of Mwh?

As already mentioned Mwh consists of a GTPase binding domain (GBD) and a formin homology 3 (FH3) domain (Strutt and Warrington, 2008; Yan *et al.,* 2008). These domains are normally found in formin group of proteins, which regulates the actin cytoskeleton where the GBD domain is involved in inhibiting the actin nucleation function of an FH2 domain and FH3 domain regulates the subcellular localisation of the protein (Wallar and Alberts, 2003). It was suggested that Mwh might act as a dominant negative protein by inhibiting other formins due to the presence of the GBD domain and Fz mediated Rho GTPases might inhibit this inhibition. Further RhoA was also found to interact with Mwh in the *Drosophila* wing (Yan *et al.,* 2010) suggesting a potential interaction between these two in cytoskeleton regulation. To prove the hypothesis I wanted to dissect out the function of the GBD and FH3 domain and the C terminal end of unknown domain structure and the relation of Mwh and RhoA in the cell cytoskeleton.

Aim of the study:

As formin proteins are important regulators of actin cytoskeleton, I speculated that Mwh, which is a formin like protein might also have a potential role in actin cytoskeleton regulation. I hypothesized that the presence of a GBD domain in Mwh might indicate a potential interaction with Rho GTPases (as Mwh was reported to interact with RhoA in the *Drosophila* wing) in modulating the cytoskeletal structure. Although Mwh does not have a well defined FH1 and FH2 domain for actin nucleation, the presence of the GBD domain can render an autoinhibition to its own C terminal end and the binding of Rho GTPases to the

GBD domain can disrupt this autoinhibiton (Figure 4.1). I also hypothesized that, Mwh GBD domain can also bind with DID domains of other formins present in *Drosophila* to render inactivity.

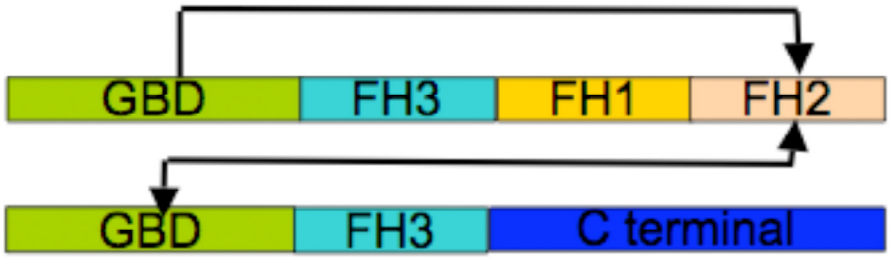

Figure 4.1: Proposed Hypothesis of my tissue culture assay: Mwh with its GBD domain can autoinhibit the C terminal end of itself and can also inhibit the FH1 and FH2 domains of other formins by dimerisation with the GBD domain. It is possible that like other formins binding of a Rho GTPases to the GBD domain reduces this inhibition.

Results:

To support my hypothesis, a number of deletion mutant constructs of Mwh were made by PCR amplifying the DNA fragments of each corresponding domain (Nterminal, GBD, FH3 and Cterminal) and then subcloning it into the pEGFPC-1 vector (Clontech) (Figure 4.2).

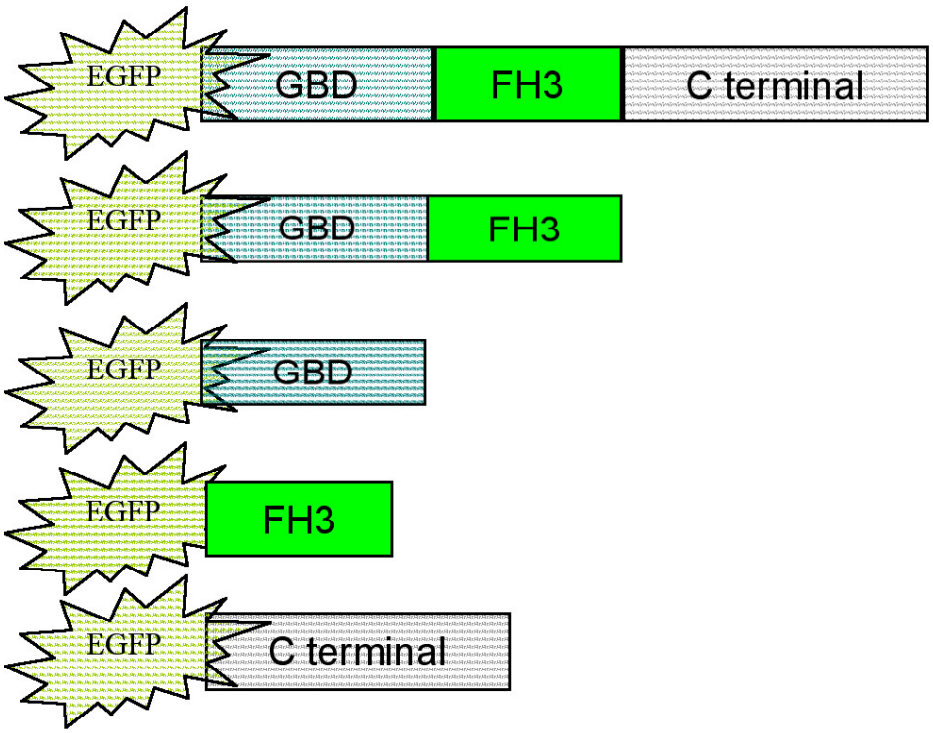

Figure 4.2: Deletion mutant constructs of Mwh used in this assay. All the constructs were tagged with EGFP at the N terminal end. Full length Mwh consisted of GBD, FH3 and C terminal domains. Deletion mutant constructs of Mwh were made carrying only the N terminal, GBD, FH3 and C terminal domain (each tagged with EGFP at the N terminus).

Although Mwh does not have a vertebrate homolog, deletion mutants were overexpressed and analysed in mammalian Swiss 3T3 fibroblast cells, as it has a distinct actin cytoskeleton structure. Cells were transfected with any one of the four different deletion mutant constructs of Mwh, and the full length Mwh (Strutt and Warrington, 2008) construct along with the empty vector served as controls (tissue culture and transfection method are discussed in detail in chapter 4 “Material and methods”). After transfection and immunostaining the phenotype of each construct was rated blindly for various parameters and scored for either the absence or presence of a complete phenotype or else for the presence of an intermediate phenotype of each of the parameters. Each and every experiment was repeated 5 times (see Table 4.2).

Actin Phenotype rating chart:

Phenotypes looked for	Present/normal	Absent/Abnormal	Medium/Intermediate phenotype
Stress Fibres	Y/N	Y/N	Y/N
Actin Ruffles	Y/N	Y/N	Y/N
Cell Shape	Y/N	Y/N	Y/N
Cell Size	Y/N	Y/N	Y/N

Table 4.1: Chart showing the parameters selected for rating each cell in this assay. Each cell was looked into for the above-mentioned parameters and scored accordingly.

The GBD domain of Mwh causes stress fibres reduction in 3T3 cells:

To define the function of different domains of Mwh, I expressed the different deletion mutant constructs in Swiss 3T3 fibroblasts and compared them with control cells expressing EGFP alone. After transfecting cells, actin phenotype rating of each cell was quantitated by eye (in a blind scoring). It was found that cells transfected with GBD or the N terminal construct was able to reduce the stress fibre formation as compared to cells transfected with other constructs, untransfected cells or cells transfected with empty vector.

I tried to categorise the respective transfected cells into three different categories viz. 1.percentage of cells with complete absence of stress fibres, 2. Intermediate phenotype and 3. Normal stress fibers. It was found that cells transfected with N terminal or GBD deletion mutants of Mwh has 37% and 35% more cells with reduction of stress fibres as compared to the control empty vector (Table 4.1, Figure 4.3 and 4.5). Intermediate phenotype of actin stress fibres were in the range of 30% to 40 % in all mutant constructs along with control and was not significantly changed in any of them (Figure 4.5). As compared to the control batch, which showed 65% of cells with normal actin stress fibre organisation, GBD and N terminal deletion mutant batches had 28% and 23% of cells respectively showing normal stress fibres phenotype (Figure 4.5). Cells transfected with C terminal deletion construct behaved almost like wild type cells

in every experiment and the FH3 deletion construct transfected cells exhibited moderate phenotype in most cases (Figures 4.4 and 4.5). When a statistical analysis (one way ANOVA) was done (by taking 5 repetitions into account) the reduction of stress fibres was found to be highly significant in cells transfected with GBD and N terminal constructs as compared to the control (Figure 4.5). Other constructs (the FH3 and C terminal) were not able to show any significant reduction in stress fibre formation (as compared to the control) (Figure 4.5). C terminal Mwh construct caused negligible reduction in stress fibres as compared to others (behaving almost like the wild type control) and the FH3 Mwh construct had 15% more reduction in stress fibres than that of control empty vector, although not statistically significant (Figures 4.4 and 4.5). Conversely the N terminal and GBD deletion mutants were able to cause approximately 30% more reduction in actin stress fibre formation when compared to the control (Figures 4.4 and 4.5).

These observations suggest that the GBD domain of Mwh is involved in actin stress fibre formation, further study may show that it does this by possibly interacting with members of Rho GTPases or interacting partners of Rho GTPases.

	Number of cells with:		
Different Constructs	**Normal Stress fibres**	**Medium stress fibres**	**Loss of stress fibres**
Control empty vector	65	30	5
N term	23	40	37
C term	53	33	16
GBD	28	37	35
FH3	37	30	13

Table 4.2: Raw data of different types of stress fibres obtained in the blind fold study on 3T3 cells after transfection with different deletion mutants of Mwh.

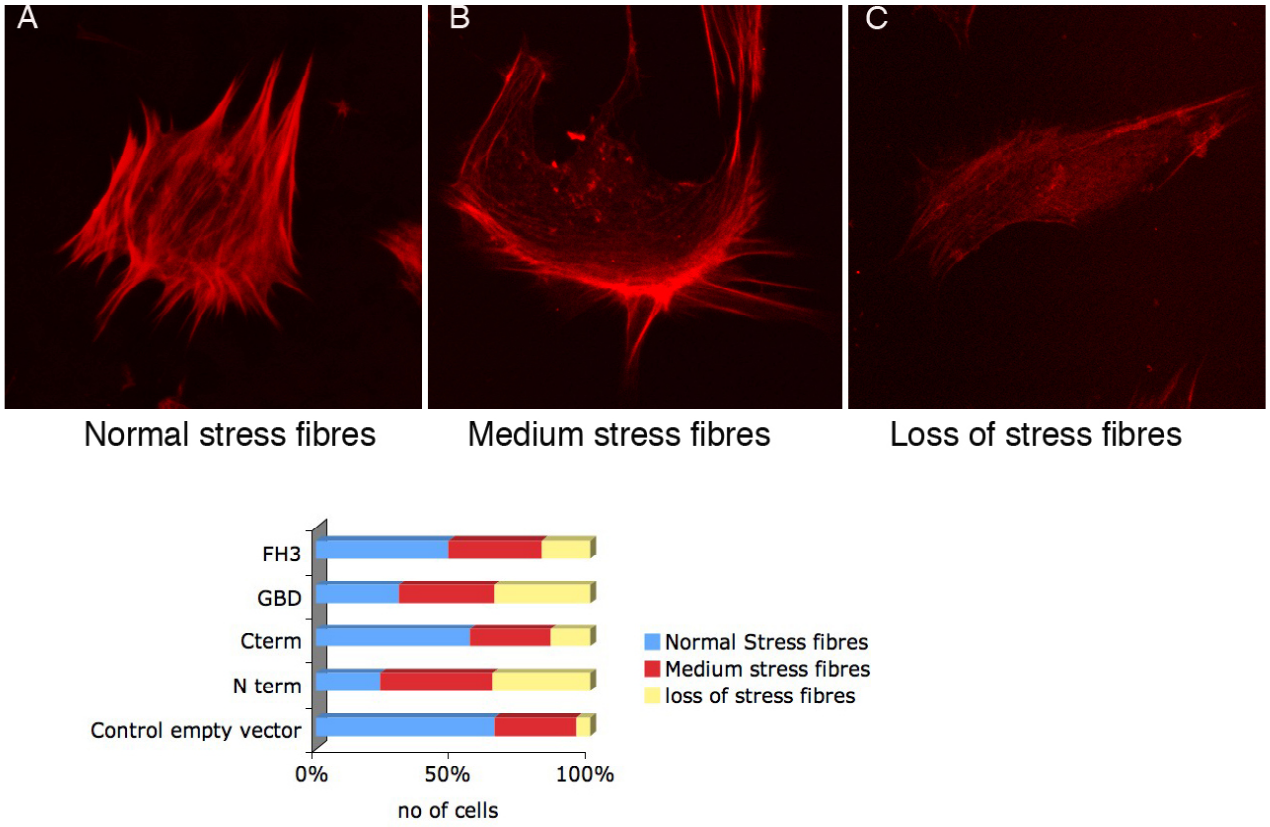

Figure 4.3: (A-C) The three different types of stress fibre phenotype quantified in 3T3 cells. (A) Presence of normal stress fibres, (B) presence of medium stress fibres (intermediate phenotype), (C) absence of stress fibres. (D) Horizontal bar graph of the relative frequency of actin stress fibre organization in different deletion mutant constructs of Mwh (normal stress fibres, blue; medium stress fibres, red; absence of stress fibres, yellow) scored in 5 different experiments (n= 100 for each constructs in each experimental set up).X axis of the graph shows percentage of cells belonging to different categories mentioned and Y axis of the graph shows different constructs used in this assay.

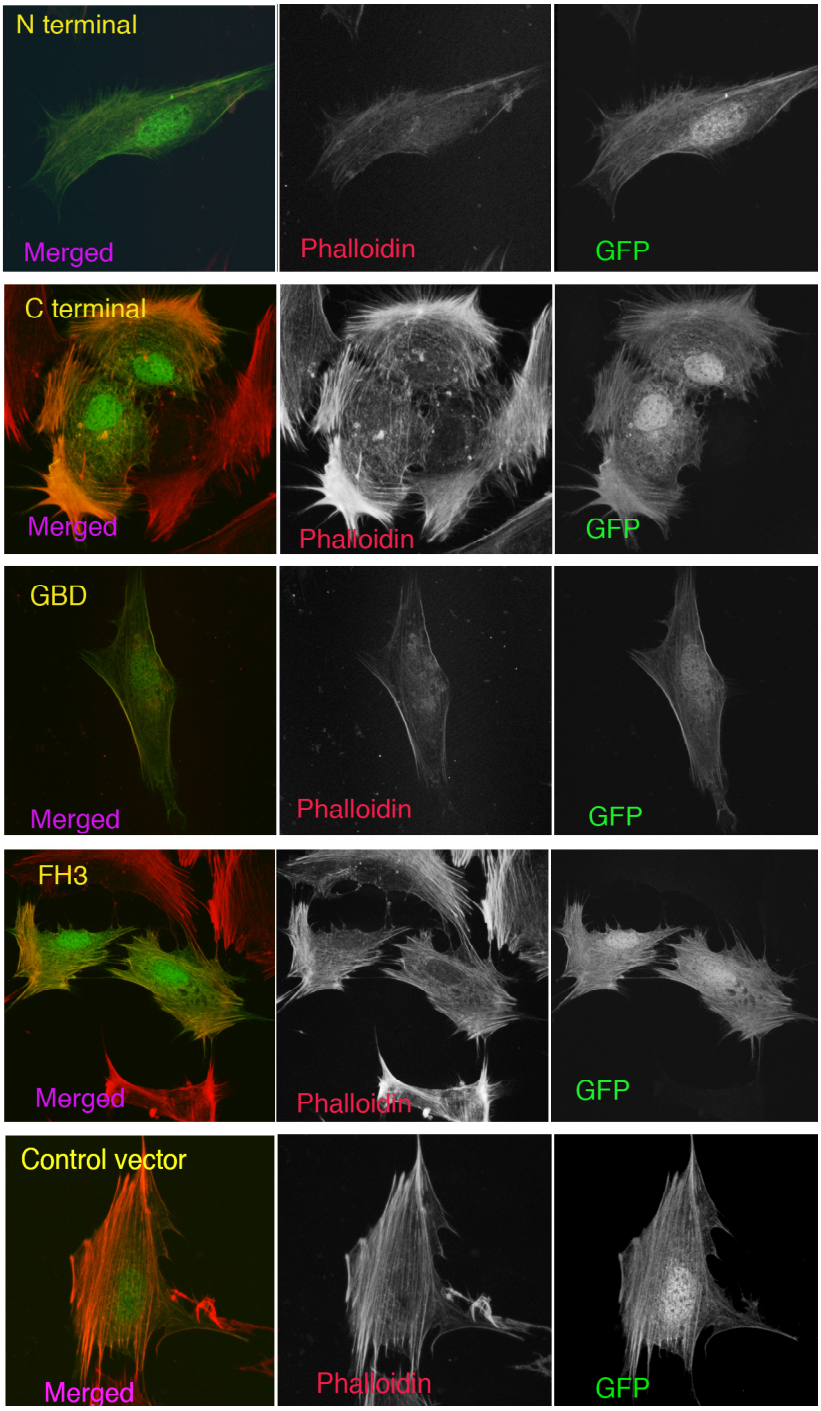

Figure 4.4: 3T3 cells transfected with different deletion mutants of Mwh constructs and stained for Phalloidin and GFP. Cells transfected with the N terminal or the GBD domain causes a reduction in stress fibres formation. Control vector and other deletion mutant constructs do not show any statistically significant stress fibre reduction (one Way ANOVA was used in this assay).

One-Way ANOVA for 5 Independent Samples

(A) Values Entered

Control(1)	Nterm (2)	Cterm (3)	GBD (4)	FH3 (5)
3	36	11	37	14
4	34	7	33	10
4	31	8	38	11
7	32	13	32	9
9	36	6	37	8

(B) Data Summary

	Samples					
	1	2	3	4	5	Total
N	5	5	5	5	5	25
Σ X	27	169	45	177	52	470
Mean	5.4	33.8	9	35.4	10.4	18.8
Σ X²	171	5733	439	6295	562	13200
Variance	6.3	5.2	8.5	7.3	5.3	181.8333
Std.Dev.	2.51	2.2804	2.9155	2.7019	2.3022	13.4846
Std.Err.	1.1225	1.0198	1.3038	1.2083	1.0296	2.6969

(C) ANOVA Summary

Source	SS	df	MS	F	P
Treatment [between groups]	4233.6	4	1058.4	162.33	<.0001
Error	130.4	20	6.52		
Ss/Bl					
Total	4364	24			

(D) Tukey HSD Test (test for significance)

HSD[.05]=4.85; HSD[.01]=6.06
M1(Control) vs M2 (N term) P<.01
M(Control) vs M3 (Cterm) nonsignificant
M1(Control) vs M4 (GBD) P<.01
M1 (Control)vs M5(FH3) P<.05
M2 vs M3 P<.01
M2 vs M4 nonsignificant
M2 vs M5 P<.01
M3 vs M4 P<.01
M3 vs M5 nonsignificant
M4 vs M5 P<.01

HSD = the absolute [unsigned] difference between any two sample means required for significance at the designated level. HSD[.05] for the .05 level; HSD[.01] for the .01 level.

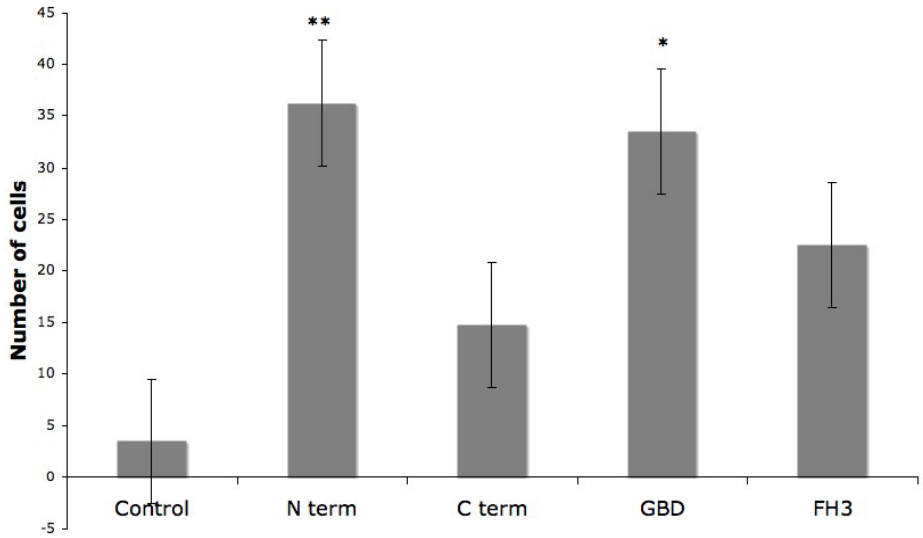

Figure 4.5: Analysis of data with one way ANOVA test with 5 independent samples (Control, Nterm, Cterm, GBD and FH3) and graphical representation of actin stress fibre reduction in each Mwh deletion mutant construct. Error bar represents standard error; each experiment is repeated 5 times and averaged for each construct (n= 100, in each case). X-axis of the graph represents phenotype shown by different deletion mutants and Y-axis of the graph shows total number of cells showing the phenotype. The reduction of stress fibre in N terminal and GBD deletion mutant was found to be statistically significant (in the case of N terminal and GBD $p < 0.01$ and in the case of FH3 the p value was found to be 0.05).

Formation of actin ruffles in GBD Mwh construct:

The GBD construct of Mwh when expressed in 3T3 cells significantly reduced stress fibres, but was found to form long actin ruffle like membranous projections from the cell periphery. Actin ruffles are Rac1 induced membranous projections composed of F actin filaments (Ridley *et al.,* 1992). But the increase in actin ruffles by the GBD deletion mutant construct was found to be not statistically significant (Figure 4.6). As compared to the controls used, 23% more cells transfected with GBD deletion mutant had long actin like ruffles (Figure 4.6). Cells transfected with the N terminal deletion mutant construct also had higher number of actin ruffles in them (increased by 14% as compared to the control) and cells transfected with FH3 deletion mutant had a 12% increase in actin ruffle formation, but none of the constructs could cause a significant increase in actin ruffles formation as compared to the control in this assay (Figure 4.6). No noteworthy actin ruffle formation was detected in the C terminal deletion mutant construct (Figure 4.6). Therefore I conclude that although GBD Mwh construct were found to have more actin ruffles when examined by eye, the change was not statistically significant (by one way ANOVA test, raw data not shown).

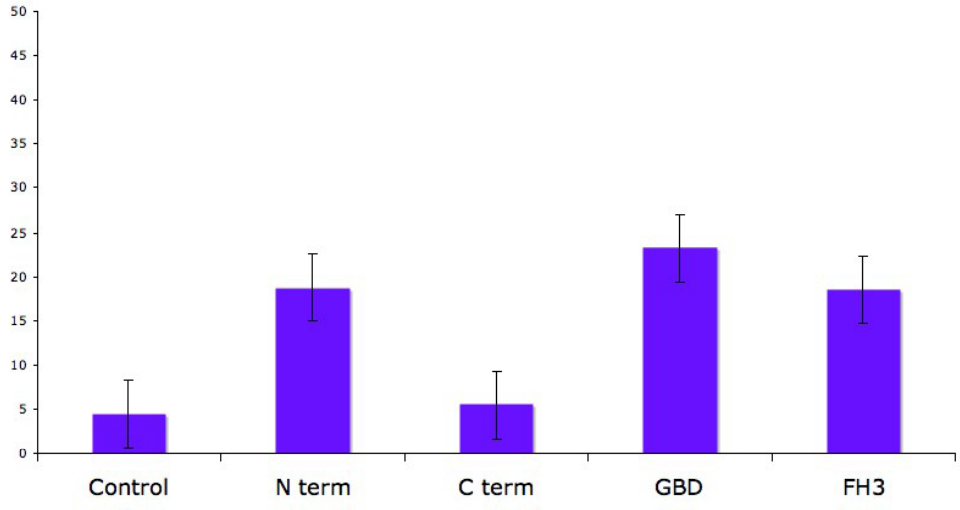

Figure 4.6: Graphical representation of the percentage of actin ruffles present in each construct. Error bar represents Standard error, each experiment was repeated 5 times and averaged for each construct (n= 100, in each case). X-axis of the graph represents phenotype shown by different deletion mutants and Y-axis of the graph shows total number of cells showing the phenotype. As compared to the control some of the deletion mutant constructs of Mwh shows an increase in actin ruffle formation from the cell periphery, which was found to be not significant in my assay (by one way ANOVA test).

Role of Mwh deletion mutant in controlling cell size/ morphology:

Although some of the deletion mutants were able to show altered cell morphology frequently (such as presence of abnormally flattened cells or large round cells), when cell morphology and cell size of the transfected cells in the assay were investigated, to find out whether any of the domains of Mwh are involved in providing distinct cell morphology or maintaining viability of the cell, the overall cell morphology/size found in different deletion constructs was not affected significantly as compared to the control (Figures 4.7 and 4.8).This suggests Mwh deletion mutant proteins may not be causing any change in overall cell shape and size when overexpressed in 3T3 cells or may not be detectable in my experimental assay.

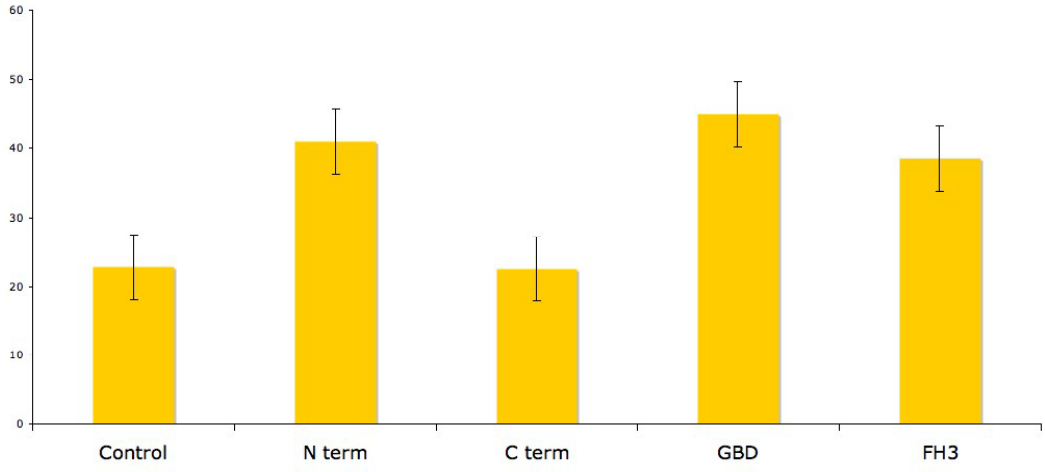

Figure 4.7: Graphical representation of percentage of cells with abnormal morphology present in each constructs. Error bar represents Standard error, each experiment was repeated 5 times and averaged for each construct (n= 100, in each case). X-axis of the graph represents phenotype shown by different deletion mutants and Y-axis of the graph shows total number of cells showing the phenotype. As compared to the control vector none of the deletion mutants could show a significant change in cell morphology my assay (by one way ANOVA test). .

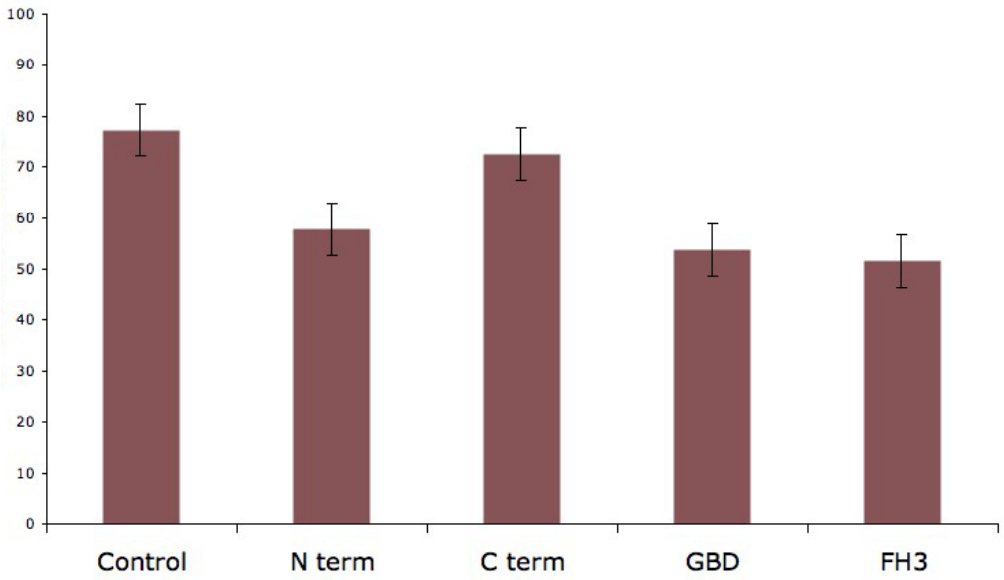

Figure 4.8: Graphical representation of percentage of cells with abnormal size (small cells) present in each constructs. Error bar represents Standard error, each experiment was repeated 5 times and averaged for each construct (n= 100, in each case). X-axis of the graph represents phenotype shown by different deletion mutants and Y-axis of the graph shows total number of cells showing the phenotype. As compared to the control vector none of the deletion mutants could show a significant change in cell morphology my assay (by one way ANOVA test). .

Thus, taken together, these results indicate that in Swiss 3T3 Fibroblast cells either the GBD domain or the N terminal domain (possibly due to the presence of GBD) of Mwh is able to significantly reduce the formation of actin stress fibres.

Discussion:

Expression of N terminal and GBD deletion constructs of Mwh in 3T3 cells induced a reduction in total actin stress fibre numbers, a phenotype which is similar to the one exhibited by RhoA mutant cells (Ridley and Hall, 1992). No significant changes were found with other deletion mutant (C terminal or FH3) or control (empty vector) constructs. Reduction of stress fibres by the N terminal and the GBD domain suggest a possible interaction between GBD of *Drosophila* Mwh and RhoA in mammalian cells.

Based on the results, I propose that binding of Mwh to RhoA protein via its GBD domain and the sequestering of the activated RhoA could prevent the later from

interacting with its downstream targets (such as myosin, alpha actinin, palladin, or downstream effectors of Rho such as dia). Thus RhoA might play a dominant negative role in this interaction resulting in actin stress fibre reduction.

Another plausible explanation is that RhoA protein and the GBD domain of Mwh are competing against each other simultaneously to bind to the stress fibres and to other interacting proteins associated with this process. But in the presence of excess amounts of GBD, RhoA might not be able to bind to its interacting partners resulting in the reduction of stress fibres. As previously noted in a conventional formin, binding of Rho GTPases to the GBD domain increases activity of the formin by reducing autoinhibition and releases the DAD domain containing FH2 for actin polymerization. In this particular scenario it is also possible that, although Rho GTPases are binding to GBD to reduce its function, the pool of available GBD domains in a cell is larger as compared to that of endogenous RhoA, therefore not all of the GBD is relived of its autoinhibition, eventually leading to reduction of actin stress fibres. Taken together my results indicate that the GBD domain of Mwh has a unique function in mammalian 3T3 cells in actin stress fibre formation and thus regulating the actin cytoskeleton.

Future Directions:

Some of the useful objectives of future studies will be to look at the total level of RhoA *in vivo* in the absence and presence of Mwh and colocalisation of RhoA with different deletion mutants of Mwh in 3T3 cells. Physical interaction study (co-IP) of Mwh with mammalian RhoA could also provide some clue about the interaction. Since Rho GTPases may participate in crosstalk and operates simultaneously in a number of different signalling pathways (Burridge, 1999), other notable Rho GTPases (Rac1, cdc42) could also be used in the interaction assay to gain insight of Mwh and Rho GTPases interaction in mammalian cells.

As the N terminal end of a conventional formin exhibits an autoinhibitory effect, it would also be interesting to check whether Mwh also possesses this kind of

autoinhibition due to the presence of the GBD domain at the N terminal end (by pull down assays), which will give us insight about the function of the GBD domain in Mwh.

Finally as Mwh does not have any vertebrate homologs, it would be important to examine the effect of different deletion mutants of Mwh in a *Drosophila* cell line. Although *Drosophila* cell lines do not have a distinct actin cytoskeleton as that of 3T3 cells, previous data showed Mwh causes formation of projections from the *Drosophila* S2 cell boundary and loss of actin bundles at the cell periphery (Strutt and Warrington, 2008). It was also seen that cells transfected with full-length Mwh construct causes formation of filopodia like extensions in the S2 cells (Strutt and Warrington, 2008). Further study with the deletion mutants in S2 cells can provide some useful insight about the role of different domains of Mwh in regulating the *Drosophila* actin cytoskeleton.

Another potential assay could be to look for potential interactions between other *Drosophila* formins and Mwh in cells of *Drosophila* origin using similar type of deletion mutants of Mwh. Obvious candidates for this study would be *dia, Daam, Formin 3* or any other formins present in *Drosophila.*

In conclusion, my result provides evidence that the GBD domain of Mwh shows a novel function in mammalian 3T3 cells by reducing the actin stress fibre formation suggesting a possible interaction of RhoA and Mwh. Further studies may provide some insights on the mechanism and function of Mwh in regulating actin cytoskeleton along with Rho GTPases.

General Discussion:

The aim of my thesis was to find out the role of PCP effector protein Mwh in the formation of a single distally pointed trichome in the *Drosophila* wing. To start with I first did an *in vivo* RNAi screen in the *Drosophila* wing with around 180 genes which were previously reported by our lab to produce multiple hairs (H.Strutt, C. Thomas unpublished data).

Those genes were further looked at by crossing the RNAi lines corresponding to each gene with a wing specific driver (*ptc-Gal4, UAS- Dcr2*) and immunostaining with Mwh protein in the *Drosophila* pupal wing just before trichome formation (32 hrs at 25ºC). A number of hits were found in my screen to regulate Mwh localisation by either increasing or decreasing Mwh protein levels. I then further tried to validate these hits with another independent set of RNAi line from the KK source of VDRC, which are designed to have less off targets effects and also are inserted at the same position to reduce the positional effect of other nearby genes.

Genes such as *Rab23, Tsp29Fb, Mo25, c12.1, cip4, staufen, microtubule star, septin 2, and pnut* were found to alter the distribution of Mwh protein in the screen and may therefore regulate it directly. Among them *staufen, microtubule star, septin 2, pnut* were found to increase and *Rab23, Tsp29Fb, Mo25, c12.1, cip4* were found to decrease Mwh protein level when knocked down by RNAi. Additionally, other genes were found which appeared to have a role in regulating cell size, timing of trichome formation and trichome morphology.

Among the hits which caused a decrease in Mwh localization, *Rab23*, a putative vesicular trafficking protein, which belongs to the Rab family of small GTPases caused a very strong reduction of Mwh (Fig 3.8). This was further proved by another independent set of RNAi line from VDRC. Rab23 was found to produce multiple hairs in the *Drosophila* wing when mutated and increased apical actin

level also were seen at the pupal wing of Rab23 mutant flies which is similar to PCP effector protein mutation (Pataki et al., 2010). PCP core protein Pk was found to associate with Rab23 in the apicoproximal region of the wing cell although no such association was seen with any of the effector proteins (In, Fy, Frtz and Mwh). As Rab23 mutants phenocopies PCP effector mutation and it regulates Mwh localisation in the pupal wing, it will be interesting to study the role of Rab23 in Mwh localisation and function. Further study may reveal the significance of vesicular trafficking and trafficking related proteins (such as Rab23) in PCP establishment and propagation.

Staufen is one of the hits which caused a stong increase in Mwh when knocked down by RNAi in my screen. This phenotype was further confirmed by another independent RNAi line of Staufen from the KK source. One of the widely studied roles of Staufen is actin mediated mRNA transport (Micklem *et al.,* 2000). Although the exact role played by Staufen in regulating Mwh still remains elusive, it is possible that in the absence of Staufen, Mwh is either not transported properly or as Staufen is a member of the RNAi machinery, it somehow down regulates a second gene which in turn causes accumulation of Mwh.

In case of other hits of my screen, validation with another independent set of line was either not possible (due to absence of other RNAi lines) or not confirmatory (due to the lines being not strong enough) to conclude their effect in Mwh localisation. Loss of function study of to those genes can shed some useful information about their role in Mwh localisation.

One of the drawback of the screen was around 2% of the total lines which caused a decrease in Mwh also produced large cells. I was unable to identify whether these genes causes large cells and also regulate Mwh localisation in the *Drosophila* wing. When I tried overexpressing UAS CyclinE to reduce the large cells and reexamine Mwh localisation, instead of reducing the large cell phenotype it caused an increase in the size of the cells. Therefore, it was not

possible to dissect out the role of those genes in Mwh localisation and function under my experimental conditions.

It is also possible that genes which regulates Mwh localisation might not phenocopy the multiple wing hair phenotype seen in *mwh* and other PCP effectors which arises the possibility that I might have not looked at all the potential genes which could regulate Mwh in the screen. Another potential drawback of the screen is genes (if any) which act downstream of Mwh cannot be find as hits in my experimental condition.

In spite of having some drawbacks , the *in vivo* RNAi screen in the *Drosophila* wing was the most efficient one to find out novel regulators of PCP effector protein Mwh. Other experimental approaches such as yeast two hybrid, gel shift assay with *Drosophila* kinases or *in vitro* siRNA mediated high throughput cellular assays could also have been used as alternate approaches, but *in vivo* RNAi was the only way to find out novel *in vivo* regulators of Mwh in *Drosophila*.

Mwh is a formin like protein with an undefined C terminal domain and a GBD and FH3 domain at its N terminus (Strutt and Warrington, 2008; Yan et al., 2008). To find out the roles of the GBD, FH3 and C terminal domain of Mwh, I made a number of deletion mutant constructs tagged with GFP. These constructs were then transfected to mammalian 3T3 cells to find out whether they regulate the well defined actin cytoskeleton structure of the 3T3 cells. The GBD deletion mutant of Mwh was found to cause significant reduction of actin stress fibres. RhoA, a very well studied small RhoGTPase is known to regulate the stress fibre formation in cells (Ridley and Hall, 1992) which hints at a possible interaction between the GBD domain of Mwh and RhoA.

Expression of the N terminal domain of Mwh which consists of the GBD and the FH3 domain in 3T3 cells could also induce a reduction in actin stress fibre formation. But FH3 domain alone cannot significantly reduce the actin stress fibre

formation suggesting the role of the GBD domain in regulating the actin stress fibre formation in 3T3 cells. No significant changes were found with other deletion mutant (C terminal) or control (empty vector) constructs.

Further studies can provide some useful insight on how the GBD domain of Mwh regulates the actin cytoskeleton by inhibiting stress fibre formation. It is possible that binding of Mwh to RhoA via its GBD domain sequesters the activated RhoA which in turn prevents the later from interacting with its downstream targets (such as myosin, alpha actinin, palladin, or downstream effectors of Rho such as dia). Thus RhoA might play a dominant negative role in this interaction resulting in actin stress fibre reduction.

Another possibility is that RhoA and the GBD domain of Mwh are competing against each other simultaneously to bind to the stress fibres and to other interacting proteins associated with this process and in the presence of excess amounts of GBD, RhoA might not be able to bind to its interacting partners resulting in the reduction of stress fibres. As previously noted in a conventional formin, binding of Rho GTPases to the GBD domain increases activity of the formin by reducing autoinhibition and releases the DAD domain containing FH2 for actin polymerization. In this particular scenario it is also possible that, although Rho GTPases are binding to GBD to reduce its function, the pool of available GBD domains in a cell (when I overexpress GBD) is larger as compared to that of endogenous RhoA, therefore not all of the GBD is relived of its autoinhibition, eventually leading to reduction of actin stress fibres. Taken together my results indicate that the GBD domain of Mwh has an unique function in mammalian 3T3 cells in actin stress fibre formation and thus regulating the actin cytoskeleton.

One obvious drawback of this study is that Mwh does not have a mammalian homolog. In the mammalian cells reduction of stress fibres by the GBD domain of Mwh could also be due to increase in other unknown proteins which occurs due

to the overexpression of the GBD domain. Another possible drawback is I have looked at the actin cytoskeleton phenotype of Mwh in mammalian 3T3 cells as they have a very well defined actin cytoskeleton structure. But studying the effect of these deletion mutant constructs of Mwh in *Drosophila* S2 cells could provide more useful insight about the function of different domains of Mwh in regulating PCP in *Drosophila*.

In conclusion, my thesis work has contributed in finding out potential novel regulators of Mwh in the *Drosophila* wing which will help to fill the gaps in our knowledge in understanding how downstream effector proteins of the PCP pathway mediates the formation of distally pointed trichomes in the *Drosophila* wing by interacting with the actin cytoskeleton. Also the *in vitro* work in mammalian 3T3 cells provides some useful clues on the probable mechanism by which Mwh might regulate the actin cytoskeleton. It also hints at the possible function of the GBD domain of Mwh.

Further study with loss of function mutant analysis *in vivo* and biochemical analysis *in vitro* can provide better understanding of the pathway that leads to the formation of a single distally pointing trichome downstream of the core PCP cues, and also how Mwh regulates this pathway by modifying the actin cytoskeleton.

Bibliography

Adler, P. N., Liu, J., Charlton, J., 2000. Cell size and the morphogenesis of wing hairs in Drosophila. Genesis. 28, 82-91.

Adler, P. N., Vinson, C., Park, W. J., Conover, S., Klein, L., 1990. Molecular structure of frizzled, a Drosophila tissue polarity gene. Genetics. 126, 401-16.

Adler, P. N., Zhu, C., Stone, D., 2004. Inturned localizes to the proximal side of wing cells under the instruction of upstream planar polarity proteins. Curr Biol. 14, 2046-51.

Afshar, K., Stuart, B., Wasserman, S. A., 2000. Functional analysis of the Drosophila diaphanous FH protein in early embryonic development. Development. 127, 1887-97.

Amano, M., Chihara, K., Kimura, K., Fukata, Y., Nakamura, N., Matsuura, Y., Kaibuchi, K., 1997. Formation of actin stress fibers and focal adhesions enhanced by Rho-kinase. Science. 275, 1308-11.

Assemat, E., Bazellieres, E., Pallesi-Pocachard, E., Le Bivic, A., Massey-Harroche, D., 2008. Polarity complex proteins. Biochim Biophys Acta. 1778, 614-30.

Atwood, S. X., Prehoda, K. E., 2009. aPKC phosphorylates Miranda to polarize fate determinants during neuroblast asymmetric cell division. Curr Biol. 19, 723-9.

Axelrod, J. D., 2001. Unipolar membrane association of Dishevelled mediates Frizzled planar cell polarity signaling. Genes Dev. 15, 1182-7.

Bao, J., Jana, S. S., Adelstein, R. S., 2005. Vertebrate nonmuscle myosin II isoforms rescue small interfering RNA-induced defects in COS-7 cell cytokinesis. J Biol Chem. 280, 19594-9.

Bastock, R., Strutt, H., Strutt, D., 2003. Strabismus is asymmetrically localised and binds to Prickle and Dishevelled during Drosophila planar polarity patterning. Development. 130, 3007-14.

Boutros, M., Ahringer, J., 2008. The art and design of genetic screens: RNA interference. Nat Rev Genet. 9, 554-66.

Brand, A. H., Perrimon, N., 1993. Targeted gene expression as a means of altering cell fates and generating dominant phenotypes. Development. 118, 401-15.

Brock, J., Midwinter, K., Lewis, J., Martin, P., 1996. Healing of incisional wounds in the embryonic chick wing bud: characterization of the actin pursestring and demonstration of a requirement for Rho activation. J Cell Biol. 135, 1097-107.

Burridge, K., 1999. Crosstalk between Rac and Rho. Science. 283, 2028-9.

Byers, H. R., White, G. E., Fujiwara, K., 1984. Organization and function of stress fibers in cells in vitro and in situ. A review. Cell Muscle Motil. 5, 83-137.

Casal, J., Lawrence, P. A., Struhl, G., 2006. Two separate molecular systems, Dachsous/Fat and Starry night/Frizzled, act independently to confer planar cell polarity. Development. 133, 4561-72.

Castrillon, D. H., Wasserman, S. A., 1994. Diaphanous is required for cytokinesis in Drosophila and shares domains of similarity with the products of the limb deformity gene. Development. 120, 3367-77.

Cereijido, M., Contreras, R. G., Shoshani, L., 2004. Cell adhesion, polarity, and epithelia in the dawn of metazoans. Physiol Rev. 84, 1229-62.

Choi, K. W., Benzer, S., 1994. Rotation of photoreceptor clusters in the developing Drosophila eye requires the nemo gene. Cell. 78, 125-36.

Chou, Y. H., Chien, C. T., 2002. Scabrous controls ommatidial rotation in the Drosophila compound eye. Dev Cell. 3, 839-50.

Chrzanowska-Wodnicka, M., Burridge, K., 1996. Rho-stimulated contractility drives the formation of stress fibers and focal adhesions. J Cell Biol. 133, 1403-15.

Collier, S., Gubb, D., 1997. Drosophila tissue polarity requires the cellautonomous activity of the fuzzy gene, which encodes a novel transmembrane protein. Development. 124, 4029-37.

Collier, S., Lee, H., Burgess, R., Adler, P., 2005. The WD40 repeat protein fritz links cytoskeletal planar polarity to frizzled subcellular localization in the Drosophila epidermis. Genetics. 169, 2035-45.

Copeland, J. W., Treisman, R., 2002. The diaphanous-related formin mDia1 controls serum response factor activity through its effects on actin polymerization. Mol Biol Cell. 13, 4088-99.

Das, G., Jenny, A., Klein, T. J., Eaton, S., Mlodzik, M., 2004. Diego interacts with Prickle and Strabismus/Van Gogh to localize planar cell polarity complexes. Development. 131, 4467-76.

de la Pompa, J. L., James, D., Zeller, R., 1995. Limb deformity proteins during avian neurulation and sense organ development. Dev Dyn. 204, 156-67.

Dickinson, A. J., Sive, H. L., 2009. The Wnt antagonists Frzb-1 and Crescent locally regulate basement membrane dissolution in the developing primary mouth. Development. 136, 1071-81.

Dietzl, G., Chen, D., Schnorrer, F., Su, K. C., Barinova, Y., Fellner, M., Gasser, B., Kinsey, K., Oppel, S., Scheiblauer, S., Couto, A., Marra, V., Keleman, K., Dickson, B. J., 2007. A genome-wide transgenic RNAi library for conditional gene inactivation in Drosophila. Nature. 448, 151-6.

Djiane, A., Riou, J., Umbhauer, M., Boucaut, J., Shi, D., 2000. Role of frizzled 7 in the regulation of convergent extension movements during gastrulation in Xenopus laevis. Development. 127, 3091-100.

Dow, L. E., Humbert, P. O., 2007. Polarity regulators and the control of epithelial architecture, cell migration, and tumorigenesis. Int Rev Cytol. 262, 253-302.

Eaton, S., Simons, K., 1995. Apical, basal, and lateral cues for epithelial polarization. Cell. 82, 5-8.

Eaton, S., Wepf, R., Simons, K., 1996. Roles for Rac1 and Cdc42 in planar polarization and hair outgrowth in the wing of Drosophila. J Cell Biol. 135, 1277-89.

Emmons, S., Phan, H., Calley, J., Chen, W., James, B., Manseau, L., 1995. Cappuccino, a Drosophila maternal effect gene required for polarity of the egg and embryo, is related to the vertebrate limb deformity locus. Genes Dev. 9, 2482-94.

Etienne-Manneville, S., Hall, A., 2002. Rho GTPases in cell biology. Nature. 420, 629-35.

Evangelista, M., Zigmond, S., Boone, C., 2003. Formins: signaling effectors for assembly and polarization of actin filaments. J Cell Sci. 116, 2603-11.
Fang, X., Adler, P. N., 2010. Regulation of cell shape, wing hair initiation and the actin cytoskeleton by Trc/Fry and Wts/Mats complexes. Dev Biol. 341, 360-74.

Fanto, M., Weber, U., Strutt, D. I., Mlodzik, M., 2000. Nuclear signaling by Rac and Rho GTPases is required in the establishment of epithelial planar polarity in the Drosophila eye. Curr Biol. 10, 979-88.

Feiguin, F., Hannus, M., Mlodzik, M., Eaton, S., 2001. The ankyrin repeat protein Diego mediates Frizzled-dependent planar polarization. Dev Cell. 1, 93-101.

Feltri, M. L., Suter, U., Relvas, J. B., 2008. The function of RhoGTPases in axon ensheathment and myelination. Glia. 56, 1508-17.

Fire, A., Xu, S., Montgomery, M. K., Kostas, S. A., Driver, S. E., Mello, C. C., 1998. Potent and specific genetic interference by double-stranded RNA in Caenorhabditis elegans. Nature. 391, 806-11.

Fradkin, L. G., Kamphorst, J. T., DiAntonio, A., Goodman, C. S., Noordermeer, J. N., 2002. Genomewide analysis of the Drosophila tetraspanins reveals a subset with similar function in the formation of the embryonic synapse. Proc Natl Acad Sci U S A. 99, 13663-8.

Fricke, R., Gohl, C., Dharmalingam, E., Grevelhorster, A., Zahedi, B., Harden, N., Kessels, M., Qualmann, B., Bogdan, S., 2009. Drosophila Cip4/Toca-1 integrates membrane trafficking and actin dynamics through WASP and SCAR/WAVE. Curr Biol. 19, 1429-37.

Geng, W., He, B., Wang, M., Adler, P. N., 2000. The tricornered gene, which is required for the integrity of epidermal cell extensions, encodes the Drosophila nuclear DBF2-related kinase. Genetics. 156, 1817-28.

Gerdes, J. M., Davis, E. E., Katsanis, N., 2009. The vertebrate primary cilium in development, homeostasis, and disease. Cell. 137, 32-45.

Goode, B. L., Eck, M. J., 2007. Mechanism and function of formins in the control of actin assembly. Annu Rev Biochem. 76, 593-627.

Goshima, G., Wollman, R., Goodwin, S. S., Zhang, N., Scholey, J. M., Vale, R. D., Stuurman, N., 2007. Genes required for mitotic spindle assembly in Drosophila S2 cells. Science. 316, 417-21.

Gray, R. S., Abitua, P. B., Wlodarczyk, B. J., Szabo-Rogers, H. L., Blanchard, O., Lee, I., Weiss, G. S., Liu, K. J., Marcotte, E. M., Wallingford, J. B., Finnell, R. H., 2009. The planar cell polarity effector Fuz is essential for targeted membrane trafficking, ciliogenesis and mouse embryonic development. Nat Cell Biol. 11, 1225-32.

Grebe, M., 2004. Ups and downs of tissue and planar polarity in plants. Bioessays. 26, 719-29.

Gubb, D., Garcia-Bellido, A., 1982. A genetic analysis of the determination of cuticular polarity during development in Drosophila melanogaster. J Embryol

Exp Morphol. 68, 37-57.

Guo, N., Hawkins, C., Nathans, J., 2004. Frizzled6 controls hair patterning in mice. Proc Natl Acad Sci U S A. 101, 9277-81.

Habas, R., Kato, Y., He, X., 2001. Wnt/Frizzled activation of Rho regulates vertebrate gastrulation and requires a novel Formin homology protein Daam1. Cell. 107, 843-54.

Hall, A., 1998. Rho GTPases and the actin cytoskeleton. Science. 279,509-14.
Haramis, A. G., Brown, J. M., Zeller, R., 1995. The limb deformity mutation disrupts the SHH/FGF-4 feedback loop and regulation of 5' HoxD genes during limb pattern formation. Development. 121, 4237-45.

Hariharan, I. K., Hu, K. Q., Asha, H., Quintanilla, A., Ezzell, R. M., Settleman, J., 1995. Characterization of rho GTPase family homologues in Drosophila melanogaster: overexpressing Rho1 in retinal cells causes a late developmental defect. EMBO J. 14, 292-302.

He, B., Adler, P. N., 2002. The frizzled pathway regulates the development of arista laterals. BMC Dev Biol. 2, 7.

He, Y., Emoto, K., Fang, X., Ren, N., Tian, X., Jan, Y. N., Adler, P. N., 2005. Drosophila Mob family proteins interact with the related tricornered (Trc) and warts (Wts) kinases. Mol Biol Cell. 16, 4139-52.

Heisenberg, C. P., Tada, M., Rauch, G. J., Saude, L., Concha, M. L., Geisler, R., Stemple, D. L., Smith, J. C., Wilson, S. W., 2000. Silberblick/Wnt11 mediates convergent extension movements during zebrafish gastrulation. Nature. 405, 76-81.

Hergovich, A., Kohler, R. S., Schmitz, D., Vichalkovski, A., Cornils, H., Hemmings, B. A., 2009. The MST1 and hMOB1 tumor suppressors control human centrosome duplication by regulating NDR kinase phosphorylation. Curr Biol. 19, 1692-702.
Hertzog, M., Chavrier, P., 2011. Cell polarity during motile processes: keeping on track with the exocyst complex. Biochem J. 433, 403-9.

Heydeck, W., Zeng, H., Liu, A., 2009. Planar cell polarity effector gene Fuzzy regulates cilia formation and Hedgehog signal transduction in mouse. Dev Dyn. 238, 3035-42.

Higgs, H. N., 2005. Formin proteins: a domain-based approach. Trends Biochem Sci. 30, 342-53.

Hotulainen, P., Paunola, E., Vartiainen, M. K., Lappalainen, P., 2005.

Actindepolymerizing nfactor and cofilin-1 play overlapping roles in promoting rapid F-actin depolymerization in mammalian nonmuscle cells. Mol Biol Cell. 16, 649-64.

Ikeda, M., Mitsuda, N., Ohme-Takagi, M., 2009. Arabidopsis WUSCHEL is a bifunctional transcription factor that acts as a repressor in stem cell regulation and as an activator in floral patterning. Plant Cell. 21, 3493-505.

Jenny, A., Darken, R. S., Wilson, P. A., Mlodzik, M., 2003. Prickle and Strabismus form a functional complex to generate a correct axis during planar cell polarity signaling. EMBO J. 22, 4409-20.

Jessen, J. R., Topczewski, J., Bingham, S., Sepich, D. S., Marlow, F., Chandrasekhar, A., Solnica-Krezel, L., 2002. Zebrafish trilobite identifies new roles for Strabismus in gastrulation and neuronal movements. Nat Cell Biol. 4, 610-5.

Jiang, J., Hui, C. C., 2008. Hedgehog signaling in development and cancer. Dev Cell. 15, 801-12.

Johnson, D. I., 1999. Cdc42: An essential Rho-type GTPase controlling eukaryotic cell polarity. Microbiol Mol Biol Rev. 63, 54-105.

Karner, C., Wharton, K. A., Jr., Carroll, T. J., 2006. Planar cell polarity and vertebrate organogenesis. Semin Cell Dev Biol. 17, 194-203.

Katoh, K., Kano, Y., Amano, M., Kaibuchi, K., Fujiwara, K., 2001. Stress fiber organization regulated by MLCK and Rho-kinase in cultured human fibroblasts. Am J Physiol Cell Physiol. 280, C1669-79.

Kibar, Z., Vogan, K. J., Groulx, N., Justice, M. J., Underhill, D. A., Gros, P., 2001. Ltap, a mammalian homolog of Drosophila Strabismus/Van Gogh, is altered in the mouse neural tube mutant Loop-tail. Nat Genet. 28, 251-5.

Kilian, B., Mansukoski, H., Barbosa, F. C., Ulrich, F., Tada, M., Heisenberg, C. P., 2003. The role of Ppt/Wnt5 in regulating cell shape and movement during zebrafish gastrulation. Mech Dev. 120, 467-76.

Kleinebrecht, J., Selow, J., Winkler, W., 1982. The mouse mutant limbdeformity (ld). Anat Anz. 152, 313-24.

Knoblich, J. A., 2008. Mechanisms of asymmetric stem cell division. Cell. 132, 583-97.

Kolega, J., 2006. The role of myosin II motor activity in distributing myosin asymmetrically and coupling protrusive activity to cell translocation.

Mol Biol Cell. 17, 4435-45.

Kovar, D. R., 2006. Molecular details of formin-mediated actin assembly. Curr Opin Cell Biol. 18, 11-7.

Kovar, D. R., Harris, E. S., Mahaffy, R., Higgs, H. N., Pollard, T. D., 2006. Control of the assembly of ATP- and ADP-actin by formins and profilin. Cell. 124, 423-35.

Krasnow, R. E., Adler, P. N., 1994. A single frizzled protein has a dual function in tissue polarity. Development. 120, 1883-93.

Kureishi, Y., Kobayashi, S., Amano, M., Kimura, K., Kanaide, H., Nakano, T., Kaibuchi, K., Ito, M., 1997. Rho-associated kinase directly induces smooth muscle contraction through myosin light chain phosphorylation. J Biol Chem. 272, 12257-60.

Kuttenkeuler, D., Boutros, M., 2004. Genome-wide RNAi as a route to gene function in Drosophila. Brief Funct Genomic Proteomic. 3, 168-76.

Langanger, G., Moeremans, M., Daneels, G., Sobieszek, A., De Brabander, M., De Mey, J., 1986. The molecular organization of myosin in stress fibers of cultured cells. J Cell Biol. 102, 200-9.

Lawrence, P. A., Shelton, P. M., 1975. The determination of polarity in the developing insect retina. J Embryol Exp Morphol. 33, 471-86.

Lee, H., Adler, P. N., 2002. The function of the frizzled pathway in the Drosophila wing is dependent on inturned and fuzzy. Genetics. 160, 1535-47.

Leung, T., Chen, X. Q., Manser, E., Lim, L., 1996. The p160 RhoA-binding kinase ROK alpha is a member of a kinase family and is involved in the reorganization of the cytoskeleton. Mol Cell Biol. 16, 5313-27.

Lu, Q., Yan, J., Adler, P. N., 2010. The Drosophila planar polarity proteins inturned and multiple wing hairs interact physically and function together. Genetics. 185, 549-58.

Lu, X., Borchers, A. G., Jolicoeur, C., Rayburn, H., Baker, J. C., Tessier-Lavigne, M., 2004. PTK7/CCK-4 is a novel regulator of planar cell polarity in vertebrates. Nature. 430, 93-8.

Luo, H., Liu, X., Wang, F., Huang, Q., Shen, S., Wang, L., Xu, G., Sun, X., Kong, H., Gu, M., Chen, S., Chen, Z., Wang, Z., 2005. Disruption of palladin results in neural tube closure defects in mice. Mol Cell Neurosci. 29, 507-15.

Macara, I. G., Mili, S., 2008. Polarity and differential inheritance--universal attributes of life? Cell. 135, 801-12.

Mah, A. S., Jang, J., Deshaies, R. J., 2001. Protein kinase Cdc15 activates the Dbf2-Mob1 kinase complex. Proc Natl Acad Sci U S A. 98, 7325-30.

Manseau, L. J., Schupbach, T., 1989. cappuccino and spire: two unique maternal-effect loci required for both the anteroposterior and dorsoventral patterns of the Drosophila embryo. Genes Dev. 3, 1437-52.

Martin-Belmonte, F., Mostov, K., 2008. Regulation of cell polarity during epithelial morphogenesis. Curr Opin Cell Biol. 20, 227-34.

Matusek, T., Djiane, A., Jankovics, F., Brunner, D., Mlodzik, M., Mihaly, J., 2006. The Drosophila formin DAAM regulates the tracheal cuticle pattern through organizing the actin cytoskeleton. Development. 133, 957-66.

Matusek, T., Gombos, R., Szecsenyi, A., Sanchez-Soriano, N., Czibula, A., Pataki, C., Gedai, A., Prokop, A., Rasko, I., Mihaly, J., 2008. Formin proteins of the DAAM subfamily play a role during axon growth. J Neurosci. 28, 13310-9.

Mayr, T., Deutsch, U., Kuhl, M., Drexler, H. C., Lottspeich, F., Deutzmann, R., Wedlich, D., Risau, W., 1997. Fritz: a secreted frizzled-related protein that inhibits Wnt activity. Mech Dev. 63, 109-25.

McCaffrey, L. M., Macara, I. G., 2009. The Par3/aPKC interaction is essential for end bud remodeling and progenitor differentiation during mammary gland morphogenesis. Genes Dev. 23, 1450-60.

Micklem, D. R., Adams, J., Grunert, S., St Johnston, D., 2000. Distinct roles of two conserved Staufen domains in oskar mRNA localization and translation. EMBO J. 19, 1366-77.

Mii, Y., Taira, M., 2009. Secreted Frizzled-related proteins enhance the diffusion of Wnt ligands and expand their signalling range. Development. 136, 4083-8.

Millard, T. H., Sharp, S. J., Machesky, L. M., 2004. Signalling to actin assembly via the WASP (Wiskott-Aldrich syndrome protein)-family proteins and the Arp2/3 complex. Biochem J. 380, 1-17.

Minin, A. A., Kulik, A. V., Gyoeva, F. K., Li, Y., Goshima, G., Gelfand, V. I., 2006. Regulation of mitochondria distribution by RhoA and formins. J Cell Sci. 119, 659-70.

Mohr, S., Bakal, C., Perrimon, N., 2010. Genomic screening with RNAi: results and challenges. Annu Rev Biochem. 79, 37-64.

Montcouquiol, M., 2007. [Planar polarity in mammals: similarity and divergence with Drosophila Melanosgaster]. J Soc Biol. 201, 61-7.

Montcouquiol, M., Kelley, M. W., 2003. Planar and vertical signals control cellular differentiation and patterning in the mammalian cochlea. J Neurosci. 23, 9469-78.

Moseley, J. B., Sagot, I., Manning, A. L., Xu, Y., Eck, M. J., Pellman, D., Goode, B. L., 2004. A conserved mechanism for Bni1- and mDia1-induced actin assembly and dual regulation of Bni1 by Bud6 and profilin. Mol Biol Cell. 15, 896-907.

Nachury, M. V., Loktev, A. V., Zhang, Q., Westlake, C. J., Peranen, J., Merdes, A., Slusarski, D. C., Scheller, R. H., Bazan, J. F., Sheffield, V. C., Jackson, P. K., 2007. A core complex of BBS proteins cooperates with the GTPase Rab8 to promote ciliary membrane biogenesis. Cell. 129, 1201-13.
Naumanen, P., Lappalainen, P., Hotulainen, P., 2008. Mechanisms of actin stress fibre assembly. J Microsc. 231, 446-54.

Nelson, W. J., 2009. Remodeling epithelial cell organization: transitions between front-rear and apical-basal polarity. Cold Spring Harb Perspect Biol. 1, a000513.

Neufeld, T. P., Rubin, G. M., 1994. The Drosophila peanut gene is required for cytokinesis and encodes a protein similar to yeast putative bud neck filament proteins. Cell. 77, 371-9.

Niederman, R., Pollard, T. D., 1975. Human platelet myosin. II. In vitro assembly and structure of myosin filaments. J Cell Biol. 67, 72-92.

Otomo, T., Rosen, M. K., 2005. [Structure and function of Formin homology 2 domain]. Tanpakushitsu Kakusan Koso. 50, 1088-93.

Paladi, M., Tepass, U., 2004. Function of Rho GTPases in embryonic blood cell migration in Drosophila. J Cell Sci. 117, 6313-26.

Parast, M. M., Otey, C. A., 2000. Characterization of palladin, a novel protein localized to stress fibers and cell adhesions. J Cell Biol. 150, 643-56.

Park, T. J., Haigo, S. L., Wallingford, J. B., 2006. Ciliogenesis defects in embryos lacking inturned or fuzzy function are associated with failure of planar cell polarity and Hedgehog signaling. Nat Genet. 38, 303-11.

Park, W. J., Liu, J., Sharp, E. J., Adler, P. N., 1996. The Drosophila tissue polarity gene inturned acts cell autonomously and encodes a novel protein. Development. 122, 961-9.

Pataki, C., Matusek, T., Kurucz, E., Ando, I., Jenny, A., Mihaly, J., 2010. Drosophila Rab23 is involved in the regulation of the number and planar polarization of the adult cuticular hairs. Genetics. 184, 1051-65.

Pellegrin, S., Mellor, H., 2005. The Rho family GTPase Rif induces filopodia through mDia2. Curr Biol. 15, 129-33.

Peng, J., Wallar, B. J., Flanders, A., Swiatek, P. J., Alberts, A. S., 2003. Disruption of the Diaphanous-related formin Drf1 gene encoding mDia1 reveals a role for Drf3 as an effector for Cdc42. Curr Biol. 13, 534-45.

Petersen, J., Nielsen, O., Egel, R., Hagan, I. M., 1998. FH3, a domain found in formins, targets the fission yeast formin Fus1 to the projection tip during conjugation. J Cell Biol. 141, 1217-28.

Pruyne, D., Evangelista, M., Yang, C., Bi, E., Zigmond, S., Bretscher, A., Boone, C., 2002. Role of formins in actin assembly: nucleation and barbedend association. Science. 297, 612-5.

Qian, D., Jones, C., Rzadzinska, A., Mark, S., Zhang, X., Steel, K. P., Dai, X., Chen, P., 2007. Wnt5a functions in planar cell polarity regulation in mice. Dev Biol. 306, 121-33.

Quinlan, M. E., Hilgert, S., Bedrossian, A., Mullins, R. D., Kerkhoff, E., 2007. Regulatory interactions between two actin nucleators, Spire and Cappuccino. J Cell Biol. 179, 117-28.

Raff, M. C., Hart, I. K., Richardson, W. D., Lillien, L. E., 1990. An analysis of the cell-cell interactions that control the proliferation and differentiation of a bipotential glial progenitor cell in culture. Cold Spring Harb Symp Quant Biol. 55, 235-8.

Ren, N., Zhu, C., Lee, H., Adler, P. N., 2005. Gene expression during Drosophila wing morphogenesis and differentiation. Genetics. 171, 625-38.
Ridley, A. J., 1996. Rho: theme and variations. Curr Biol. 6, 1256-64.

Ridley, A. J., Hall, A., 1992. The small GTP-binding protein rho regulates the assembly of focal adhesions and actin stress fibers in response to growth factors. Cell. 70, 389-99.

Ridley, A. J., Hall, A., 1994. Signal transduction pathways regulating Rhomediated stress fibre formation: requirement for a tyrosine kinase. EMBO J.

13, 2600-10.

Rivero, F., Muramoto, T., Meyer, A. K., Urushihara, H., Uyeda, T. Q., Kitayama, C., 2005. A comparative sequence analysis reveals a common GBD/FH3-FH1-FH2-DAD architecture in formins from Dictyostelium, fungi and metazoa. BMC Genomics. 6, 28.

Rosales-Nieves, A. E., Johndrow, J. E., Keller, L. C., Magie, C. R., Pinto-Santini, D. M., Parkhurst, S. M., 2006. Coordination of microtubule and microfilament dynamics by Drosophila Rho1, Spire and Cappuccino. Nat Cell Biol. 8, 367-76.

Ross, A. J., May-Simera, H., Eichers, E. R., Kai, M., Hill, J., Jagger, D. J., Leitch, C. C., Chapple, J. P., Munro, P. M., Fisher, S., Tan, P. L., Phillips, H. M., Leroux, M. R., Henderson, D. J., Murdoch, J. N., Copp, A. J., Eliot, M. M., Lupski, J. R., Kemp, D. T., Dollfus, H., Tada, M., Katsanis, N., Forge, A., Beales, P. L., 2005. Disruption of Bardet-Biedl syndrome ciliary proteins perturbs planar cell polarity in vertebrates. Nat Genet. 37, 1135-40.

Sagot, I., Klee, S. K., Pellman, D., 2002. Yeast formins regulate cell polarity by controlling the assembly of actin cables. Nat Cell Biol. 4, 42-50.

Sakumura, Y., Tsukada, Y., Yamamoto, N., Ishii, S., 2005. A molecular model for axon guidance based on cross talk between rho GTPases. Biophys J. 89, 812-22.

Schwartzberg, P. L., 2007. Formin the way. Immunity. 26, 139-41.

Sharma, N., Berbari, N. F., Yoder, B. K., 2008. Ciliary dysfunction in developmental abnormalities and diseases. Curr Top Dev Biol. 85, 371-427.

Shimada, A., Nyitrai, M., Vetter, I. R., Kuhlmann, D., Bugyi, B., Narumiya, S., Geeves, M. A., Wittinghofer, A., 2004. The core FH2 domain of diaphanousrelated formins is an elongated actin binding protein that inhibits polymerization. Mol Cell. 13, 511-22.

Smith, L. A., Bukanov, N. O., Husson, H., Russo, R. J., Barry, T. C., Taylor, A. L., Beier, D. R., Ibraghimov-Beskrovnaya, O., 2006. Development of polycystic kidney disease in juvenile cystic kidney mice: insights into pathogenesis, ciliary abnormalities, and common features with human disease. J Am Soc Nephrol. 17, 2821-31.

Snaith, H. A., Armstrong, C. G., Guo, Y., Kaiser, K., Cohen, P. T., 1996. Deficiency of protein phosphatase 2A uncouples the nuclear and centrosome cycles and prevents attachment of microtubules to the kinetochore in Drosophila microtubule star (mts) embryos. J Cell Sci. 109 (Pt 13), 3001-12.

Stram, Y., Kuzntzova, L., 2006. Inhibition of viruses by RNA interference. Virus Genes. 32, 299-306.

Strutt, D., 2008. The planar polarity pathway. Curr Biol. 18, R898-902.

Strutt, D., 2009. Gradients and the specification of planar polarity in the insect cuticle. Cold Spring Harb Perspect Biol. 1, a000489.

Strutt, D., Strutt, H., 2007. Differential activities of the core planar polarity proteins during Drosophila wing patterning. Dev Biol. 302, 181-94.

Strutt, D., Warrington, S. J., 2008. Planar polarity genes in the Drosophila wing regulate the localisation of the FH3-domain protein Multiple Wing Hairs to control the site of hair production. Development. 135, 3103-11.

Strutt, D. I., 2001. Asymmetric localization of frizzled and the establishment of cell polarity in the Drosophila wing. Mol Cell. 7, 367-75.

Strutt, D. I., 2002. The asymmetric subcellular localisation of components of the planar polarity pathway. Semin Cell Dev Biol. 13, 225-31.

Strutt, D. I., Weber, U., Mlodzik, M., 1997. The role of RhoA in tissue polarity and Frizzled signalling. Nature. 387, 292-5.

Strutt, H., Strutt, D., 2005. Long-range coordination of planar polarity in Drosophila. Bioessays. 27, 1218-27.

Strutt, H., Strutt, D., 2008. Differential stability of flamingo protein complexes underlies the establishment of planar polarity. Curr Biol. 18, 1555-64.

Suzuki, A., Ohno, S., 2006. The PAR-aPKC system: lessons in polarity. J Cell Sci. 119, 979-87.

Tada, M., Smith, J. C., 2000. Xwnt11 is a target of Xenopus Brachyury: regulation of gastrulation movements via Dishevelled, but not through the canonical Wnt pathway. Development. 127, 2227-38.

Takeya, R., Sumimoto, H., 2003. Fhos, a mammalian formin, directly binds to F-actin via a region N-terminal to the FH1 domain and forms a homotypic complex via the FH2 domain to promote actin fiber formation. J Cell Sci. 116, 4567-75.

Tanaka, H., Takasu, E., Aigaki, T., Kato, K., Hayashi, S., Nose, A., 2004. Formin3 is required for assembly of the F-actin structure that mediates tracheal fusion in Drosophila. Dev Biol. 274, 413-25.

Taylor, J., Abramova, N., Charlton, J., Adler, P. N., 1998. Van Gogh: a new Drosophila tissue polarity gene. Genetics. 150, 199-210.

Totsukawa, G., Yamakita, Y., Yamashiro, S., Hartshorne, D. J., Sasaki, Y., Matsumura, F., 2000. Distinct roles of ROCK (Rho-kinase) and MLCK in spatial regulation of MLC phosphorylation for assembly of stress fibers and focal adhesions in 3T3 fibroblasts. J Cell Biol. 150, 797-806.

Tree, D. R., Shulman, J. M., Rousset, R., Scott, M. P., Gubb, D., Axelrod, J. D., 2002. Prickle mediates feedback amplification to generate asymmetric planar cell polarity signaling. Cell. 109, 371-81.

Usui, T., Shima, Y., Shimada, Y., Hirano, S., Burgess, R. W., Schwarz, T. L., Takeichi, M., Uemura, T., 1999. Flamingo, a seven-pass transmembrane cadherin, regulates planar cell polarity under the control of Frizzled. Cell. 98, 585-95.

Van Aelst, L., D'Souza-Schorey, C., 1997. Rho GTPases and signaling networks. Genes Dev. 11, 2295-322.

Van Aelst, L., Symons, M., 2002. Role of Rho family GTPases in epithelial morphogenesis. Genes Dev. 16, 1032-54.

Verkhovsky, A. B., Borisy, G. G., 1993. Non-sarcomeric mode of myosin II organization in the fibroblast lamellum. J Cell Biol. 123, 637-52.

Vinson, C. R., Adler, P. N., 1987. Directional non-cell autonomy and the transmission of polarity information by the frizzled gene of Drosophila. Nature. 329, 549-51.

Vinson, C. R., Conover, S., Adler, P. N., 1989. A Drosophila tissue polarity locus encodes a protein containing seven potential transmembrane domains. Nature. 338, 263-4.

Wallar, B. J., Alberts, A. S., 2003. The formins: active scaffolds that remodel the cytoskeleton. Trends Cell Biol. 13, 435-46.

Wallar, B. J., Stropich, B. N., Schoenherr, J. A., Holman, H. A., Kitchen, S. M., Alberts, A. S., 2006. The basic region of the diaphanous-autoregulatory domain (DAD) is required for autoregulatory interactions with the diaphanousrelated formin inhibitory domain. J Biol Chem. 281, 4300-7.

Wallingford, J. B., Rowning, B. A., Vogeli, K. M., Rothbacher, U., Fraser, S. E., Harland, R. M., 2000. Dishevelled controls cell polarity during Xenopus gastrulation. Nature. 405, 81-5.

Wang, C. C., Chan, D. C., Leder, P., 1997. The mouse formin (Fmn) gene: genomic structure, novel exons, and genetic mapping. Genomics. 39, 303-11.

Wang, F., Dai, J., Daum, J. R., Niedzialkowska, E., Banerjee, B., Stukenberg, P. T., Gorbsky, G. J., Higgins, J. M., 2010. Histone H3 Thr-3 phosphorylation by Haspin positions Aurora B at centromeres in mitosis. Science. 330, 231-5.

Wang, Y., Nathans, J., 2007. Tissue/planar cell polarity in vertebrates: new insights and new questions. Development. 134, 647-58.

Wang, Y., Ng, E. L., Tang, B. L., 2006. Rab23: what exactly does it traffic? Traffic. 7, 746-50.

Watanabe, N., Kato, T., Fujita, A., Ishizaki, T., Narumiya, S., 1999. Cooperation between mDia1 and ROCK in Rho-induced actin reorganization. Nat Cell Biol. 1, 136-43.

Watanabe, N., Madaule, P., Reid, T., Ishizaki, T., Watanabe, G., Kakizuka, A., Saito, Y., Nakao, K., Jockusch, B. M., Narumiya, S., 1997. p140mDia, a mammalian homolog of Drosophila diaphanous, is a target protein for Rho small GTPase and is a ligand for profilin. EMBO J. 16, 3044-56.

Winter, C. G., Wang, B., Ballew, A., Royou, A., Karess, R., Axelrod, J. D., Luo, L., 2001. Drosophila Rho-associated kinase (Drok) links Frizzled-mediated planar cell polarity signaling to the actin cytoskeleton. Cell. 105, 81-91.

Wong, L. L., Adler, P. N., 1993. Tissue polarity genes of Drosophila regulate the subcellular location for prehair initiation in pupal wing cells. J Cell Biol. 123, 209-21.

Xu, N., Keung, B., Myat, M. M., 2008. Rho GTPase controls invagination and cohesive migration of the Drosophila salivary gland through Crumbs and Rhokinase. Dev Biol. 321, 88-100.

Xu, Y., Moseley, J. B., Sagot, I., Poy, F., Pellman, D., Goode, B. L., Eck, M. J., 2004. Crystal structures of a Formin Homology-2 domain reveal a tethered dimer architecture. Cell. 116, 711-23.

Yamanaka, T., Ohno, S., 2008. Role of Lgl/Dlg/Scribble in the regulation of epithelial junction, polarity and growth. Front Biosci. 13, 6693-707.

Yan, J., Huen, D., Morely, T., Johnson, G., Gubb, D., Roote, J., Adler, P. N., 2008. The multiple-wing-hairs gene encodes a novel GBD-FH3 domaincontaining protein that functions both prior to and after wing hair initiation. Genetics. 180, 219-28.

Yan, J., Lu, Q., Fang, X., Adler, P. N., 2009. Rho1 has multiple functions in Drosophila wing planar polarity. Dev Biol. 333, 186-99.

Yasuda, S., Taniguchi, H., Oceguera-Yanez, F., Ando, Y., Watanabe, S., Monypenny, J., Narumiya, S., 2006. An essential role of Cdc42-like GTPases in mitosis of HeLa cells. FEBS Lett. 580, 3375-80.

Yun, U. J., Kim, S. Y., Liu, J., Adler, P. N., Bae, E., Kim, J., Park, W. J., 1999. The inturned protein of Drosophila melanogaster is a cytoplasmic protein located at the cell periphery in wing cells. Dev Genet. 25, 297-305.

Zeller, R., Jackson-Grusby, L., Leder, P., 1989. The limb deformity gene is required for apical ectodermal ridge differentiation and anteroposterior limb pattern formation. Genes Dev. 3, 1481-92.

Zeng, H., Hoover, A. N., Liu, A., 2010. PCP effector gene Inturned is an important regulator of cilia formation and embryonic development in mammals. Dev Biol. 339, 418-28.